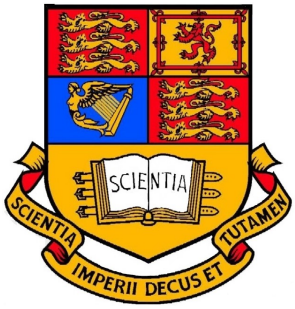

Imperial College London

MSc. Quantum Fields and Fundamental Forces

Gravitational Aspects of False Vacuum Decay

Candidate:
Usama Syed Aqeel

Supervisor:
Prof. Arttu Rajantie

Submitted in partial fulfilment for the degree of Master of Science of Imperial College London

Abstract

The possibility for quantum field theories to possess unstable vacua in flat, curved and gravitational cases are investigated. The state of higher energy density becomes unstable due to barrier penetration and thus permits a transition to the lower energy density state. In the limit of small $\hbar$ it is possible to reduce the gravitational system to a set of coupled ordinary differential equations solved using a Runge-Kutta method.

Humanity's deepest desire for knowledge is justification enough for our continuing quest. And our goal is nothing less than a complete description of the universe we live in.

Stephen Hawking (ABHOT)

Contents

Introduction

Motivation for this Report

Scalar fields are ubiquitous in physics from the *inflaton field* which is a candidate for the root cause of cosmological inflation, to the nature of the *Higgs field* [14; 19] by which particles acquire masses, to *dilatons* in Kaluza-Klein models. The second case here is of vital importance and is the main motivation for this report. An interesting exercise is when the potential of this scalar field possesses a false minimum. Due to the renormalisation group running coupling of the effective Higgs potential the masses of the Higgs scalar and the top quark ($m_{\mathrm{H}} = 125.18 \pm 0.16$ GeV, $m_t = 173.1 \pm 0.9$ GeV respectively [33]) place the Standard Model in a metastable state. As a result, there is a lower vacuum energy state that the electroweak vacuum can decay into [10].

False Vacuum Decay is the study of systems with classically stable states being rendered metastable under quantum fluctuations. One could consider a potential in a scalar field configuration with two non-degenerate minima. The minimum that is not global is called the false vacuum. If a system such as a scalar field is resting within this false vacuum, then in the classical case, it will remain unperturbed in this state. However, if one considers quantum fluctuations, the system will eventually seek the true vacuum (global minimum of the potential) in order to achieve equilibrium. This process is often likened to the nucleation of bubbles within the boiling process of super-heated liquids. Consider a homogeneous liquid within a container which is free of defects. This frees up the container from nucleation sites for vapour bubbles to form. This system exhibits two phases - a liquid phase and a vapour phase. Thermal fluctuations in the liquid cause bubbles of vapour to materialise in the fluid phase. If the volume of the bubble is too small, then the loss in surface tension does not compensate for the gain in volume. If the bubble is sufficiently large, then it will expand until the entire liquid

is converted to vapour.

The study of false vacuum decay has been of great interest since the early 1970s, with the seminal work of Voloshin, Kobrazev and Okun [21] and Coleman and Callan [4; 8] building on the work of Banks, Bender and Wu [1]. It was found, as in the analogy, that the phenomenon of barrier penetration results in a rapidly expanding bubble of true vacuum accelerating to the speed of light. As the bubble expands, it converts false vacuum to true vacuum. Notably, Coleman found that the solution to such a problem *boils* down to finding a classical solution to the Euclidean equations of motion, called the *bounce*. In doing so, one can calculate the action, B, of such a process occurring and thus the probability of decay rate per unit volume, Γ/V.

The inclusion of thermal as well as quantum fluctuations is also a huge area of interest in the literature and many fascinating analyses namely by Garriga [11] and Linde [23] tackle the same problem but in finite temperature. Their results will often be mentioned without proof, as the main focus of this report will be on the limit of zero temperature, however, the results of these papers are too irresistible to not include.

Structure of this Report

In Chapter 1 Theory Toolbox, we will develop the tools required to solve the problem of false vacuum decay such as the action principle and the path integral. In Chapter 2 Quantum Tunnelling will introduce the problem of WKB tunnelling and tunnelling in the heat kernel formalism and show how these are two sides of the same coin. We shall further introduce the notion of a metastable state as well as solving some heat kernels for simple systems such as the Single-Well Potential and the Double-Well Potential.

In Chapter 3 Instantons in Quantum Field Theory, we will apply our new skills to the study of a scalar field in a potential with a non-degenerate set of minima and show how the state with higher energy is rendered metastable due to barrier penetration. We then proceed to Chapter 4 Numerical Results in Minkowski Spacetime wherein we shall solve the scalar field equation using the Runge-Kutta method, shooting method and Newton-Raphson root-finding method to confirm the validity of the thin-wall approximation.

In Chapter 5 Instantons in de Sitter Space, we will introduce scalar dynamics on de Sitter space and solve the new equation of motion in Chapter 6 Numerical Problem in Fixed de Sitter Space. We also introduce the Hawking-Moss instanton and the pesky oscillating instantons as well as the sought after Coleman-de Luccia instanton in 6.2 Types of Solutions. We determine whether or not these solutions are important to consider.

Finally, in Chapter 7 Gravitational Instantons, we use a Friedmann-Robertson-Walker ansatz for the metric to solve the Friedmann equation coupled to the scalar field equation and show that the resulting spacetime is a de Sitter space. In Chapter 8 Numerical Results with Gravity we also introduce the Fixed Background approximation and show that under certain conditions that Coleman-de Luccia solutions cease and only the Hawking-Moss solution contributes. In this limit, the resulting spacetime is a static de Sitter spacetime.

Chapter 1

Theory Toolbox

In this section, many of the theoretical concepts, useful to our discussion, are introduced. At times we will be precise on derivations of the tools we require and at others we shall be terse when the tools are considered trivial.

1.1 Classical Fields in Flat Space

Consider the space-time dependent fields $\Phi^i(x^\mu)$, the action is defined as a functional of these fields. The Lagrangian density, $\mathcal{L}$, is a function of the fields, $\Phi^i(x^\mu)$, and their derivatives, $\partial_\mu \Phi^i$. Integrating the density over a spatial volume element gives the Lagrangian, L,

$$L = \int \mathrm{d}^3x \mathcal{L}(\Phi^i, \partial_\mu \Phi^i), \tag{1.1.1}$$

so the action for a classical field is,

$$S = \int \mathrm{d}t L = \int \mathrm{d}^4x \mathcal{L}(\Phi^i, \partial_\mu \Phi^i). \tag{1.1.2}$$

The Euler-Lagrange equations come from stationary action upon application of the arbitrary variations,

$$\begin{aligned} \Phi^i &\rightarrow \Phi^i + \delta\Phi^i \\ \partial_\mu \Phi^i &\rightarrow \partial_\mu \Phi^i + \delta(\partial_\mu \Phi^i) = \partial_\mu \Phi^i + \partial_\mu(\delta\Phi^i). \end{aligned}$$

Since $\delta\Phi^i$ is assumed to be small, we can Taylor expand the Lagrangian,

$$\mathcal{L}(\Phi^i + \delta\Phi^i, \partial_\mu\Phi^i + \partial(\delta\Phi^i)) = \mathcal{L}(\Phi^i, \partial_\mu\Phi^i) + \frac{\partial\mathcal{L}}{\partial\Phi^i}\delta\Phi^i + \frac{\partial\mathcal{L}}{\partial(\partial_\mu\Phi^i)}\partial_\mu(\delta\Phi^i) + ...$$

The corresponding action transforms as $S \to S + \delta S$ with,

$$\delta S = \int \mathrm{d}^4x \left(\frac{\partial\mathcal{L}}{\partial\Phi^i}\delta\Phi^i + \frac{\partial\mathcal{L}}{\partial(\partial_\mu\Phi^i)}\partial_\mu(\delta\Phi^i)\right).$$

The second term can be integrated by Stokes' Theorem and by dropping boundary terms (as $\delta\Phi(\pm\infty) \to 0$) we are left with the Euler-Lagrange equation for a field,

$$\frac{\delta S}{\delta\Phi^i} = \frac{\partial\mathcal{L}}{\partial\Phi^i} - \partial_\mu\left(\frac{\partial\mathcal{L}}{\partial(\partial_\mu\Phi^i)}\right) = 0. \tag{1.1.3}$$

The simplest field we could describe would be a real scalar field which takes space-time coordinates and maps them onto the real numbers,

$$\phi : \mathbb{M}^4 \longmapsto \mathbb{R}. \tag{1.1.4}$$

A typical scalar field is the temperature variation in a room. At every point in the room, we assign a single temperature, and the temperature of the entire room is described by the scalar distribution. In quantum field theory, scalar fields give rise to spin-less particles, such as the π^0-meson or the Higgs field [3]. The Lagrangian must contain terms dependent on ϕ and $\partial_\mu\phi$. The relativistically covariant Lagrangian of a scalar field is,

$$\mathcal{L} = \frac{1}{2}\eta^{\mu\nu}\partial_\mu\phi\partial_\nu\phi - U(\phi). \tag{1.1.5}$$

The equation of motion for this field is simply,

$$\partial_\mu\partial^\mu\phi + U'(\phi) = 0. \tag{1.1.6}$$

Using the Taylor expansion of $U(\phi)$ about a local minimum ϕ_0, we can write,

$$U(\phi - \phi_0) = U(\phi_0) + \frac{1}{2!}U''(\phi_0)(\phi - \phi_0)^2 + ...$$

We are free to add a constant to the potential, so we can redefine the vacuum state to have vanishing potential, $U(\phi - \phi_0) \simeq \frac{1}{2}U''(\phi_0)(\phi - \phi_0)^2$. If $U''(\phi_0) = m^2$ and $\phi_0 = 0$,

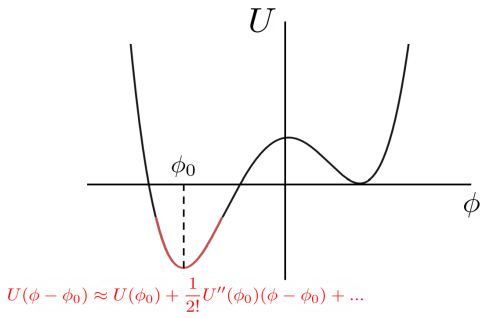

Figure 1.1.1: Here is a potential which has two degenerate minima, one at ϕ_0. If we expand the potential about the ϕ_0, we see that very close to the minimum, the potential is approximated as a parabola (in red). Expanding the potential will give the particle a mass.

we have $U(\phi) = \frac{1}{2}m^2\phi^2$ as we see in Figure 1.1.1.
Applying this approximate potential to the equation of motion, we obtain the Klein-Gordon Equation,

$$\partial_\mu \partial^\mu \phi + m^2 \phi = 0. \tag{1.1.7}$$

If we expand $\phi(x)$ in terms of Fourier modes, where $k_\mu = (E, k_i)$ we have

$$\begin{aligned} \int \frac{\mathrm{d}^4 k}{(2\pi)^4} \widetilde{\phi}(k)[\partial^\mu \partial_\mu + m^2] e^{ik_\mu x^\mu} &= 0 \\ -k^\mu k_\mu + m^2 = -E^2 + |\mathbf{k}|^2 + m^2 &= 0 \end{aligned}$$

and so we obtain the Einstein Energy-Momentum Relation $E^2 = m^2 + |\mathbf{k}|^2$ of a particle with rest-mass m.

Another central construction in Field Theory and General Relativity is the energy-momentum tensor $T_{\mu\nu}$. We proceed to derive this tensor using the symmetries of the Lagrangian under a spacetime translation of the scalar field by a vector a^μ,

$$\begin{aligned} \phi(x^\mu) \to \phi(x') &= \phi(x^\mu + a^\mu) \\ &= \phi(x) + a^\mu \partial_\mu \phi + ... \end{aligned}$$

Under these translations, the change induced on the scalar field to leading order is

$\delta\phi = a^\mu \partial_\mu \phi$. How does the Lagrangian change under translations? Well, it is a function of ϕ, but also a function of space-time position, so its change is two-fold. Let's first deal with changes with respect to ϕ

$$\delta\mathcal{L} = \frac{\partial\mathcal{L}}{\partial\phi}\delta\phi + \frac{\partial\mathcal{L}}{\partial(\partial_\mu\phi)}\partial_\mu\delta\phi \tag{1.1.8}$$

Using the Euler-Lagrange equations (1.1.3), we can replace the first term and combine the two terms by the Leibniz product rule,

$$\delta\mathcal{L} = \partial_\mu\left(\frac{\partial\mathcal{L}}{\partial(\partial_\mu\phi)}\right)\delta\phi + \frac{\partial\mathcal{L}}{\partial(\partial_\mu\phi)}\partial_\mu\delta\phi = \partial_\mu\left(\frac{\partial\mathcal{L}}{\partial(\partial_\mu\phi)}\delta\phi\right). \tag{1.1.9}$$

Moreover, as $\mathcal{L}$ is a scalar function depending on x^μ [28] another way to write this is,

$$\delta\mathcal{L} = a^\mu\partial_\mu\mathcal{L}. \tag{1.1.10}$$

Combining (1.1.9) and (1.1.10), we have the continuity equation,

$$\partial_\mu j^\mu = a^\nu\partial_\mu\left(\partial^\mu\phi\partial_\nu\phi - \delta^\mu_\nu\mathcal{L}\right) = 0, \tag{1.1.11}$$

j^μ is the conserved Nöther current and is given by,

$$j^\mu = a^\nu\left(\partial^\mu\phi\partial_\nu\phi - \delta^\mu_\nu\mathcal{L}\right) = a^\nu T^\mu{}_\nu, \tag{1.1.12}$$

and finally, we have the energy-momentum tensor of the scalar field theory,

$$T_{\mu\nu} = \partial_\mu\phi\partial_\nu\phi - \eta_{\mu\nu}\mathcal{L}. \tag{1.1.13}$$

1.2 Action Principle For General Relativity

The energy-momentum tensor appears in the Einstein Field Equations (EFEs) which are the dynamical equations of motion given by,

$$G_{\mu\nu} = 8\pi G_N\, T_{\mu\nu}, \tag{1.2.1}$$

where G_N is Newton's Universal Gravitational constant, $G_{\mu\nu} = R_{\mu\nu} - \frac{1}{2}Rg_{\mu\nu}$ is the *Einstein tensor*. $R_{\mu\nu}$ and R are the *Ricci tensor* and *scalar* respectively [3]. The con-

struction of $T_{\mu\nu}$ is slightly different in curved spaces, though the formula is essentially the same but with appropriate replacements for the metric. These variables are all dependent on the metric tensor $g_{\mu\nu}$ through the Christoffel connection, $\Gamma_{\rho\sigma}{}^{\mu}$, [31; 3] and its derivatives, $\partial_\nu \Gamma_{\rho\sigma}{}^{\mu}$,

$$\Gamma_{\rho\sigma}{}^{\mu} = \frac{1}{2} g^{\mu\nu} \left(\partial_\sigma g_{\rho\nu} + \partial_\rho g_{\sigma\nu} - \partial_\nu g_{\rho\sigma} \right). \tag{1.2.2}$$

This is the unique connection which is both metric-compatible (the covariant derivative of the metric vanishes, $\nabla_\rho g_{\nu\mu} = 0$) and torsion-free ($\Gamma_{\rho\sigma}{}^{\mu} = \Gamma_{\sigma\rho}{}^{\mu}$). The Riemann Tensor is determined by,

$$R^{\mu}{}_{\nu\rho\sigma} = \partial_\rho \Gamma_{\nu\sigma}{}^{\mu} - \partial_\sigma \Gamma_{\nu\rho}{}^{\mu} + \Gamma_{\rho\lambda}{}^{\mu} \Gamma_{\nu\sigma}{}^{\lambda} - \Gamma_{\sigma\lambda}{}^{\mu} \Gamma_{\nu\rho}{}^{\lambda}. \tag{1.2.3}$$

Once we know the Riemann Tensor, the Ricci tensor is easily determined,

$$R_{\mu\nu} = R^{\rho}{}_{\mu\rho\nu}, \tag{1.2.4}$$

then we can obtain the Ricci Scalar by calculating the *trace* of $R_{\mu\nu}$,

$$R = g^{\mu\nu} R_{\mu\nu}. \tag{1.2.5}$$

So, of the dynamical equations of motion of general relativity, we see that the most fundamental degree of freedom is the $g_{\mu\nu}$ as each of the participants of (1.2.1) all explicitly depend on it. $T_{\mu\nu}$ contains the information about the matter in the universe (spinors and tensors). In the action for the metric, we must treat $g_{\mu\nu}(x)$ as a classical field (dynamical variable). We introduce the *Lagrangian Density* over a manifold $\mathcal{M}$.

For a general classical field Φ^i on a d-dimensional pseudo-Riemannian (Lorentzian) manifold covered by an appropriate coordinate chart $\{x^\mu\}$, the Lagrangian density $\mathcal{L} = \mathcal{L}(\Phi^i, \partial\Phi^i)$ is a local function defined as,

$$L = \int d^{d-1}x \sqrt{|g|} \mathcal{L}(\Phi^i, \partial\Phi^i), \tag{1.2.6}$$

where, L is the Lagrangian of the system. From this, the action can be written in terms of the Lagrangian density (hereby Lagrangian),

$$S[\Phi^i] = \int_{\mathcal{M}} \mathrm{d}t\, \mathrm{d}^{d-1}x \sqrt{|g|}\mathcal{L}(\Phi^i, \partial\Phi^i) = \int_{\mathcal{M}} \mathrm{d}^d x \sqrt{|g|}\mathcal{L}(\Phi^i, \partial\Phi^i) \tag{1.2.7}$$

where $\int_{\mathcal{M}}$ denotes integration over the entire manifold and g is the metric determinant. This action must be diffeomorphism invariant. A diffeomorphism is a *bijective*[1] homeomorphism over a manifold $\mathcal{M}$ to another manifold $\mathcal{N}$ in the following sense,

$$\begin{aligned} f : \mathcal{M} &\longmapsto \quad \mathcal{N} = f(\mathcal{M}), \\ p &\longrightarrow \quad\ \ p' = f(p). \end{aligned} \tag{1.2.8}$$

We see that a diffeomorphism is a smooth re-labelling of points on $\mathcal{M}$. By far the simplest action to write is the Einstein-Hilbert Action, S_{EH}. In d-dimensions, this is nothing but,

$$S_{\mathrm{EH}}[g^{\mu\nu}] = \frac{1}{2}M_p^2 \int \mathrm{d}^d x \sqrt{|g|}R, \tag{1.2.9}$$

where $M_p = (8\pi G)^{-\frac{1}{2}}$ is the reduced Planck Mass in natural units. The dynamical variable is in fact $g^{\mu\nu}$ and so we must make the variations $g^{\mu\nu} \to g^{\mu\nu} + \delta g^{\mu\nu}$ to obtain the vacuum EFEs,

$$G_{\mu\nu} = 0. \tag{1.2.10}$$

To summarise, we need the actions to have the following simple properties, that the Lagrangian:

1. is a local functional in our tensor fields. *Tensor* also refers to *scalar* fields as a scalar field $f(x) \in \mathcal{J}_0^0$,
2. must be invariant under group symmetries of the fields (if a function $f(x)$ is $\mathbb{Z}_2$ invariant, the action must respect this),
3. must be a scalar function under diffeomorphism (differential analogue of space-time Lorentz invariance)

That's the beauty of the action principle. It allows us to intuitively build theories from the blocks outlined above.

[1] Bijective means one-to-one and onto - essentially means, $p \in \mathcal{M}$ is mapped to one and one point only $f(p) \in \mathcal{N}$. So the inverse mapping f^{-1} is well-defined.

We can now easily incorporate a scalar field, $\phi(x)$, in a potential $U(\phi)$ along with the S_{EH},

$$S[\phi, g^{\mu\nu}] = \int \mathrm{d}^d x \sqrt{|g|} \left(\frac{1}{2} g^{\mu\nu} \nabla_\mu \phi \nabla_\nu \phi - U(\phi) + \frac{1}{2} M_p^2 R \right). \tag{1.2.11}$$

We can see that the scalar field Lagrangian is that of the Klein-Gordon scalar but with obvious replacements, $\eta_{\mu\nu} \to g_{\mu\nu}$ and $\partial_\mu \to \nabla_\mu$. The variations required to obtain the EFEs are $g^{\mu\nu} \to g^{\mu\nu} + \delta g^{\mu\nu}$ and will give us $G_{\mu\nu} = M_p^{-2} T_{\mu\nu}$, where the stress-energy tensor $T_{\mu\nu}$, can be calculated as a functional derivative of the ϕ part of S,

$$T_{\mu\nu} = \frac{2}{\sqrt{|g|}} \frac{\delta S_\phi}{\delta g^{\mu\nu}}. \tag{1.2.12}$$

This derivation is very different from that of the energy-momentum tensor (1.1.13), however the calculation leads us to the following form of the energy-momentum tensor,

$$T_{\mu\nu} = \nabla_\mu \phi \nabla_\nu \phi - g_{\mu\nu} \mathcal{L}, \tag{1.2.13}$$

which is exactly the same as the flat case we discussed. Effectively, this demonstrates Einstein's Equivalence Principle. Variations in $\phi \to \phi + \delta\phi$, will give us the Klein-Gordon Equation on a curved space-time,

$$\frac{1}{\sqrt{|g|}} \partial_\mu \left[\sqrt{|g|} g^{\mu\nu} \partial_\nu \phi \right] = -\frac{\mathrm{d}U}{\mathrm{d}\phi}. \tag{1.2.14}$$

Since this is a tensorial equation, we can consider (1.2.14) in a local inertial frame $g_{\mu\nu} \to \eta_{\mu\nu}$ for which we will obtain (1.1.6). We will focus on the Euclidean analogue of (1.2.11) in the section on instantons in gravitational fields.

1.3 The Path Integral

1.3.1 The Free Propagator

The purpose of the path integral is to establish an action principle to quantum mechanics and particularly to quantum field theory (where the action principle is absolutely necessary). We consider the possible set of trajectories of a particle between two points q and q_0. Hamilton's principle allows us to throw away all the trajectories, except the one that extremises the action S. So the classical particle has a predetermined and

unique trajectory which depends on its initial position and velocity. This is of course not possible in quantum mechanics as we have lost determinism of the absolute state of a particle. Naturally, we could consider every possible trajectory a particle can take and see what happens. Starting with the wave function, we can write,

$$\psi(q,t) = \langle q| \exp(-i\hat{H}t) |\psi(0)\rangle \,, \tag{1.3.1}$$

[28; 26]. We then introduce the completeness relation in terms of the set of position eigenstates at initial time t_0, $\{|q_0\rangle\}$ given by $\mathbb{1} = \int \mathrm{d}q_0 \, |q_0\rangle \langle q_0|$. For instance, in the case of a free particle moving in one-dimension, between positions x_0 to x the Hamiltonian is quite simply,

$$\hat{H} = \frac{\hat{p}^2}{2m},$$

and our free propagator is,

$$D_0(x, x_0; t) = \langle x| e^{-i\frac{\hat{p}^2}{2m}t} |x_0\rangle \,. \tag{1.3.2}$$

We are of course always free to introduce a set of basis eigenstates, since our Hamiltonian is dependent only on $\hat{p}$, let us introduce its eigenstates as a complete set such that $\mathbb{1} = \int \frac{\mathrm{d}p}{2\pi} \, |p\rangle \langle p|$,

$$\begin{aligned} D_0(x, x_0; t) &= \frac{1}{2\pi} \int \mathrm{d}p \, \langle x| \, e^{-i\frac{\hat{p}^2}{2m}t} \, |p\rangle \, \langle p|x_0\rangle \,, \\ &= \frac{1}{2\pi} \int \mathrm{d}p e^{-i\frac{p^2}{2m}t} \, \langle x|p\rangle \, \langle p|x_0\rangle \,. \end{aligned}$$

Here, we can use $\langle x|p\rangle = e^{ipx}$,

$$D_0(x, x_0; t) = \frac{1}{2\pi} \int \mathrm{d}p e^{-i\frac{p^2}{2m}t + ip(x-x_0)},$$

we can write,

$$D_0(x, x_0; t) = \frac{1}{2\pi} \exp\left[\frac{im(x-x_0)^2}{2t}\right] \int_{-\infty}^{\infty} \mathrm{d}p \exp\left[\frac{-it}{2m}\left(p - \frac{m(x-x_0)}{t}\right)^2\right], \tag{1.3.3}$$

which is a Gaussian integral but with an imaginary exponent. Using the routine in Appendix A Gaussian Integrals, we can evaluate the integral,

$$D_0(x, x_0; t) = \sqrt{\frac{m}{2\pi i t}} \exp\left(\frac{im(x - x_0)^2}{2t}\right). \tag{1.3.4}$$

There are factors of i in both the exponent and in the prefactor, which make this object hard to visualise. However, if we analytically continue this solution by Wick rotation, $t \to -i\tau$, we have,

$$D_0(x, x_0; -i\tau) = \sqrt{\frac{m}{2\pi\tau}} \exp\left(-\frac{m(x - x_0)^2}{2\tau}\right). \tag{1.3.5}$$

This describes a distribution that is a δ-function at $\tau = 0$ which spreads out over time with a Gaussian profile. This is the Green's Function of the heat equation [31],

$$\frac{\partial u(x,t)}{\partial t} = \kappa \frac{\partial^2 u(x,t)}{\partial x^2}. \tag{1.3.6}$$

Interestingly, if we look at the Schödinger equation and perform a Wick rotation, we obtain a heat equation

$$\frac{\partial \psi(x,\tau)}{\partial \tau} = \kappa \frac{\partial^2 \psi(x,\tau)}{\partial x^2}. \tag{1.3.7}$$

with the thermal diffusivity coefficient $\kappa = \frac{\hbar}{2m}$. So Wick rotation transforms the propagator of the Schrödinger equation into a Green's function of the heat equation. For this reason, (1.3.5) is often called the *heat kernel* of $\hat{H}$, which we define as,

$$D(x, x_0; -i\tau) = \langle x | e^{-\hat{H}\tau} | x_0 \rangle. \tag{1.3.8}$$

1.3.2 The Particle in a Potential Case

In the case of the particle in non-zero potential $V(q)$ we have actually done most of the work already. We follow the derivation found in [26]. Looking closely at the exponential factor for small δt, we have,

$$e^{-i\hat{H}\delta t} = e^{-i(\frac{1}{2m}\hat{p}^2 + V(q))\delta t} = e^{-i\frac{1}{2m}\hat{p}^2\delta t} e^{-iV(q)\delta t}[1 + \mathcal{O}(\delta t^2)],$$

we should note that the extra terms comes from the commutators in the Baker-Campbell-Hausdorff (BCH) formula for operators. This is because for non-commuting

operators $\hat{A}$ and $\hat{B}$,

$$\exp(\hat{A})\exp(\hat{B}) = \exp\left(\hat{A}+\hat{B}+\frac{1}{2}[\hat{A},\hat{B}]+...\right) \neq \exp\left(\hat{A}+\hat{B}\right),$$

but for a small δt factor in the exponent,

$$\exp(\hat{A}\delta t)\exp(\hat{B}\delta t) = \exp\left(\hat{A}\delta t+\hat{B}\delta t+\frac{1}{2}\delta t^2[\hat{A},\hat{B}]+...\right) \approx \exp\left((\hat{A}+\hat{B})\delta t\right).$$

Now the key to this is to calculate as before using the same technique for the free case. So to leading order, our amplitude is given by,

$$\begin{aligned}\langle q_{r+1}|\exp(-i\hat{H}\delta t)|q_r\rangle &= \langle q_{r+1}|\, e^{-\frac{i}{2m}\hat{p}^2}e^{-iV(\hat{q})\delta t}\,|q_r\rangle\,,\\ &= e^{-iV(q)\delta t}\langle q_{r+1}|\, e^{-i\frac{\hat{p}^2}{2m}\delta t}\,|q_r\rangle\,,\end{aligned}$$

and what remains to be evaluated is the free propagator from (1.3.4),

$$\langle q_{r+1}|\exp(-i\hat{H}\delta t)|q_r\rangle = \sqrt{\frac{m}{2\pi i\delta t}}\exp\left(i\left[\frac{1}{2}m\left(\frac{q_{r+1}-q_r}{\delta t}\right)^2 - V(q_r)\right]\delta t\right), \quad (1.3.9)$$

and now returning to the propagator $D(q,q_0;T)$ we have,

$$D(q,q_0;T) = \left(\frac{m}{2\pi i\delta t}\right)^{\frac{1}{2}(n+1)}\int\prod_{r=1}^{n}\mathrm{d}q_r\exp\left(i\sum_{r=0}^{n}\left[\frac{1}{2}m\left(\frac{q_{r+1}-q_r}{\delta t}\right)^2 - V(q_r)\right]\delta t\right). \quad (1.3.10)$$

The exponent here is of course a discrete-lattice form of the action of our system $S[q] = \int \mathrm{d}t\left(\frac{1}{2}m\dot{q}^2 - V(q)\right) = \int \mathrm{d}tL(q,\dot{q})$, where $L(q,\dot{q})$ is of course the Lagrangian as we have become so acquainted with. Usually, $L(q,\dot{q}) = T(\dot{q}) - V(q)$, where T and V are, respectively, the kinetic and potential energy of the system. In the limit as $\delta t \to 0$, we have,

$$D(q,q_0;T) = \langle q|\exp(-i\hat{H}t)|q_0\rangle = \int [\mathrm{d}q]e^{iS[q]}, \quad (1.3.11)$$

where in the limit that $\delta t \to 0$,

$$\sqrt{\frac{m}{2\pi i\delta t}}\prod_{r=1}^{n}\sqrt{\frac{m}{2\pi i\delta t}}\,\mathrm{d}q_r \to [\mathrm{d}q], \quad (1.3.12)$$

is the functional integration measure. The great thing about the right hand side of (1.3.10) is that we have eliminated any trace of operators. We have a purely algebraic construction.

Chapter 2

Quantum Tunnelling

Now that we have introduced the path integral in this section we discuss the process of tunnelling first in the Wentzel–Kramers–Brillouin (WKB) approximation. The WKB approximation was independently developed and used by Gregor Wentzel, Hendrik Kramers and Léon Brillouin in 1926 to solve certain wave-mechanical problems, is of paramount importance for approximations made in quantum mechanics. This is one of several instances in mathematical physics where many individuals develop the same tool but the common name refers to only a few of them for brevity. These methods were also studied in depth by Harold Jeffreys in 1923 and as far back as the first half of the nineteenth century by George Green. A more pedagogical discussion of the results of the WKB approximation can be found in texts such as [31] and for a more quantum tunnelling focused approach [13]. It will be seen that the tunnelling in the path integral regime agrees with that of the WKB approximation.

2.1 WKB Tunnelling

For a particle moving in a rectangular potential barrier with height, U, and width, a, given as

$$V(x) = \begin{cases} U & 0 \leq x \leq a, \\ 0 & \text{otherwise.} \end{cases}$$

Thus the Schödinger equation for this one-dimensional system is given by,

$$\frac{\mathrm{d}^2\psi}{\mathrm{d}x^2} - \frac{2m}{\hbar^2}[V(x) - E]\psi(x). \tag{2.1.1}$$

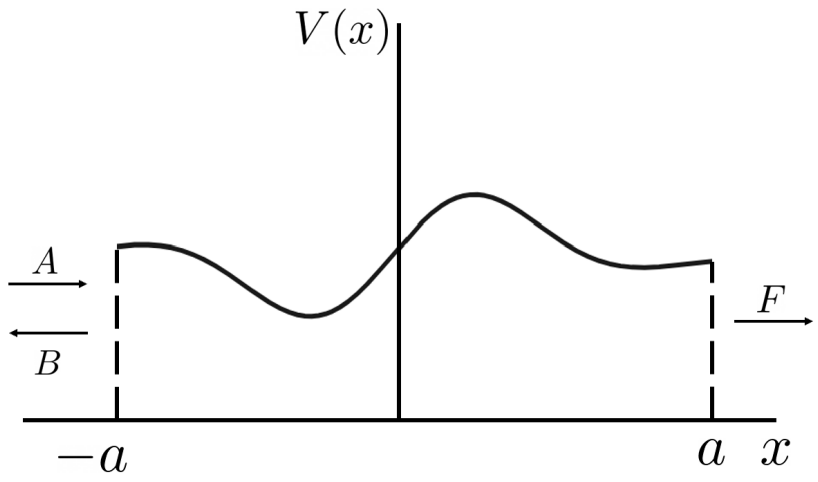

Figure 2.1.1: Bumpy-topped potential barrier.

In the case that, $E < V(x)$, in the non-classical region $(0 \leq x \leq a)$ The transmission coefficient, $T(E)$, can be readily determined as a function of the particle energy, E, as,

$$T(E)^{-1} = 1 + \frac{U^2}{4E(U-E)} \sinh^2\left(\frac{a}{\hbar}\sqrt{2m(U-E)}\right). \tag{2.1.2}$$

However, if we have a more complicated potential, Figure (2.1.1) we may not be able to obtain an exact closed-form solution for $T(E)$. Fortunately, we have the WKB solution to give us a semi-classical approximation for T, [13]. The power of the WKB solution is that it can deal with situations where, $E < V(x)$ and so $p(x)$ will be imaginary $p(x) = i\sqrt{2m(V(x)-E)}$, as is the requirement for tunnelling. The corresponding solution of the Schrödinger equation will be,

$$\psi(x) = \frac{A}{\sqrt{|p(x)|}} \exp\left(\pm\frac{1}{\hbar}\int |p(x)|\,\mathrm{d}x\right). \tag{2.1.3}$$

Now we consider the bumpy-topped potential in Figure (2.1.1).

- To the left, $(x < -a)$ the solution of the time-independent Schrödinger equation is,

  $$\psi(x < -a) = Ae^{ikx} + Be^{-ikx},$$

  where A is the incident wave amplitude and B is the reflected wave amplitude and $k = \sqrt{2mE/\hbar}$.

- To the right ($x > a$) the solution is,

$$\psi(x > a) = Fe^{ikx},$$

There is no e^{-ikx} term here because, we are assuming that the source of the particles is on the left of the potential. The transmission coefficient is the modulus-square of the ratio of the transmitted wave amplitude and the incident wave amplitude,

$$T = \frac{|F|^2}{|A|^2}.$$

- Inside the non-classical region ($-a < x < a$) we have,

$$\psi(-a < x < a) = \frac{C}{\sqrt{|p(x)|}} \exp\left(+\frac{1}{\hbar}\int_{-a}^{a} |p(x)|\,\mathrm{d}x\right) + \frac{D}{\sqrt{|p(x)|}} \exp\left(-\frac{1}{\hbar}\int_{-a}^{a} |p(x)|\,\mathrm{d}x\right).$$

Within the non-classical region we can see that if the barrier is very high or broad, that the coefficient C, must be very small (zero for an infinitely broad barrier). The relative amplitude of the incident and transmitted waves is determined by the total decrease of the exponential over the non-classical region,

$$\frac{|F|}{|A|} \propto \exp\left(-\frac{1}{\hbar}\int_{-a}^{a} |p(x)|\,\mathrm{d}x\right),$$

so that,

$$T = A' \exp\left(-\frac{2}{\hbar}\int_{-a}^{a} |p(x)|\,\mathrm{d}x\right), \tag{2.1.4}$$

which is the tunnelling coefficient for some generally-shaped potential barrier provided $\hbar$ is small.

2.2 Tunnelling using the Path Integral

Now we would like to translate tunnelling in terms the path integral formulation and we will see that there is an alternative approach which yields the same results as the WKB approach [7]. Consider for now some general potential $V(x)$. If we consider the amplitude of the particle moving from x_0 to x within time T, the path integral is given

by,

$$\langle x|\, e^{-i\hat{H}T/\hbar}\, |x_0\rangle = \int [\mathrm{d}x] e^{+\frac{i}{\hbar}S[x]}. \tag{2.2.1}$$

Note that we have reinstated $\hbar$ as we want a semiclassical[1] approximation expanded in orders of $\hbar$. When we usually calculate path integrals, we would like to expand about the classical trajectory of the particle such as,

$$x(t) = x_c(t) + f(t), \tag{2.2.2}$$

where $x_c(t)$ is the classical trajectory obeying the same boundary conditions as the general $x(t)$. The function $f(t)$ vanishes on the boundary. This is the same prescription that we established when deriving the Euler-Lagrange equations. However if $E < V(x)$ in some region, then the classical equation of motion has no well-defined solution.

Fortunately, we have Wick rotation $t = -i\tau$ which allows us to soldier on through this conundrum [36]. τ is known as the Euclidean time and all other affected quantities have the prefix *Euclidean* attached to them. For example, the total energy of a particle in this system is given by,

$$E = \frac{1}{2}m\left(\frac{\mathrm{d}x}{\mathrm{d}t}\right)^2 + V(x), \tag{2.2.3}$$

once we perform Wick rotation, we obtain the total Euclidean energy,

$$E_E = -\frac{1}{2}m\left(\frac{\mathrm{d}x}{\mathrm{d}\tau}\right)^2 + V(x). \tag{2.2.4}$$

The Euler-Lagrange equation under Wick rotation gives the condition for the classical path,

$$-m\frac{\mathrm{d}^2x_c}{\mathrm{d}\tau^2} + V'(x_c) = 0. \tag{2.2.5}$$

This is a funny sort of version of Newton's Second Law, but with the potential inverted. So if we have a potential barrier which is larger that the total energy of the particle, under Wick rotation, tunnelling becomes a particle moving on the inverted version of

[1] Semiclassical refers to a regime for which the momenta in our problem are larger that $\hbar$.

the potential barrier. Next, we focus on the effect on the action $S[x]$,

$$S[x] = \int_{-T/2}^{T/2} \mathrm{d}t \left[\frac{1}{2} m \left(\frac{\mathrm{d}x}{\mathrm{d}t} \right)^2 - V(x) \right] = i \int \mathrm{d}\tau \left[\frac{1}{2} m \left(\frac{\mathrm{d}x}{\mathrm{d}\tau} \right)^2 + V(x) \right]. \tag{2.2.6}$$

This new quantity is called the Euclidean action S_E [4; 6; 7; 8],

$$S_E = \int \mathrm{d}\tau \left[\frac{1}{2} m \left(\frac{\mathrm{d}x}{\mathrm{d}\tau} \right)^2 + V(x) \right]. \tag{2.2.7}$$

We can perform a change of variables as $\frac{1}{2} m \left(\frac{\mathrm{d}x}{\mathrm{d}\tau} \right)^2 = V(x)$ and we can rewrite S_E as,

$$S_E = \int_{x_0}^{x} \mathrm{d}x \sqrt{2mV(x)}, \tag{2.2.8}$$

and so the path integral is now from x_0 at Euclidean time $-\frac{T}{2}$ to x at Euclidean time $\frac{T}{2}$,

$$\langle x | \, e^{\hat{H}T/\hbar} \, | x_0 \rangle = A \exp\left(-\frac{1}{\hbar} \int_{x_0}^{x} \mathrm{d}x \sqrt{2mV(x)} \right). \tag{2.2.9}$$

This is recognised as the heat kernel of $\hat{H}$. The tunnelling coefficient T is,

$$T = A \exp\left(-\frac{2}{\hbar} \int_{x_0}^{x} \mathrm{d}x \sqrt{2mV(x)} \right), \tag{2.2.10}$$

which agrees with the exponential suppression from WKB approximation (2.1.4) with $E = 0$.

2.3 Heating up the Kernels

We will now consider a more detailed derivation of (2.2.9). Consider the heat kernel of a general $\hat{H}$,

$$\langle x_f | \, e^{-\hat{H}T/\hbar} \, | x_i \rangle = N \int [\mathrm{d}x] e^{-S[x]/\hbar}, \tag{2.3.1}$$

where N is a normalisation factor which is required since the Euclidean continuation is different from the usual path integral. $|x_i\rangle$ and $|x_f\rangle$ are the eigenstates of the position operator. In order to understand this expression a bit better we can introduce the

complete set of eigenstates of $\hat{H}$, such that $\hat{H}\,|n\rangle = E_n\,|n\rangle$, so the left side of (2.3.1) becomes,

$$\langle x_f|\, e^{-\hat{H}T/\hbar}\,|x_i\rangle = \sum_n e^{-E_nT/\hbar}\,\langle x_f|n\rangle\,\langle n|x_i\rangle \xrightarrow{T\to\infty} e^{-E_0T/\hbar}\,\langle x_f|0\rangle\,\langle 0|x_i\rangle\,. \tag{2.3.2}$$

We see that the vacuum state $|0\rangle$ dominates at large T [8]. In the case of the right side, S is the Euclidean action,

$$S = \int_{-\frac{T}{2}}^{\frac{T}{2}} \mathrm{d}\tau \left[\frac{1}{2}m\left(\frac{\mathrm{d}x}{\mathrm{d}\tau}\right)^2 + V(x)\right], \tag{2.3.3}$$

the $[\mathrm{d}x]$ measure is of course an integration over all functions $x(\tau)$ which obey the boundary conditions $x\,(-T/2) = x_i$ and $x\,(+T/2) = x_f$.

We define x_c as the classical Euclidean trajectory that minimises the action S and obeys the boundary conditions. We introduce a complete set of orthonormal functions, $\{x_n(\tau)\}$, which vanish on the boundary, $x_n(\pm T/2) = 0$. Thus a general path, $x(\tau)$ between $\tau = \pm T/2$ can be written as,

$$x(\tau) = x_c(\tau) + \sum_{n=1}^{\infty} c_n x_n(\tau), \tag{2.3.4}$$

where the c_n indicate the weight of each x_n that appears in the infinite sum. Orthonormality implies that $\int_{-\frac{T}{2}}^{\frac{T}{2}} \mathrm{d}\tau\; x_n(\tau)x_m(\tau) = \delta_{nm}$. With these considerations we can now define the measure of integration,

$$[\mathrm{d}x] = \prod_n (2\pi\hbar)^{-\frac{1}{2}}\,\mathrm{d}c_n. \tag{2.3.5}$$

Taking the functional derivative of S evaluated at the classical path gives,

$$\frac{\delta S}{\delta x_c} = -\frac{\mathrm{d}^2x_c}{\mathrm{d}\tau^2} + V'(x_c) = 0. \tag{2.3.6}$$

The second variational derivative of the action S can be determined easily by applying

the fluctuations $x_c \to x_c + \sum_n c_n x_n(\tau)$ and then Taylor Expanding,

$$\begin{aligned}\frac{\delta^2 S}{\delta x_c^2} &= -\frac{\mathrm{d}^2}{\mathrm{d}\tau^2}\left[x_c + \sum_n c_n x_n(\tau)\right] + V'\left(x_c + \sum_n c_n x_n(\tau)\right), \\ &= \left[-\frac{\mathrm{d}^2 x_c}{\mathrm{d}\tau^2} + V'(x_c)\right] + \sum_n \left[-\frac{\mathrm{d}^2 x_n}{\mathrm{d}\tau^2} + V''(x_c)\, x_n(\tau)\right],\end{aligned} \tag{2.3.7}$$

whereby, the first term vanishes due to (2.3.6). Thus the second variational derivative of the action with respect to x_c is given by,

$$\begin{aligned}\frac{\delta^2 S}{\delta x_c^2} = \sum_{n=1}^{\infty}\left[-\frac{\mathrm{d}^2 x_n}{\mathrm{d}\tau^2} + V''(x_c)x_n\right] &= \sum_{n=1}^{\infty}\lambda_n x_n, \\ -\frac{\mathrm{d}^2 x_n}{\mathrm{d}\tau^2} + V''(x_c)x_n &= \lambda_n x_n.\end{aligned} \tag{2.3.8}$$

As the differential operator (2.3.8) is in Sturm-Liouville form [31],

$$-\frac{\mathrm{d}}{\mathrm{d}\tau}\left[p(\tau)\frac{\mathrm{d}x_n}{\mathrm{d}\tau}\right] + q(\tau)x_n = \lambda_n w(\tau) x_n, \tag{2.3.9}$$

we have chosen the orthonormal set $\{x_n(\tau)\}$ to be eigenfunctions of (2.3.8). Thus (2.3.8) is expressed as an eigenvalue equation.

Putting all of this together, the heat kernel is written,

$$\begin{aligned}&\langle x_f|\, e^{-\hat{H}T/\hbar}\,|x_i\rangle = \\ &N\int\prod_n \frac{\mathrm{d}c_n}{\sqrt{2\pi\hbar}} e^{-S_c/\hbar}\exp\left(-\frac{1}{2\hbar}\int_{-\frac{T}{2}}^{\frac{T}{2}}\mathrm{d}\tau'\sum_{n,m} c_n c_m x_m(\tau')\left[\ddot{x}_n(\tau') + V''(x_c)x_n(\tau')\right] + \ldots\right), \\ = \;& N\int\prod_n \frac{\mathrm{d}c_n}{\sqrt{2\pi\hbar}} e^{-S_c/\hbar}\exp\left(\sum_n -\frac{\lambda_n}{2\hbar}c_n^2\right)[1+\mathcal{O}(\hbar)], \\ = \;& N\prod_n \lambda_n^{-\frac{1}{2}} e^{-S_c/\hbar}[1+\mathcal{O}(\hbar)],\end{aligned}$$

where the action has been expanded about the classical solution. We shall drop the $[1+\mathcal{O}(\hbar)]$ factor from here on, but the reader should implicitly account for its presence. The final equality can be written more explicitly in terms of a functional determinant,

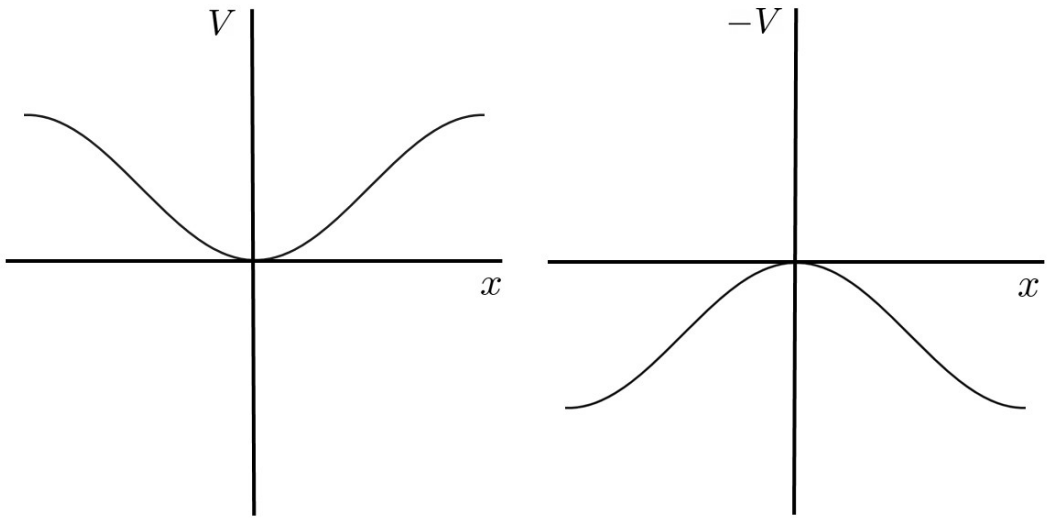

Figure 2.3.1: The single well potential becomes inverted in the mechanical analogy under Wick rotation.

$$\langle x_f | \, e^{-\hat{H}T/\hbar} \, | x_i \rangle = N e^{-S_c/\hbar} [\det(-\partial_\tau^2 + V''(x_c))]^{-\frac{1}{2}}, \tag{2.3.10}$$

A major roadblock of these calculations is evaluating functional determinants, but it depends purely on the nature of the potential $V(x_c)$, so this is a natural stopping point.

2.3.1 Single-Well Potential

Consider the single well potential in Figure 2.3.1 which we can write to leading order as $V(x) \approx \frac{1}{2}\omega^2 x^2$. We are free to redefine $V(0) = 0$ by adding a constant, we will not be afforded the same leniency when in curved spaces, we may as well make use of this invariance here. The classical trajectory of the particle is when $x_i = x_f = 0$. The only well behaved solution that does not instantly become singular is the one where $x_c(\tau) = 0$. The heat kernel of interest is,

$$\langle x = 0 | \, e^{-\hat{H}T/\hbar} \, | x = 0 \rangle = N [\det(-\partial_\tau^2 + \omega^2)]^{-\frac{1}{2}}. \tag{2.3.11}$$

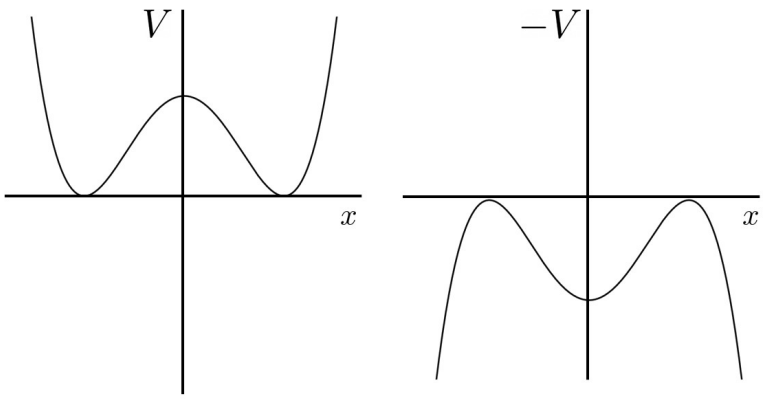

Figure 2.3.2: The double well potential becomes inverted in the mechanical analogy under Wick rotation.

We employ the method of evaluating functional determinants in Appendix B Functional Determinants to write,

$$\langle x=0|\, e^{-\hat{H}T/\hbar}\, |x=0\rangle \xrightarrow{T\to\infty} \left(\frac{\omega}{\pi\hbar}\right)^{\frac{1}{2}} e^{-\frac{1}{2}\omega T}. \tag{2.3.12}$$

Using (2.3.2), we can determine the ground state energy in the limit $T \to \infty$,

$$e^{-E_0 T/\hbar} |\, \langle x=0|n=0\rangle\, |^2 = \left(\frac{\omega}{\pi\hbar}\right)^{\frac{1}{2}} e^{-\frac{1}{2}\omega T}, \tag{2.3.13}$$

so the ground state energy is $E_0 = \frac{1}{2}\hbar\omega$ and the probability of the particle being at the origin is $|\, \langle x=0|n=0\rangle\, |^2 = (\omega/\pi\hbar)^{\frac{1}{2}}$ as expected from standard calculations in quantum mechanics for a particle with unit mass [7].

2.3.2 Double-Well Potential

A less trivial example of tunnelling is of a symmetric potential $V(x)$ with two vacua placed at $\pm a$, such that $V(\pm a) = 0$. This configuration complicates things slightly, as the vacuum is not unique.

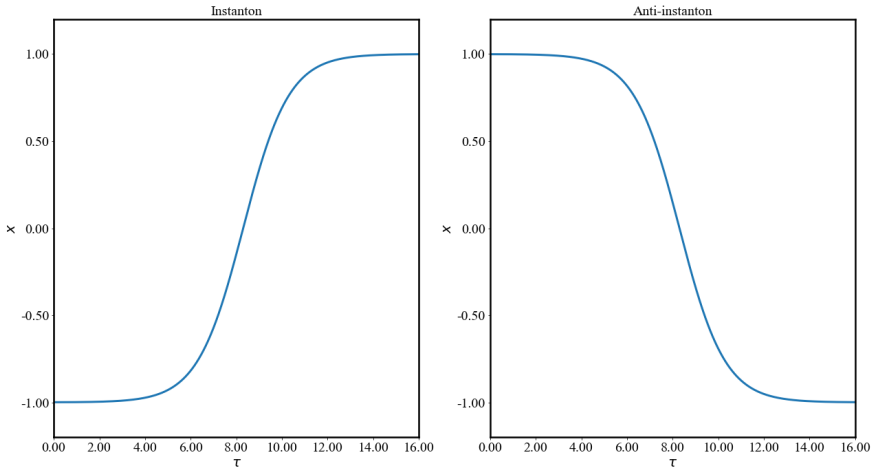

Figure 2.3.3: The instanton, which is a smooth curve connecting the particle with boundary conditions $x(\pm T/2) = \pm a$ (a is normalised to 1). The anti-instanton is the time-reversal of this which smoothly connects the boundary values of x.

For instance, we must calculate the amplitudes,

$$\langle a| e^{-\hat{H}T} |a\rangle = \langle -a| e^{-\hat{H}T} |-a\rangle , \tag{2.3.14}$$

$$\langle a| e^{-\hat{H}T} |-a\rangle = \langle -a| e^{-\hat{H}T} |a\rangle . \tag{2.3.15}$$

Clearly, this complicates matters somewhat. Two obvious examples are where the particle remains at $x = \pm a$. Though these are solutions by right, there is a more interesting solution which starts at $x = -a$ at $-T/2$ and ends at $x = a$ at $T/2$ seen in Figure 3.1.1. The solution being when we push $T \to \infty$. The classical equation of motion can be obtained by considering the total energy $E = 0$ which gives us,

$$\frac{\mathrm{d}x}{\mathrm{d}\tau} = \sqrt{2V(x)}, \tag{2.3.16}$$

(2.3.16) is can be integrated to give,

$$\tau = \tau_1 + \int_0^x \mathrm{d}x' [2V(x')]^{-\frac{1}{2}}. \tag{2.3.17}$$

The solution (2.3.17) is aptly named the *instanton* centred at τ_1. The instanton is a *particle-like* solution to the classical equation of motion but it exists in time (hence *instant-*). It has a localised structure, much like solitons (or classical lumps). We can construct an identical solution to the instanton but played backwards in time, called

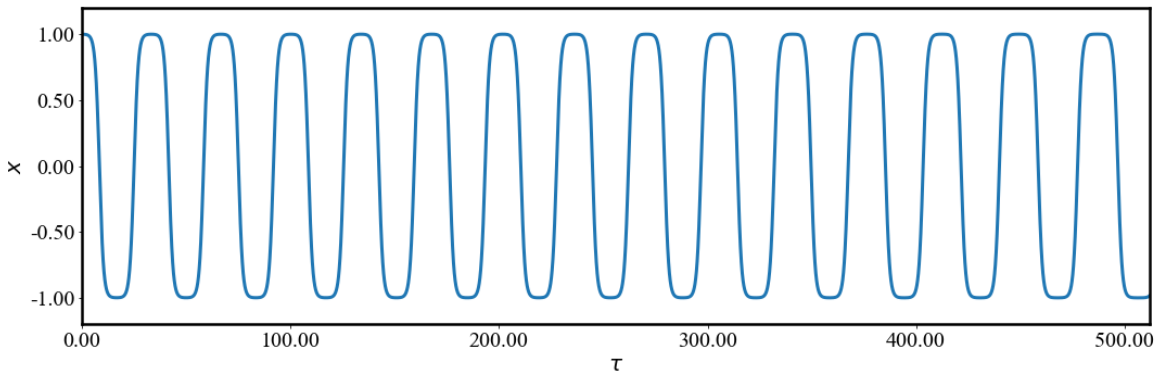

Figure 2.3.4: Several kinks over a large time period

the *anti-instanton* which takes our particle from $x = a$ at $-T/2$ to $x = -a$ at $T/2$. There is also a more general solution which connects instanton to anti-instanton (called the *kink* solution).

The action of these objects S_0 is given by,

$$S_0 = \int \mathrm{d}\tau \left[\frac{1}{2}\left(\frac{\mathrm{d}x}{\mathrm{d}\tau}\right)^2 + V(x)\right] = \int \mathrm{d}\tau \left(\frac{\mathrm{d}x}{\mathrm{d}\tau}\right)^2 = \int_{-a}^{a} \mathrm{d}x\sqrt{2V(x)}, \tag{2.3.18}$$

which is our usual barrier penetration factor.

About a classical turning point of the potential, (2.3.16) becomes,

$$\frac{\mathrm{d}x}{\mathrm{d}\tau} \propto \omega(a-x), \tag{2.3.19}$$

$$(a-x) \propto e^{-\omega\tau/2}, \tag{2.3.20}$$

which shows that the width of the instanton is of $\mathcal{O}(\frac{1}{\omega})$. Assuming that ω is huge, this makes the instanton very narrow in width and so highly localised. Hence, it is possible within the time T, to fit a set of instantons followed by anti-instantons widely separated with respect to the width $\frac{1}{\omega}$. These are approximate solutions of the equations of motion and have *approximately* stationary action [7].

Suppose we have n of these objects connected to each other, we require the following facts for our solution:

1. if the action of one of these objects is S_0, then the action for n widely-separated objects is nS_0.

2. evaluation of the functional determinant requires us to split the time interval T into $-T/2 = \tau_0 < \tau_1 < ... < \tau_{n-1} < \tau_n = T/2$. If the instanton was very large, then the particle would spend a longer time around $x = 0$ and so $V'' = \omega^2$. The small width of these objects stops this from being the case, however, if it were, then the functional determinant would become that for the single well,

$$\sqrt{\frac{\omega}{\pi\hbar}}e^{-\omega T/2}.$$

   Thus we attach a simple correction K which pertains to a single (anti-)instanton, giving us,

$$\sqrt{\frac{\omega}{\pi\hbar}}e^{-\omega T/2}K^n. \tag{2.3.21}$$

3. the integration over time can be evaluated by integration over the centres of our objects τ_i,

$$\int_{-T/2}^{T/2}\mathrm{d}\tau_1\int_{-T/2}^{\tau_1}\mathrm{d}\tau_2...\int_{-T/2}^{\tau_{n-1}}\mathrm{d}\tau_n \equiv \frac{T^n}{n!}.$$

Assembling the solution therefore is simple as we put these ingredients together,

$$\langle -a|e^{-\hat{H}T}|-a\rangle = \sqrt{\frac{\omega}{\pi\hbar}}e^{-\omega T/2}\sum_{\text{even } n}\frac{(Ke^{-S_0/\hbar}T)^n}{n!}, \tag{2.3.22}$$

and,

$$\langle a|e^{-\hat{H}T}|-a\rangle = \sqrt{\frac{\omega}{\pi\hbar}}e^{-\omega T/2}\sum_{\text{odd } n}\frac{(Ke^{-S_0/\hbar}T)^n}{n!}. \tag{2.3.23}$$

We can generalise both of these formulae into one,

$$\langle \pm\, a|e^{-\hat{H}T}|-a\rangle = \sqrt{\frac{\omega}{\pi\hbar}}e^{-\omega T/2}\frac{1}{2}\left[\exp(Ke^{-S_0/\hbar}T) \mp \exp(-Ke^{-S_0/\hbar}T)\right]. \tag{2.3.24}$$

The ground state energy is,

$$E_\pm = \frac{1}{2}\hbar\omega \pm \hbar K e^{-S_0/\hbar}. \tag{2.3.25}$$

This is interesting as we see the barrier-penetration factor $e^{-S_0/\hbar}$ from the WKB ap-

proximation. Essentially, the wavefunction is smeared over the classical turning points. (2.3.25) is slightly disingenuous as the second term is smaller than the $\mathcal{O}(\hbar^2)$ corrections of the first term, so we do not have the right to keep it in our formula, [7; 8]. However, it is the leading order contribution to $\Delta E = E_+ - E_- = 2\hbar K e^{-S_0/\hbar}$, so we ought to keep it.

Now we shall evaluate K - the correction to a single instanton. If we take the first derivative of the equation of motion (2.3.6), we have,

$$-\frac{\mathrm{d}^2}{\mathrm{d}\tau^2}\dot{x}_c + V''(x_c)\dot{x}_c = 0. \tag{2.3.26}$$

Comparing this to the eigenvalue equation (2.3.8) we can see that (2.3.26) is alluding to an eigenfunction, x_1, of the differential operator with eigenvalue zero. By one-to-one comparison, we see that $x_1 = S_0^{-1/2}\dot{x}_c$. The normalisation is achieved by the action (2.3.18). In order to evaluate the functional determinants, we integrate over the expansion coefficients. However, if we did integrate over the c_1 coefficient, our functional determinant would be hopelessly divergent. If we instead change the centre of the instanton infinitesimally, $\mathrm{d}\tau_1$, then the change in the solution is,

$$\mathrm{d}x = (\mathrm{d}x_c/\,\mathrm{d}\tau)\,\mathrm{d}\tau_1, \tag{2.3.27}$$

and the induced change in the expansion coefficient is,

$$\mathrm{d}x = x_1\,\mathrm{d}c_1. \tag{2.3.28}$$

Thus we have the infinitesimal change in the expansion coefficient, dc_1, to be,

$$(2\pi\hbar)^{-1/2}\,\mathrm{d}c_1 = (S_0/2\pi\hbar)^{-1/2}\,\mathrm{d}\tau_1. \tag{2.3.29}$$

We that in evaluating the functional determinant, we do not include the integration over the zero eigenvalue. But we ought to include a factor of $(S_0/2\pi\hbar)^{-1/2}$. Therefore, the contribution from one instanton is going to be,

$$\langle a|\, e^{\hat{H}T}\,|-a\rangle = NT\,(S_0/2\pi\hbar)^{1/2}\,e^{-S_0/\hbar}\left(\widetilde{\det}[\partial_\tau^2 + V''(x_c)]\right)^{-1/2}, \tag{2.3.30}$$

where $\widetilde{\det}$ refers to the functional determinant excluding the zero eigenvalue. The value

of K is therefore,

$$K = (S_0/2\pi\hbar)^{1/2} \left| \frac{\det[-\partial_\tau^2 + \omega^2]}{\widetilde{\det}[-\partial_\tau^2 + V''(x_c)]} \right|^{\frac{1}{2}}. \tag{2.3.31}$$

The detailed derivation of this expression was originally formulated by Coleman and Callan, [8; 7]. We have assumed that all of the eigenvalues are positive, except for the one zero mode x_1. This is not a baseless assumption as from the one-dimensional Schrödinger equation, the eigenfunction of lowest eigenvalue has no nodes. The next eigenfunction has one node. Since the instanton, x_c, is a monotonically increasing function, its first derivative (and so the zero mode) is nodeless. Therefore, x_1, is the only zero mode and all other eigenvalues $\lambda_{n>1}$ are positive □.

2.3.3 Metastable States

Suppose now, that we have the potential in Figure 2.3.5. If we neglect barrier penetration, in the semiclassical limit, $V(x)$ has an energy eigenstate at the bottom of the well at $x = 0$ ($E = \frac{1}{2}\hbar\omega + ...$). We would like to calculate the corrections to E due to barrier penetration. Under Wick rotation, we observe that the classical equation of motion has a solution in which the particle begins at $x = 0$, bounces off $x = \varsigma$ and then returns to $x = 0$. Computing the transition matrix element, from $x = 0$ to $x = 0$, by summing over this configuration (as before), we have,

$$\langle 0| e^{-\hat{H}T/\hbar} |0\rangle = \sqrt{\frac{\omega}{\pi\hbar}} e^{-\omega T/2} \exp(-KTe^{-S_0/\hbar}). \tag{2.3.32}$$

The ground state energy for this process is given by,

$$E_0 = \frac{1}{2}\hbar\omega + \hbar K e^{-S_0\hbar}. \tag{2.3.33}$$

Now, from the description of this motion, the solution $x_c(\tau)$ has a maximum (unlike the instanton from before). Therefore, the zero mode, x_1 which is proportional to $\dot{x}_c$ has a node.

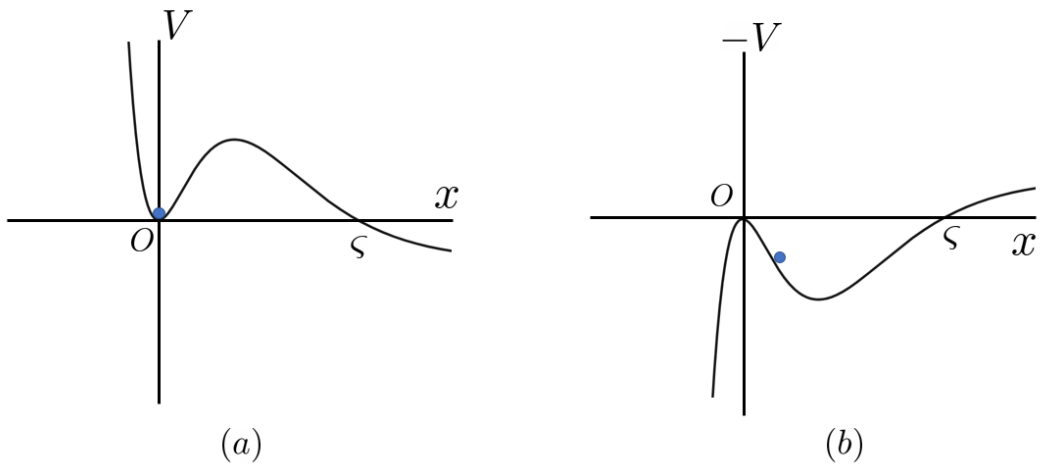

Figure 2.3.5: (a) An example of an unstable potential with a vacuum state at $x = 0$ however it is no the global minimum of V since there exist regions in the domain of x such that $V(x) < V(0)$, therefore, (b) this vacuum state is unstable. A method of understanding this instability is the fact that when the particle reaches ς, it achieves rest since $V(\varsigma) = 0$, however, this is not a classical stationary point of the potential.

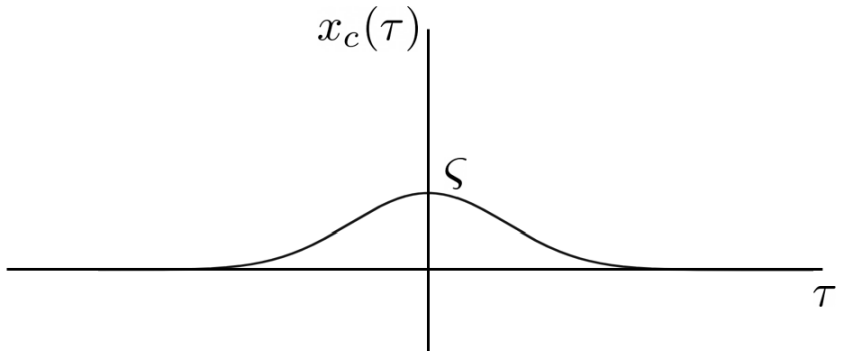

Figure 2.3.6: The classical solution to the unstable potential has a node at $\tau = 0$, therefore, the zero mode $\propto \mathrm{d}x/\,\mathrm{d}\tau$ has one node at $\tau = 0$. This means that there must be a negative mode which has no nodes.

Thus, there is mode with a negative eigenvalue. Recalling that K is constructed by the inverse square root of the eigenvalue product and thus is imaginary. But this eigenvalue is not within the spectrum of eigenvalues of $\hat{H}$. We conclude that a *metastable* state has an imaginary energy contribution and thus we define,

$$\Gamma = \hbar|K|e^{-S_0/\hbar}, \tag{2.3.34}$$

where $|K|$ is the modulus of the functional determinant contributions. Γ is noticed as

the imaginary part of the energy in (2.3.33) provided K is an imaginary number. A more elegant formulation of this calculation was performed by Coleman and Callan in [8]. This Γ factor is associated to the rate of decay of an unstable state. Γ is a measure of the instability of the vacuum state and allows permits tunnelling. The heat kernel obtains a further exponential suppression which remains after Wick rotation.

Chapter 3

Instantons in Quantum Field Theory

We are now ready to apply what we have learned but extending to the case of a field with an unstable vacuum state. What follow are essentially the same steps as the quantum mechanical case, however, field theories present their own sets of idiosyncrasies and complications. In this section, we will describe the relevant calculations for a single scalar field in an metastable potential as well as discuss the issues of regularisation and renormalisation in order to deal with ultraviolet divergences that quantum field theories so often possess.

3.1 The False Vacuum

Consider the scalar field $\phi(x)$ in a potential $U(\phi)$. The potential contains a set of minima ϕ_{fv} and ϕ_{tv}, for now which may or may not be degenerate. The action for this system in the $(+---)$ signature is,

$$S[\phi] = \int \mathrm{d}^4x \left(\frac{1}{2}\partial_\mu \phi \partial^\mu \phi - U(\phi) \right). \tag{3.1.1}$$

We always have the freedom to add a constant to U such that $U(\phi_{\text{fv}}) = 0$. ϕ_{fv} is rendered unstable by barrier penetration under quantum fluctuations.

Our aim is not to compute Γ, the probability of decay per unit time, but rather Γ/V which is the probability of decay per unit time-volume, which is the Γ that in a given

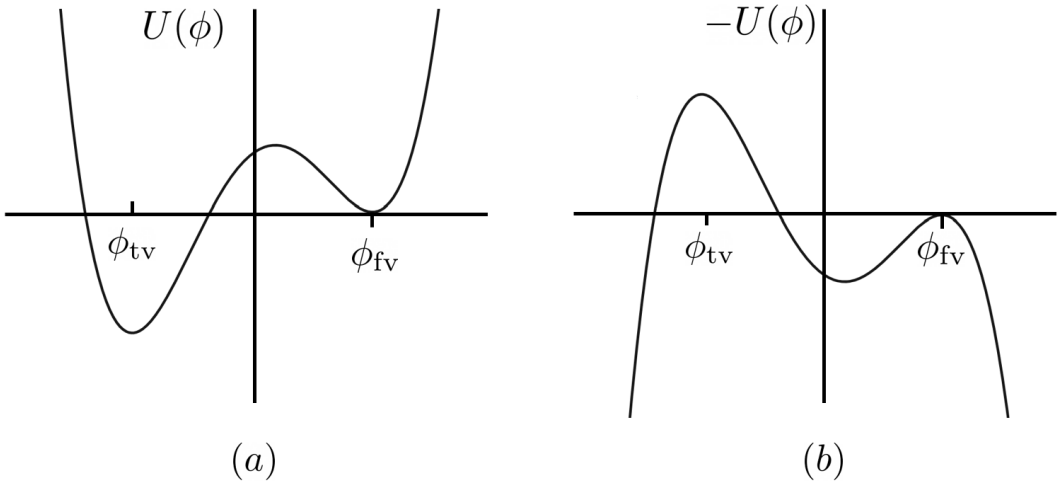

Figure 3.1.1: (a) Shows the scalar field resting in a potential at the false vacuum $\phi_{\rm fv}$. Classically, $\phi_{\rm fv}$ is a stable minimum point of the potential - small oscillations of the scalar about $\phi_{\rm fv}$ are stable. Under quantum fluctuations this minimum is rendered unstable, due to barrier penetration and it is possible for the scalar field to tunnel into the true vacuum $\phi_{\rm tv}$. (b) Under Wick Rotation $t = -i\tau$, we effectively flip the potential and the barrier penetration problem becomes a particle rolling in Euclidean space-time.

spatial volume V that a critical bubble will form is proportional to the volume (if the bubble is very large). It should be noted that the calculation is performed at absolute zero. Were it not for cosmology, this question would be pointless. An infinitely old universe would necessarily be in the true vacuum, no matter the instability of U. But the universe is not infinitely old, therefore it is possible that at the time of the Big Bang, that the ϕ settled near $\phi_{\rm fv}$ and as the universe cooled, its fate was sealed to lie in the false vacuum.

Suppose that the scalar field initially rests in the state $|\phi_{\rm fv}\rangle$ and we would like for the particle to move to the state $|\phi_{\rm tv}\rangle$. We are interested in a solution which smoothly connects these vacua together. The amplitude of ϕ given these conditions will be,

$$\langle\phi_{\rm tv}|\, e^{-i\hat{H}T}\, |\phi_{\rm fv}\rangle = \int [{\rm d}\phi] e^{iS[\phi]/\hbar}. \tag{3.1.2}$$

The Wick rotation procedure is identical to the case of quantum mechanics, and the

Euclidean action is,

$$S_E[\phi] = \int \mathrm{d}^4x \left[\frac{1}{2}\left(\frac{\partial\phi}{\partial\tau}\right)^2 + \frac{1}{2}(\partial_i\phi)^2 + U(\phi)\right] = \int_{-\infty}^{\infty} \mathrm{d}\tau\mathcal{L}_E, \tag{3.1.3}$$

where ∂_i indicates the derivatives with respect to x, y and z. The heat kernel for a scalar field is given by,

$$\langle\phi_{\mathrm{tv}}|\, e^{-i\hat{H}T}\, |\phi_{\mathrm{fv}}\rangle = N\int [\mathrm{d}\phi] e^{-S_E[\phi]/\hbar}. \tag{3.1.4}$$

Again we have included the normalisation N because the fundamental evaluation of this path integral is different to Feynman's sum over histories. The Euclidean equation of motion are obtained by taking the variations of S_E with respect to ϕ,

$$\begin{aligned} \frac{\delta S_E}{\delta\phi} = \frac{\mathrm{d}U}{\mathrm{d}\phi} - \frac{\partial^2\phi}{\partial\tau^2} - \nabla^2\phi &= 0, \\ \frac{\partial^2\phi}{\partial\tau^2} + \nabla^2\phi &= \frac{\mathrm{d}U}{\mathrm{d}\phi}. \end{aligned} \tag{3.1.5}$$

For the solution described above, we have the following boundary condition,

$$\phi(\tau, +\infty) = \phi(+\infty, \vec{x}) = \phi_{\mathrm{fv}}, \tag{3.1.6}$$

This is an appropriate boundary condition because, if this tunnelling process occurs at some point in space and time, then far away from that point, the field should rest in the ϕ_{fv} state undisturbed [4; 7]. Once we have this solution called the bounce, ϕ_c, we can compute Γ/V as,

$$\frac{\Gamma}{V} = Ke^{-S_0/\hbar}, \tag{3.1.7}$$

where $S_0 = S[\phi_c]$.

What kind of solutions are we interested in? The solution must have minimum stationary action, as they are the dominant contribution [9]. The constant solution $\phi(x) = \phi_{\mathrm{fv}}$ is of no interest to us as it has no negative eigenvalues. The second variation of S_E

leads to an eigenvalue equation for fluctuations $\delta\phi$ of a constant $\phi_{\rm fv}$ solution gives,

$$-\partial_\mu\partial_\mu\delta\phi + U''(\phi_{\rm fv})\delta\phi = \lambda_n\delta\phi. \tag{3.1.8}$$

Choosing $\delta\phi = T(\tau)X(x)Y(y)Z(z)$ allows the equation to become separable. The equation for each of the components T, X, Y and Z are identical. Let's consider the equation for the T component,

$$-\frac{\mathrm{d}^2T}{\mathrm{d}\tau^2} + U''(\phi_{\rm fv})T = \lambda_n^{(\tau)}T. \tag{3.1.9}$$

$\lambda_n^{(\tau)}$ are the eigenvalues of the time components of the fluctuations. This solves to $T(\tau) = A\sin(\epsilon_n\tau) + B\cos(\epsilon_n\tau)$, and we obtain eigenvalues for the time-component of the fluctuations about $\phi_{\rm fv}$ to be,

$$\lambda_n^\tau = \epsilon_n + U''(\phi_{\rm fv}). \tag{3.1.10}$$

$\epsilon_n > 0$ and $U''(\phi_{\rm fv}) > 0$ then λ_n^τ is always positive. The same analysis follows for all other components X, Y and Z. It then follows that the functional derivative of the constant false vacuum solution is always real, thus it provides no contribution to the amplitude of tunnelling.

If we embed the bounce solution ϕ_c into a one-parameter family of functions (by a re-scaling of spacetime by a parameter, ζ),

$$\phi_\zeta = \phi_c(x/\zeta), \tag{3.1.11}$$

then we can write the action S as,

$$S[\phi_\zeta] = \frac{1}{2}\zeta^2\int \mathrm{d}^4x(\partial_\mu\phi_c)^2 + \zeta^4\int \mathrm{d}^4x U(\phi_c). \tag{3.1.12}$$

This must be stationary at $\zeta = 1$. Computing the derivative of $S[\phi_\zeta]$ with respect to ζ evaluated at $\zeta = 1$, we find that the action of the bounce is,

$$S_0 = \frac{1}{4}\int \mathrm{d}^4x(\partial_\mu\phi_c)^2 > 0, \tag{3.1.13}$$

which is promising as it is positive. However, since $U(\phi_c)$ is somewhere negative, we

may have worried that $S_0 < 0$, but we have eliminated this possibility. Moreover,

$$\frac{\mathrm{d}^2 S}{\mathrm{d}\zeta^2} = -\frac{1}{2}\int \mathrm{d}^4 x (\partial_\mu \phi_c)^2 < 0 \tag{3.1.14}$$

Therefore, at ϕ_c, $\delta^2 S/\delta\phi^2$ has at least one negative eigenvalue. So ϕ_c contributes to Γ/V.

3.2 Constructing the Bounce

The boundary conditions in (3.1.6) clearly allude to a solution (which at least at the boundary) is $O(4)$-invariant. Had we considered finite temperatures, this bounce would be $O(3)$-invariant as the phase transitions are dominated by thermal hopping [11]. This $O(4)$-symmetry was extended to the entire solution by [9]. Under this assumption, we can parameterise the field in terms of the Euclidean distance, ρ, of some point from the origin, $\rho = \sqrt{\tau^2 + |\vec{x}|^2}$. We see a considerable simplification of the Euclidean action for $\phi = \phi(\rho)$,

$$S_E[\phi] = 2\pi^2 \int \mathrm{d}\rho\ \rho^3 \left[\frac{1}{2}\left(\frac{\mathrm{d}\phi}{\mathrm{d}\rho}\right)^2 + U(\phi)\right], \tag{3.2.1}$$

and by taking variations $\delta\phi$ of $S[\phi]$, we find the equations of motion,

$$\frac{\delta S_E}{\delta\phi} = -\frac{\mathrm{d}}{\mathrm{d}\rho}\left(\rho^3 \frac{\mathrm{d}\phi}{\mathrm{d}\rho}\right) + \rho^3 \frac{\mathrm{d}U}{\mathrm{d}\phi} = 0, \tag{3.2.2}$$

$$\frac{\mathrm{d}^2\phi}{\mathrm{d}\rho^2} + \frac{3}{\rho}\frac{\mathrm{d}\phi}{\mathrm{d}\rho} = \frac{\mathrm{d}U}{\mathrm{d}\phi}, \tag{3.2.3}$$

which is a non-linear second order ordinary differential equation with boundary conditions $\dot{\phi}(0) = 0$ and $\dot{\phi}(+\infty) = 0$.

This is excellent because we have transformed a problem of multi-dimensional tunnelling into a problem of solving this equation with the boundary conditions (3.1.6). The problem is that we cannot exactly solve this equation analytically. We can perform numerical approximations, which are the subject of the next section, however, let us analyse the equation of motion a bit further and see where it takes us.

From a slightly different perspective, (3.2.2), seems to be nothing but Newton's Second

Law. If we make the replacements $\phi \to x$ and $\rho \to t$, we have,

$$\frac{\mathrm{d}^2 x}{\mathrm{d}t^2} + \gamma(t)\frac{\mathrm{d}x}{\mathrm{d}t} = -\frac{\mathrm{d}(-U)}{\mathrm{d}x}. \tag{3.2.4}$$

This clearly describes the dynamics of a particle in a potential $-U$ with a curious time-dependent drag term, $\gamma(t) = \frac{3}{t}$, diminishing over time. Using this mechanical analogy, we can see what happens to the energy E, of this system. For a particle in a potential $-U(x)$, the total energy is $E = \frac{1}{2}\left(\frac{\mathrm{d}x}{\mathrm{d}t}\right)^2 - U(x)$, then from (3.2.2), we see that

$$\frac{\mathrm{d}E}{\mathrm{d}t} = -\gamma(t)\frac{\mathrm{d}x}{\mathrm{d}t} \tag{3.2.5}$$

As the drag term decreases monotonically over time, it facilitates in the removal of the energy of the particle as expected. This motivates the existence of a solution which starts close to ϕ_{tv} at $\rho = 0$ but does not reach ϕ_{fv} at $\rho = \infty$. Instead, the particle oscillates to the minimum of the inverted potential and settles down to rest, we call this solution an *undershoot*. There exist a set of initial conditions $\phi(0)$ for which this is the case. As we move $\phi(0)$ closer to ϕ_{tv}, then $\max_\rho(\phi)$ will approach ϕ_{fv}. However, if we move too close to ϕ_{tv}, then the particle will overshoot. To demonstrate this requires some work. If we expand the potential about ϕ_{tv}, as $U'(\phi) = U'(\phi_{\mathrm{tv}}) + U''(\phi_{\mathrm{tv}})(\phi - \phi_{\mathrm{tv}}) + \mathcal{O}\left((\phi - \phi_{\mathrm{tv}})^2\right)$, therefore, the differential equation simplifies to

$$\left(\frac{\mathrm{d}^2}{\mathrm{d}\rho^2} + \frac{3}{\rho}\frac{\mathrm{d}}{\mathrm{d}\rho} - \mu^2\right)(\phi - \phi_{\mathrm{tv}}) \;=\; 0 \tag{3.2.6}$$

where $U''(\phi_{\mathrm{tv}}) = \mu^2$. When the initial condition of the particle is sufficiently close to ϕ_{tv}, then the particle will remain stationary for very large ρ. For this, the drag term is vanishes, therefore,

$$\left(\frac{\mathrm{d}^2}{\mathrm{d}\rho^2} - \mu^2\right)(\phi - \phi_{\mathrm{tv}}) = 0 \tag{3.2.7}$$

which can be approximated to be $\phi(\rho) \simeq |\phi_{\mathrm{tv}}|\,(e^{\mu\rho} - 1)$. This solution is not bounded by a maximum value and thus it overshoots the value $\phi = \phi_{\mathrm{fv}}$.

By continuity, we conclude that there exists a solution which obeys exactly the boundary conditions of the problem called the *bounce*, which appears in Figure 3.1.1.

3.3 Thin-Wall Approximation

We will proceed to find an analytical closed-form solution to both the *bounce* (instanton) and the Euclidean action $B = S_E[\phi_c] - S_E[\phi_{\text{fv}}]$. Consider again the one-dimensional equation of motion

$$\frac{\mathrm{d}^2\phi}{\mathrm{d}\rho^2} + \frac{3}{\rho}\frac{\mathrm{d}\phi}{\mathrm{d}\rho} = \frac{\mathrm{d}U}{\mathrm{d}\phi}, \tag{3.3.1}$$

We can denote the symmetric double-well potential with minima at $\pm a$ as $U_+(\phi) = \frac{\lambda}{8}\left(\phi^2 - a^2\right)^2$. Here, $\phi_{\text{fv}} = +a$ and $\phi_{\text{tv}} = -a$. We can break the $\mathbb{Z}_2-$symmetry of the vacua by introducing a term linear in ε,

$$U(\phi) = U_+(\phi) + \frac{\varepsilon}{2a}(\phi - a). \tag{3.3.2}$$

As we shall recall, the initial condition of ϕ is that the particle must remain at the ϕ_{tv} for very large $\rho = R$, in this regime, the drag term in negligible. If the drag term is not contributing, we require that ε be very small. This is the thin-wall approximation introduced in [4]. As a result of this approximation, we have simplified the equation to,

$$\frac{\mathrm{d}^2\phi}{\mathrm{d}\rho^2} = \frac{\mathrm{d}U_+}{\mathrm{d}\phi}$$

The beauty of this equation is that the solution is nothing but the *instanton* (2.3.17) described in the section 2.3.2 Double-Well Potential,

$$\rho = R + \pm\int_0^{\phi_1} \frac{\mathrm{d}\phi}{\sqrt{2U_+(\phi)}}, \tag{3.3.3}$$

which is an instanton centred about R. By taking the negative branch of the square-root, this is solved to be $\phi(\rho) = a\tanh(\frac{1}{2}\mu\rho)$, where $\mu = a\sqrt{\lambda}$. Excellent, we have found a solution which obeys the boundary conditions. We would now like to calculate some quantities associated to this ϕ, such as $S_E = B$ and the centre of this instanton

R. We can split our solution into three segments,

$$\phi(\rho) = \begin{cases} -a & \rho \ll R \\ a\tanh\left(\frac{1}{2}\mu(\rho - R)\right) & \rho \approx R \\ a & \rho \gg R. \end{cases}$$

This can be thought of as the true vacuum inside a very thin-walled bubble of radius approximately R surrounded by a sea of false vacuum.

The action integral is simply split up into the three cases

$$\begin{aligned} S_E &= 2\pi^2 \int \mathrm{d}\rho\ \rho^3 \left[\frac{1}{2}\left(\frac{\mathrm{d}\phi}{\mathrm{d}\rho}\right)^2 + U_+(\phi)\right] && (3.3.4) \\ &= S_E^{\text{interior}} + S_E^{\text{wall}} + S_E^{\text{exterior}} && (3.3.5) \end{aligned}$$

Now the S_E^{exterior} contribution vanishes, because $U(+a) = 0$ as well as $\dot{\phi} = 0$, therefore,

$$\begin{aligned} S_E &= 2\pi^2 \int_0^R \mathrm{d}\rho\ \rho^3(-\varepsilon) + 2\pi^2 \int \mathrm{d}\rho\ R^3 \left[\frac{1}{2}\dot{\phi}^2 + U_+(\phi)\right], \\ &= 2\pi^2 \left\{-\frac{1}{4}R^4\varepsilon + R^3 S_1\right\}, && (3.3.6) \end{aligned}$$

where we define the *surface tension of the bubble*, S_1, to be,

$$S_1 = \left|\int_{-a}^{a} \mathrm{d}\phi [2U_+(\phi)]^{1/2}\right| = \frac{2\mu^3}{3\lambda}. \quad (3.3.7)$$

In order to calculate the radius of this bubble, we can find the minimum of S_E,

$$\frac{dS_E}{\mathrm{d}R} = 2\pi^2\left[-R^3\varepsilon + 3R^2 S_1\right] = 0. \quad (3.3.8)$$

Solving for R, gives,

$$R = \frac{3S_1}{\varepsilon}, \quad (3.3.9)$$

and substituting this back into (3.3.4), one finds a closed form solution for B,

$$B = \frac{27\pi^2 S_1^4}{2\varepsilon^3}. \quad (3.3.10)$$

Therefore, Γ/V is given by,

$$\frac{\Gamma}{V} = K \ \exp\left(-\frac{27\pi^2 S_1^4}{2\varepsilon^3\hbar}\right)[1+\mathcal{O}(\hbar)]. \tag{3.3.11}$$

Here, K contains the functional determinant which we still need to take care of.

3.4 Analytic Continuation to Minkowski

Analytic continuation into Minkowski space-time leads to interesting repercussions. Once the particle tunnels through the potential, it then propagates classically in Minkowski space-time as the momentum becomes real again. The shift can be performed by rotating time in the equation of motion. The classical field jumps (at $t=0$) to a state defined by,

$$\begin{aligned} \phi(t=0,\mathbf{x}) &= \phi(\tau=0,\mathbf{x}), \\ \frac{\partial}{\partial t}\phi(t=0,\mathbf{x}) &= 0, \end{aligned}$$

afterwards, the field evolves according to,

$$-\frac{\partial^2\phi}{\partial t^2} + \nabla^2\phi = U'(\phi). \tag{3.4.1}$$

As the Minkowski field equation (3.4.1) is an analytical continuation of that of Euclidean field, the solution of (3.4.1) is just the analytical continuation for the bounce,

$$\phi(t,\mathbf{x}) = \phi\left(\rho = (|\mathbf{x}|^2 - t^2)^{\frac{1}{2}}\right) = a\tanh\left[\frac{1}{2}\mu\left(\sqrt{-x^\mu x_\mu} - R\right)\right]. \tag{3.4.2}$$

We can draw some interesting conclusions from this:

- The $O(4)$-invariant bounce becomes an $O(3,1)$-invariant bubble meaning it is Lorentz-invariant. This implies the growth of the bubble after materialization looks the same to every Lorentz observer.
- In the case of small ε, there is a thin-wall localized at $\rho = R$, separating the false and true vacua. As the bubble expands, this wall traces out a hyperboloid,

$$|\mathbf{x}|^2 - t^2 = R^2. \tag{3.4.3}$$

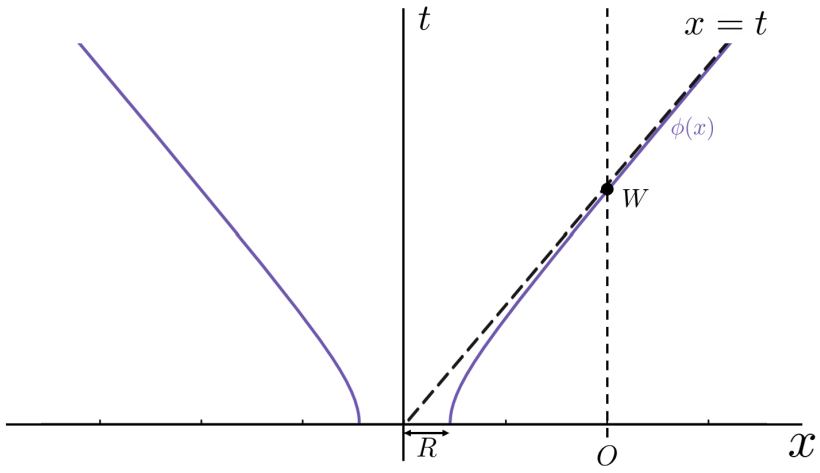

Figure 3.4.1: The space-time diagram of the classical growth of the bubble of true vacuum after materialization. We see that R is the radius of the bubble in Minkowski spacetime. The hyperbola is the path traced out by the bubble wall. The observer, O, only receives warning of the bubble after they cross the light-cone, W.

A section of the bubble wall carries rest energy per unit area, S_1, so the wall expanding with velocity, v, carries energy, $S_1(1-v^2)$ per area. Thus, if the radius of the expanding bubble is, $|\mathbf{x}|$, the surface energy of the bubble, E_{wall} is simply,

$$E_{\text{wall}} = 4\pi|\mathbf{x}|^2 S_1(1-v^2)^{\frac{1}{2}}. \tag{3.4.4}$$

As $v = \frac{\mathrm{d}|\mathbf{x}|}{\mathrm{d}t} = \frac{(|\mathbf{x}|^2-R^2)^{\frac{1}{2}}}{|\mathbf{x}|}$ so,

$$E_{\text{wall}} = 4\pi|\mathbf{x}|^2 S_1\left(1-\frac{|\mathbf{x}|^2-R^2}{|\mathbf{x}|^2}\right)^{-\frac{1}{2}} = 4\pi|\mathbf{x}|^3\frac{S_1}{R}, \tag{3.4.5}$$

but from (3.3.9) we may simplify this into,

$$E_{\text{wall}} = \frac{4}{3}\pi\varepsilon|\mathbf{x}|^3 = E_{\text{vol}}. \tag{3.4.6}$$

Under the thin-wall approximation, all the energy released by converting the false vacuum to true vacuum goes to accelerate the expansion of the bubble only. This is possibly the most efficient way to destroy the Universe.

3.5 Functional Determinant for Field Theory

The evaluation of K is essentially the same as the case of quantum mechanics but with few technical difficulties.

Vanishing Eigenvalues

As we have four dimensions, we have four possible directions to infinitesimally translate and therefore, we have four possible eigenfunctions with zero eigenvalues proportional to $\partial_\mu \phi$. We can determine their normalisations by considering their orthogonality,

$$\begin{aligned} \int \mathrm{d}^4x (\partial_\mu \phi_c)(\partial_\nu \phi_c) &= \frac{1}{4}\delta_{\mu\nu} \int \mathrm{d}^4x (\partial_\sigma \phi_c)^2, \\ &= \delta_{\mu\nu} S_0, \end{aligned} \tag{3.5.1}$$

where S_0 is defined as in (3.1.13). Thus for the case of zero eigenvalues, the only difference is that instead of one factor of $(S_0/2\pi)^{1/2}$, we have four such factors. Thus K will become,

$$K = \frac{S_0^2}{4\pi^2} \left| \frac{\widetilde{\det}\left[-\partial_\mu\partial_\mu + U''(\phi_c)\right]}{\det\left[-\partial_\mu\partial_\mu + U''(\phi_{\mathrm{fv}})\right]} \right|^{-\frac{1}{2}}, \tag{3.5.2}$$

where $\widetilde{\det}$ is the functional determinant ignoring the zero eigenvalues.

Renormalisation

Our dynamics are in terms of non-renormalised quantities. It is an interesting exercise to discuss the renormalised form of Γ/V. For instance, the action of the particle, can be defined as the renormalised action S_R plus the standard renormalisation counterterms from the n-loop diagrams [7; 8],

$$S = S_R + \sum_{n=1}^{\infty} \hbar^n S^{(n)} \simeq S_R + S^{(1)}, \tag{3.5.3}$$

where the last equality is first achieved under the semiclassical limit (small $\hbar$), and then $\hbar$ set to unity. The renormalisation counterterms remove ultraviolet divergences from the one-particle irreducible diagrams generated by the effective action,

$$\exp(\gamma[\phi]) = \exp(S_R[\phi] + S^{(1)}[\phi]) \sqrt{\det\left(-\partial_\mu\partial_\mu + U''(\phi)\right)}.$$

But we want to remove the golden nugget that is S_R from the divergences $S^{(n)}$. We shall move forward by introducing the following definitions for renormalised quantities:

- ϕ - renormalised field,
- $U(\phi)$ - potential appearing in S_R,
- $\bar{\phi}$ - bounce computed from S_R,
- $S_0 = S_R[\bar{\phi}]$.

Now, let's compute Γ/V, term by term by treating S_R as the total action. Then taking into account the renormalisation counter-terms perturbatively. The counter-terms might ruin the convention $S[\phi_{\text{fv}}] = 0$, thus we subtract this off the bounce action S_0,

$$S_0 \to S_0 - S[\phi_{\text{fv}}]. \tag{3.5.4}$$

Furthermore, adding terms to S_R will change the stationary points of S, thus changing the bounce. If we determine the difference by perturbing the bounce by $\delta\bar{\phi}$,

$$S[\bar{\phi}] \to S_0 + \int \mathrm{d}^4x \frac{\delta S_R}{\delta\bar{\phi}}\delta\bar{\phi} + S^{(1)}[\bar{\phi}] + ... \tag{3.5.5}$$

However, $\bar{\phi}$ is a stationary point of S_R, thus $\delta S_R/\delta\bar{\phi} = 0$ so we have,

$$S[\bar{\phi}] \to S_0 + S^{(1)}[\bar{\phi}]. \tag{3.5.6}$$

Similarly,

$$S[\phi_{\text{fv}}] = S_0[\phi_{\text{fv}}] + S^{(1)}[\phi_{\text{fv}}] = S^{(1)}[\phi_{\text{fv}}]. \tag{3.5.7}$$

Thus, we conclude that $S_R = S[\bar{\phi}] - S[\phi_{\text{fv}}] = S_0 + S^{(1)}[\bar{\phi}] - S[\phi_{\text{fv}}]$, leading to a renormalised expression for Γ/V,

$$\frac{\Gamma}{V} = \frac{S_0^2}{4\pi^2}\exp\left(-S_0 - S^{(1)}[\bar{\phi}] + S^{(1)}[\phi_{\text{fv}}]\right)\left|\frac{\widetilde{\det}\left[-\partial_\mu\partial_\mu + U''(\bar{\phi})\right]}{\det\left[-\partial_\mu\partial_\mu + U''(\phi_{\text{fv}})\right]}\right|^{-\frac{1}{2}}. \tag{3.5.8}$$

The purpose of this demonstration is certainly not to show the computational ease or beauty of the obtained equation. It is simply to demonstrate that we can achieve the fully renormalised version of Γ/V using the standard techniques. Though for the remainder of our discussion, we will forgo the problem of renormalisation.

Chapter 4

Numerical Results in Minkowski Spacetime

In this section, we will describe the numerical solution to the classical equation of motion. We are searching for an $O(4)$-symmetric solution to the classical equation of motion as they are the solutions which minimise the Euclidean action. Other solutions do exist, however, they are usually of higher Euclidean action and so are less likely to contribute to the decay rate, Γ.

4.1 Setting up the Numerical Problem

A natural starting point, is the action of the scalar field in the metastable potential. As we are interested in an $O(4)$-symmetric solution, we define $\phi = \phi(\rho)$. We again define this by including the $\mathbb{S}^3$ measure

$$S_E[\phi] = 2\pi^2 \int \mathrm{d}\rho \rho^3 \left(\frac{1}{2} \left(\frac{\mathrm{d}\phi}{\mathrm{d}\rho} \right)^2 + \frac{\lambda}{8} \left(\phi^2 - a^2 \right)^2 + \frac{\varepsilon}{2a} (\phi - a) \right). \tag{4.1.1}$$

There are several parameters in (4.1.1) (a, ε, λ). We could set them all to unity, however, this will only solve a particular case of our problem. Instead, we re-define the variables in terms of new units. If we make the following re-definitions

$$\phi \to ax, \quad \varepsilon \to 2\lambda a^4 E, \quad \rho \to \frac{t}{a\sqrt{\lambda}} \tag{4.1.2}$$

where x and t are variables and E is a parameter which encapsulates the energy density difference between the false and true vacua. Equivalently, the action is written

$$B = \frac{2\pi^2}{\lambda}\int_0^\infty \mathrm{d}t\; t^3\left[\frac{1}{2}\left(\frac{\mathrm{d}x}{\mathrm{d}t}\right)^2 + \frac{1}{8}\left(x^2-1\right)^2 + E(x-1)\right] = \frac{\widetilde{B}}{\lambda}. \tag{4.1.3}$$

The first differential equation to introduce is the derivative of (4.1.3) with respect to t

$$\frac{\mathrm{d}\widetilde{B}}{\mathrm{d}t} = 2\pi^2 t^3\left[\frac{1}{2}\left(\frac{\mathrm{d}x}{\mathrm{d}t}\right)^2 + \frac{1}{8}\left(x^2-1\right)^2 + E(x-1)\right] \tag{4.1.4}$$

The solution of this differential equation will give us an exact form of the B coefficient. Using the Euler-Lagrange equation, we can derive the equation of motion we need to solve

$$\frac{\mathrm{d}^2x}{\mathrm{d}t^2} + \frac{3}{t}\frac{\mathrm{d}x}{\mathrm{d}t} = \frac{1}{2}x(x^2-1) + E \tag{4.1.5}$$

The strength of redefining the parameters in (4.1.2) is that the different solutions correspond to different values of E only. We can obtain solutions for different values of the other parameters by implementing the re-definitions above. In order to solve (4.1.5) using a Runge-Kutta method we begin by defining a system of first order ODEs,

$$v = \frac{\mathrm{d}x}{\mathrm{d}t}, \tag{4.1.6}$$

then (4.1.5) becomes,

$$\frac{\mathrm{d}v}{\mathrm{d}t} = -\frac{3}{t}v + \frac{1}{2}x(x^2-1) + E. \tag{4.1.7}$$

This is a boundary value problem (BVP) and no BVP is complete without boundary conditions. However, we lack knowledge of the $x(0)$ initial condition which results in the bounce. Although we know that $v(0) = 0$. Therefore, we employ a shooting method. Shooting methods turn BVPs into initial value problems (IVP). We know that we require the bounce to have vanishing gradient, v, at infinity. We define *overshoots* have $v(\infty) > 0$ and *undershoots* have $v(\infty) < 0$, thus by continuity, we can conclude that there must be a solution which has a vanishing $v(\infty)$ at the boundary of these classes of curves.

Suppose that we manage to find an undershoot x_1 and an overshoot x_2. We would like to know what the behaviour of the mid-point of these initial conditions, thus we define

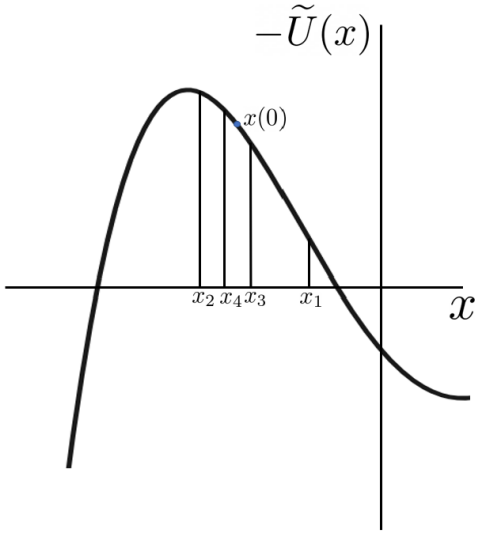

Figure 4.1.1: The interval bisection scheme. x_1 and x_3 are undershoots and x_2 and x_4 are overshoots.

$x_3 = \frac{1}{2}(x_1 + x_2)$. If x_3 results in an undershoot, then we know the between x_1 and x_3, we only have undershoots and not the bounce that we are looking for. Therefore, we will continue to find the mid-point between x_2 and x_3 as in this region, we will certainly have our bounce. If now the mid-point $x_4 = \frac{1}{2}(x_2 + x_3)$ is an overshoot, then we know that the region between x_2 and x_4 contains only overshoots, and so this region does not contain the bounce. Then we know that the bounce is in the region between x_4 and x_3. This interval bisection scheme will quickly converge onto the bounce initial condition $x(0)$ as in Figure 4.1.1. This method is also known as the *wag-the-dog method* in [13].

Furthermore, we clearly see that the $t = 0$ is a regular singular point of (4.1.7), so instead, we begin integration at ρ of $\mathcal{O}(10^{-15})$.

Additionally, we need to make a correction to the potential. For different values of E, we want the potential to vanish at their respective x_{fv} values. We can use the Newton-Raphson method [31] to locate the minimum of the potential around $x = 1$. Once we find the value of x_{fv}, we can correct the potential by subtracting off the contributions to the false vacuum, so that we have,

$$\widetilde{U}_{\text{corrected}}(x) = \frac{1}{8}(x^2 - 1)^2 + E(x - 1) - \widetilde{U}(x_{\text{fv}}) \tag{4.1.8}$$

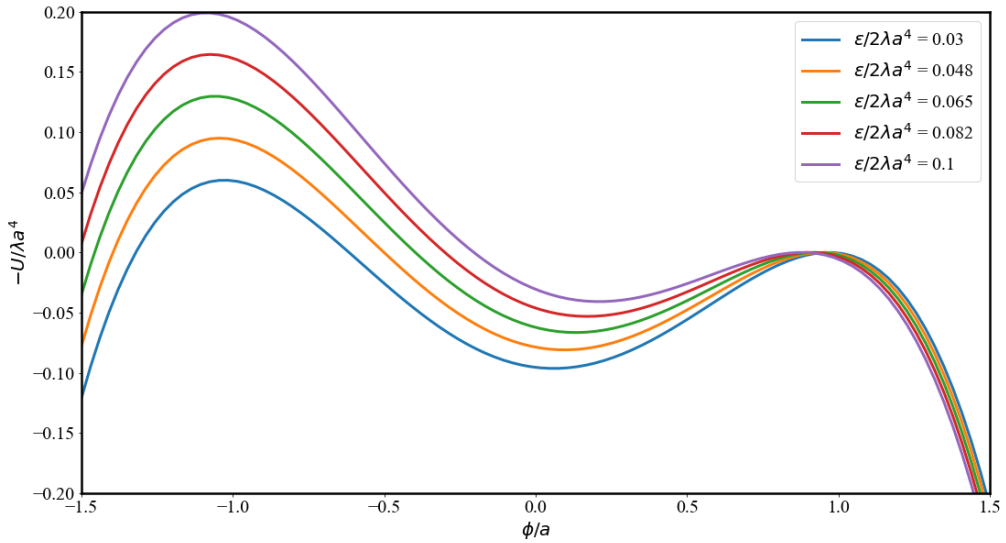

Figure 4.1.2: The corrected potential for various $E = [0.03 - 0.10]$. In the thin-wall approximation, we would like to keep E very small.

We can see that this correction indeed results in several potentials with varying E such that $\widetilde{U}(x_{\text{fv}}) = 0$ in Figure 4.1.2. The purpose of this correction is that in the calculation of B, we require the bounce to have vanishing potential and kinetic energies outside the bubble. Additionally, it helps with keeping B finite.

4.2 Verifying the Thin-Wall Approximation

The interpretation of the instanton solution in Euclidean space-time is that of a bubble of true-vacuum (ϕ_{tv}) in a sea of false vacuum (ϕ_{fv}) separated by a thin-wall. As the wall is *thin*, the bubble radius, $\widetilde{R}$, can therefore be approximated as the solution of $x(t = \widetilde{R}) = 0$. From Figure 4.2.1, we know that the $x(t)$ is a monotonically increasing function which is initially negative and becomes positive, implying that $x(t)$ crosses the t-axis only once. The radius of the bubble, $\widetilde{R}$, is somewhat arbitrary but it is approximated as the point of intersection of the instanton with the $x(t) = 0$ line. Arguably the more important quantity is B, which is calculated by integrating (4.1.4) by numerical integration over t. The trapezium rule was used to integrate this function which has errors associated with it. The results of $\widetilde{R}$ and $\widetilde{B}$ can be seen in Figure 4.2.2 as compared with the thin-wall approximation. Recalling that in the Thin-Wall

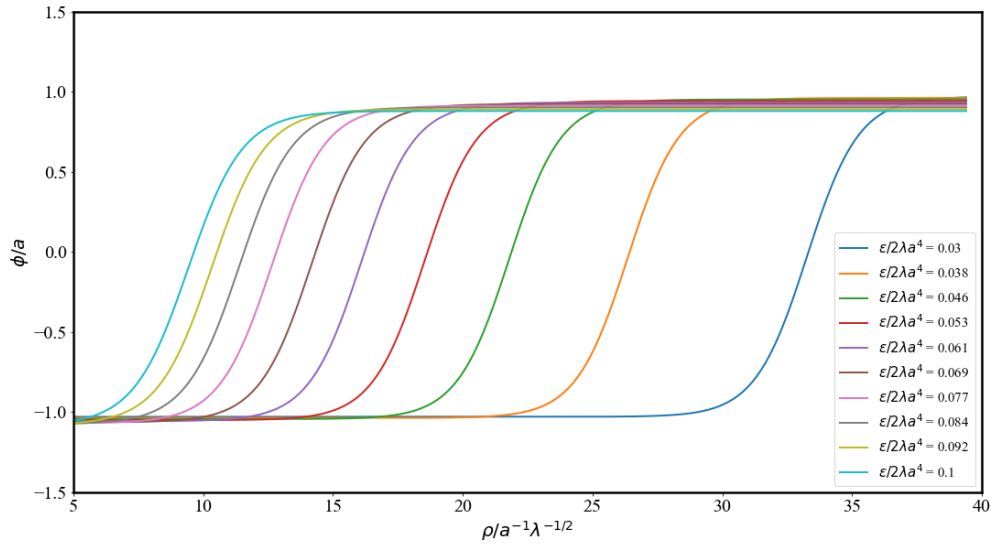

Figure 4.2.1: Several bounces plotted of different values of ε.

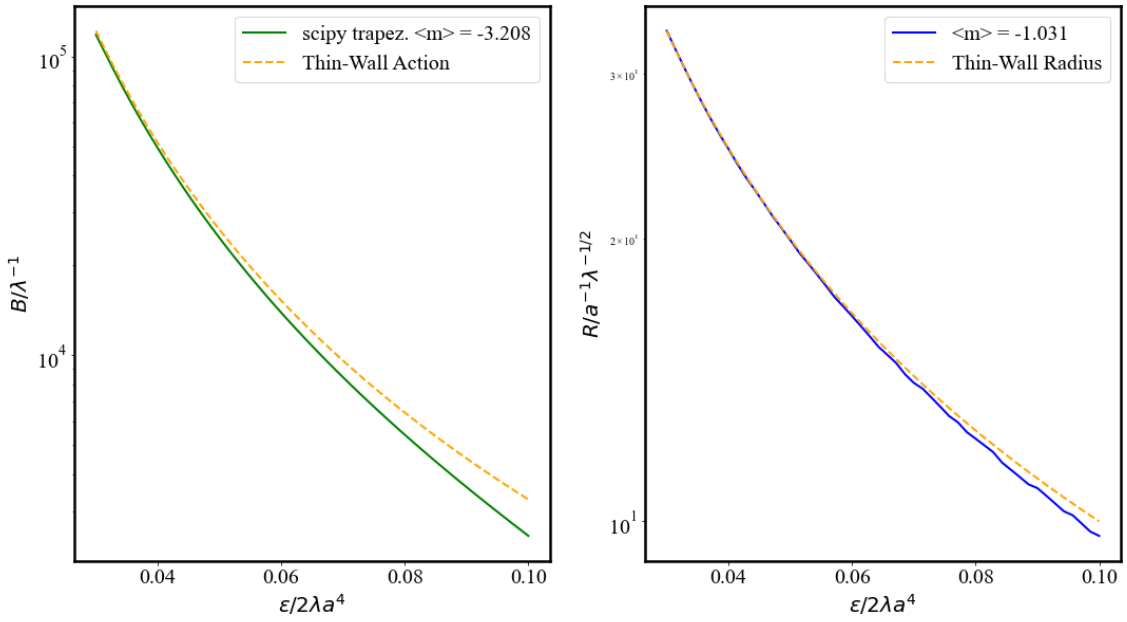

Figure 4.2.2: Plots for the action B and the radius R of the bubble on a logarithmic $y-$axis obtained from cumulative trapezium rule integration. For larger values of $E = \varepsilon/2\lambda a^4$, we see that the thin-wall results diverge from the numerical calculation.

Approximation, the dependence of R and B on ε are

$$R = \frac{3S_1}{\varepsilon}, \qquad B = \frac{27\pi^2 S_1^4}{2\varepsilon^3} \tag{4.2.1}$$

By substitution of S_1 into these expressions and removing dimensions, we find that they simplify into the following form,

$$\widetilde{R} = \frac{1}{E}, \qquad \widetilde{B} = \frac{\pi^2}{3E^3} \tag{4.2.2}$$

Taking the logarithm on either side of the equations, we have,

$$\ln(\widetilde{R}) = -\ln(E) + k_1, \qquad \ln(\widetilde{B}) = -3\ln(E) + k_2, \tag{4.2.3}$$

where $k_1 = 0$ and $k_2 = \ln(\pi^2/3)$. The average slopes of the data shown in Figure 4.2.2 were found to be $\langle \frac{\Delta B}{\Delta \varepsilon} \rangle = -3.208$ and $\langle \frac{\Delta R}{\Delta \varepsilon} \rangle = -1.031$. This is in agreement with [4] within a small region of values of E as required by the thin-wall approximation. This shows that at least within this small range, that the thin-wall approximation is quite valid. Although at large enough values of E, the calculation is bound to diverge from the thin-wall results.

In these dimensions, it is also possible to estimate the intersection points k_1 and k_2. For example, under the thin-wall approximation, the numerical calculation of k_1 was found to be $k_1^{\text{num}} = -0.097455$. Likewise, the numerical value of k_2 was found to be $k_2^{\text{num}} = 0.485521$. Though we find considerable deviations for the numerical calculations than we have here. Although our numerical calculation shows that there is considerable agreement for small values of E, we see that the thin-wall approximation breaks down for values $\varepsilon = 0.1\lambda a^4$ ($E = 0.05$, the factor of 2 comes from introducing the dimensions again).

Although, we have not developed a method for solving this problem in a very thin-wall regime, it could be the case that for $\varepsilon < 0.01\lambda a^4$ that there is further divergence and the thin-wall approximation is only valid in a small region of the values of ε. This breakdown limit is the reason for the discrepancy between the numerical and predicted values of k_1 and k_2. Consider the (4.2.3), $E = e^{k_1} = e$ is the value for which $\ln(\widetilde{R})$ vanishes, corresponding to $\varepsilon = 5.44\lambda a^4$. The numerical prediction for this E is

$E^{\text{num}} = e^{-0.097455} = 0.91$, which corresponds to $\varepsilon = 1.82\lambda a^4 \gg 0.1\lambda a^4$. This is beyond the range at which the approximation breaks down, thus the deviation in k_1 is expected. Furthermore, we have $E = e^{3k_2} = (\pi^2/3)^3$, for which $\ln(\widetilde{B})$ vanishes, which correspond to $\varepsilon = 35.62\lambda a^4$. The numerical prediction of this limit is $\varepsilon = 8.58\lambda a^4 \gg 0.1\lambda a^4$. This is again beyond the thin-wall-limit, therefore, deviations are expected between the thin-wall limit and our numerical results.

4.3 Limitations of the Solution

In this section we will summarise the limitation of our numerical calculations. There are two main limitations that we can identify with this solution which can be fixed. The first is the choice of the potential. For the calculation to work, we require that the potential has two stable minima separated by a barrier. However, we can see in Figure 4.3.1 that as E is increased, the second derivative $\widetilde{U}''(\phi_{\text{fv}}/a)$ decreases. Eventually, we reach a point $E = 0.193$ where the second derivative vanishes after which the false vacuum is ill-defined. At this point, tunnelling ceases.

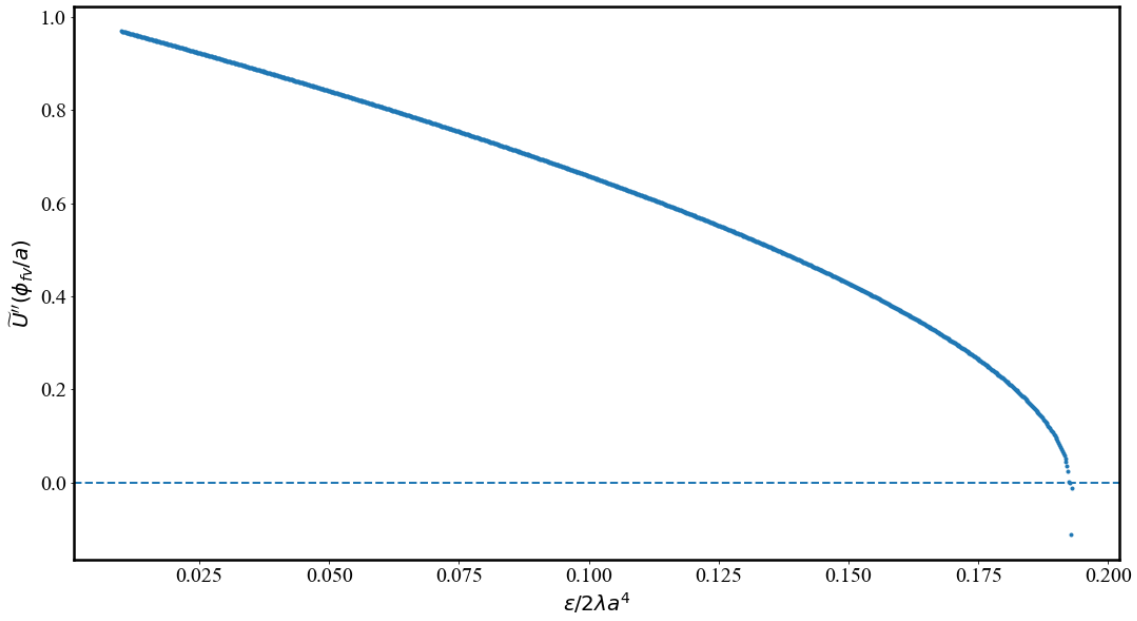

Figure 4.3.1: Plot of the value of the second derivative $\widetilde{U}''$ evaluated at the false vacuum ϕ_{fv}/a as a function of $\varepsilon/2\lambda a^4$.

We can see in Figure 4.3.2 that for the case of $E = 0.193$ that the false vacuum ceases

is no longer a minimum point of the potential.

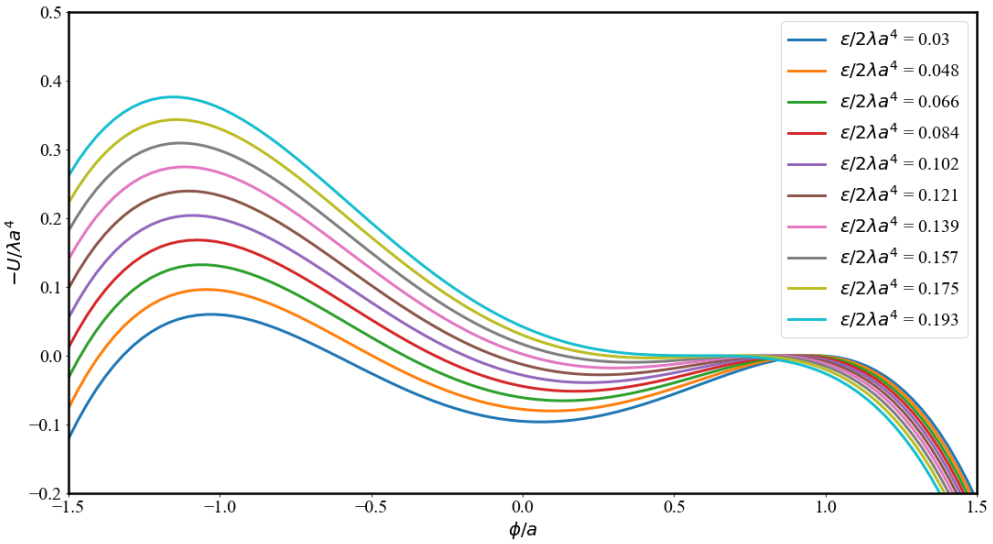

Figure 4.3.2: Plot of the potential as a function x. Of interest is the curve for which $E = 0.193$ where the domain surrounding the false vacuum $x \simeq 1$ is no longer a well but becomes a point of inflection.

Within the problem, we have stored all numerical values of the initial condition $\phi(0)/a$ as float64 objects in Spyder IDE. As we increase the value of E, the difference between the initial condition required for the bounce $\phi(0)$ and ϕ_{fv} is of order $\mathcal{O}(10^{-5})$. We can see this in Figure 4.3.3.

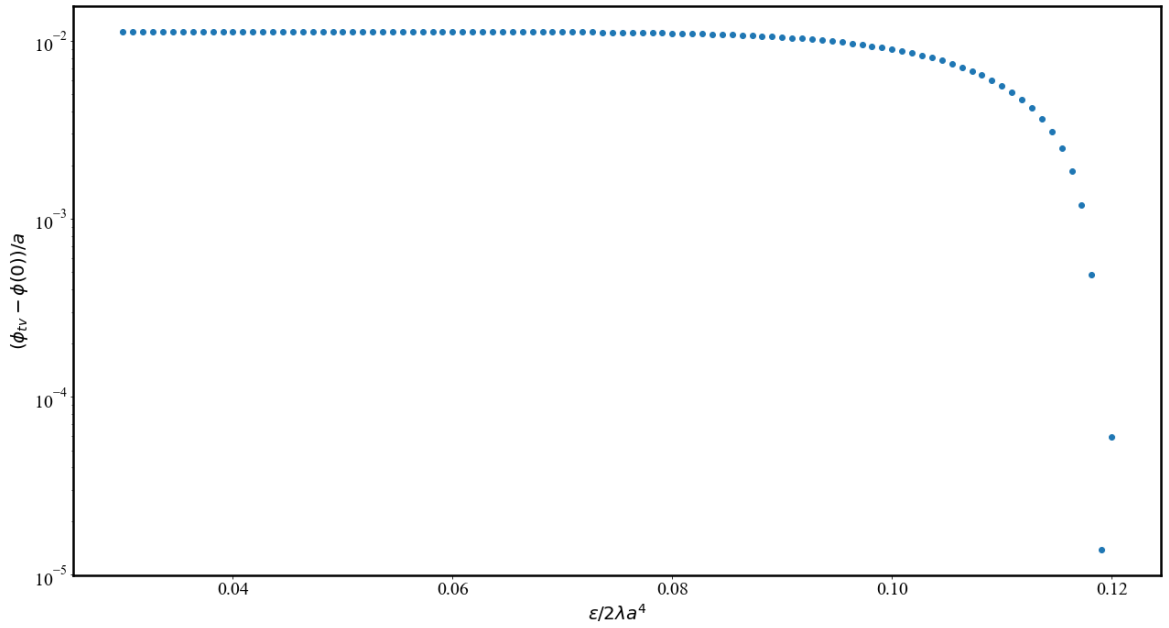

Figure 4.3.3: Plot of $(\phi_{\text{tv}} - \phi(0))/a$ against E. As E is increased, the difference between $\phi(0)/a$ and ϕ_{tv}/a decreases.

This poses another issue for us as the maximum precision for *double-precision floating-point* objects (float64 in Spyder) is of $\mathcal{O}(10^{-18})$ [20]. Thus, there is a point at which the difference is less than this maximum float precision and thus our numerical methods can no longer delineate between $\phi(0)/a$ or ϕ_{tv}/a. This is not a limitation by the physics of the problem. A possible solution is to store the numerical values of $\phi(0)/a$ in *quadruple-precision floating-point format* [18] which are float128. This format minimises round-off and overflow errors which in turn would increase the precision of the initial condition of our problem and further calculations that depend on its precision such as the calculation of B and R.

The combination of these two factors limits the precision to which we can calculate the initial condition and to obtain the bounce for larger values of E.

Chapter 5

Instantons in de Sitter Space

5.1 Welcome to de Sitter Space

de Sitter spaces (dS_D) are examples of a maximally symmetric spaces with constant positive curvature. They are also solutions to the vacuum EFEs (1.2.10). We would like to describe tunnelling phenomena on a curved manifold. We consider de Sitter space, our ultimate goal in this report is to describe the transition between universes with constant and positive energy densities facilitated by scalar field tunnelling. de Sitter spaces fit this bill, and thus we consider the case of scalar tunnelling in a fixed de Sitter background.

In General Relativity (GR), we define curved manifolds intrinsically, not extrinsically. Suppose that the Earth is our potentially curved manifold. We have Alice on the Earth. Bob in a rocket orbiting far away from the Earth, enough that he can see the entire Earth.

From Bob's perspective, the Earth is curved and very similar to a 2-sphere. Bob's perspective describes the idea of *extrinsic curvature*. What does Alice have to say about this? Unfortunately, Alice is on the Earth and she cannot immediately tell whether she is on a curved space or not (as an m-sphere is locally $\mathbb{R}^m$). However, Alice remembers from her Differential Geometry notes that she can determine if she's on a curved space by parallel transporting a vector along different paths between the same two points. We use the Christoffel connection definition of parallel transport. In Figure 5.1.1 we see that she can take the vector along a path $\overline{ABC}$. If she then takes

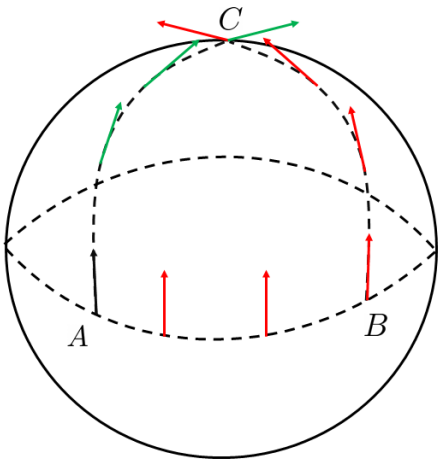

Figure 5.1.1: A diagram demonstrating the parallel transport of a vector at A to C by two different paths. The vector transported along the path $\overline{ABC}$ points in a different direction than the transport along the path $\overline{AC}$. This is due to definition of the Christoffel connection.

the vector along the path $\overline{AC}$ and compares to her previous result, she will find that the transported vectors will not be of the same orientation. Thus concluding that the space she lives on is not flat. This notion of curvature is *intrinsic*.

Unfortunately, in the case of a manifold in GR, we have the great misfortune of always having to be Alice. Thus our notion of curvature is defined by how the manifold induces a change in orientation over tensors. Effectively, the curvature of space-time is always intrinsic. Having said that, there is a very nice extrinsic visualisation of what exactly dS_D is.

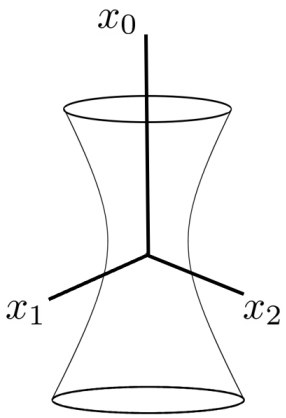

Figure 5.1.2: A three-dimensional one-branch hyperboloid is the same as dS_2

D-dimensional de Sitter space-time can be viewed as time-like *one-branch* (connected) hyperbola in $D+1$ Minkowski space-time [16]. The metric in the embedding space $\mathbb{R}^{1,D}$ is,

$$-\,\mathrm{d}s^2_{\text{embedded}} = -\,\mathrm{d}X_0^2 + \mathrm{d}X_1^2 + ... + \mathrm{d}X_D^2, \tag{5.1.1}$$

where the equation for the hyperboloid is given by,

$$-X_\mu X^\mu = \alpha^2. \tag{5.1.2}$$

We can cover this hyperboloid with a global coordinate chart. For example, in $D=4$, we have,

$$\begin{aligned} X_0 &= \alpha \sinh(t/\alpha), \\ X_1 &= \alpha \cos(t/\alpha)\cos\psi, \\ X_2 &= \alpha \cosh(t/\alpha)\sin\psi\cos\theta, \\ X_3 &= \alpha \cosh(t/\alpha)\sin\psi\sin\theta\cos\varphi, \\ X_4 &= \alpha \cosh(t/\alpha)\sin\psi\sin\theta\sin\varphi. \end{aligned} \tag{5.1.3}$$

ψ, θ, φ define an angular coordinate chart over a 3−sphere. The metric in these coordinates is,

$$-\,\mathrm{d}s^2 = -\,\mathrm{d}t^2 + \alpha\cosh^2(t/\alpha)\,\mathrm{d}\Omega_3^2, \tag{5.1.4}$$

where $\mathrm{d}\Omega_3^2$ is the metric on $\mathbb{S}^3$. Under Wick rotation ($t = -i\xi - \alpha\pi/2$), the Euclidean metric is simply,

$$\mathrm{d}s^2 = \mathrm{d}\xi^2 + \alpha^2\sin^2(\xi/\alpha)\,\mathrm{d}\Omega_3^2, \tag{5.1.5}$$

where $\xi \in (0, \alpha\pi)$. $\xi = 0$ and $\xi = \alpha\pi$ are coordinate singularities of the manifold. The extra $\pi/2$ shift allows us to represent the metric in the standard form of a 4-sphere and also defines the North and South poles as the start and limits of integration. The parameter α will hereby be called the de Sitter radius. Thus, under Wick rotation dS_3 is $\mathbb{S}^4$. The Euclidean Ricci Scalar, R_E, has a closed form,

$$R_E = \frac{12}{\alpha^2} \tag{5.1.6}$$

5.2 Scalar Dynamics in de Sitter Space

Over the de Sitter space, the Euclidean action is given by,

$$S_E[\phi] = 2\pi^2\alpha^3 \int_0^{\alpha\pi} \mathrm{d}\xi \sin^3(\xi/\alpha) \left[\frac{1}{2}\left(\frac{\mathrm{d}\phi}{\mathrm{d}\xi}\right)^2 + U(\phi)\right]. \tag{5.2.1}$$

The Euler-Lagrange equation will give,

$$\frac{\mathrm{d}^2\phi}{\mathrm{d}\xi^2} + \frac{3}{\alpha}\cot\left(\frac{\xi}{\alpha}\right)\frac{\mathrm{d}\phi}{\mathrm{d}\xi} = \frac{\mathrm{d}U}{\mathrm{d}\phi}. \tag{5.2.2}$$

This is not too dissimilar to the equation of motion in the flat case (3.3.1), only the drag term is different. The boundary conditions for the bounce are given by,

$$\dot{\phi}(0) = \dot{\phi}(\alpha\pi) = 0. \tag{5.2.3}$$

For large α we notice by Taylor expansion,

$$\cot(\xi/\alpha) = \frac{1}{\tan(\xi/\alpha)} \to \alpha/\xi. \tag{5.2.4}$$

The equation of motion thus simplifies as,

$$\ddot{\phi} + \frac{3}{\xi}\dot{\phi} = \frac{\mathrm{d}U}{\mathrm{d}\phi} \tag{5.2.5}$$

which is identical to the equation of motion of the scalar field in the flat case (replacing $\xi \to \rho$). We should expect this because as we increase α, we expect the curvature of the space-time (5.1.6) to decrease. Then under the thin-wall approximation, for large ξ, we expect that the results for R and B for flat space to be the leading order contribution. We might expect an α-dependent correction to the radius of the bubble and the action.

Chapter 6

Numerical Problem in Fixed de Sitter Space

6.1 Setting up the Numerical Problem

Firstly, we will define the Euclidean action of the scalar field in curved spacetime with the potential $U(\phi)$. In the $(\xi, \psi, \theta, \varphi)$ coordinates, we would like a solution which is symmetric with respect to the transformations in (ψ, θ, φ) - an $O(4)-$transformation, thus the solution is only dependent on ξ. For a de Sitter spacetime with a radius, α, the Euclidean action is given by,

$$S_E[\phi] = 2\pi^2\alpha^3 \int_0^{\alpha\pi} \mathrm{d}\xi \sin^3(\xi/\alpha) \left[\left(\frac{\mathrm{d}\phi}{\mathrm{d}\xi} \right)^2 + \frac{\lambda}{8}(\phi^2 - a^2)^2 + \frac{\varepsilon}{2a}(\phi - a) \right]. \tag{6.1.1}$$

We have two coordinate singularities at the boundary of our spacetime, so we require say $\xi_0 = 10^{-15}$ and $\xi_{\max} = \alpha(\pi - \xi_0)$, where $\xi_{\max}$ is the endpoint of integration. In the mechanical analogy, see that the coefficient of $\dot{\phi}$ changes sign at $\xi = \pi/2$. This means that the drag term accelerates the particle instead of decelerating it. We can see this as,

$$\frac{\mathrm{d}^2\phi}{\mathrm{d}\xi^2} = -\frac{3}{\alpha} \cot\left(\frac{\xi}{\alpha}\right) \frac{\mathrm{d}\phi}{\mathrm{d}\xi} + \frac{\mathrm{d}U}{\mathrm{d}\phi}. \tag{6.1.2}$$

If the left-hand side is interpreted as acceleration in our mechanical analogy, we can see that the $\dot{\phi}$ term becomes less negative as $\xi \to \alpha\pi/2$. Once ξ crosses this limit, the

sign of this term changes,

$$\frac{\mathrm{d}^2\phi}{\mathrm{d}\xi^2} = +\frac{3}{\alpha}\left|\cot\left(\frac{\xi}{\alpha}\right)\right|\frac{\mathrm{d}\phi}{\mathrm{d}\xi} + \frac{\mathrm{d}U}{\mathrm{d}\phi}, \tag{6.1.3}$$

and the term strictly increases monotonically, leading to the inevitable acceleration of the particle. Thus, we require that as $\xi \to \alpha\pi/2$, $\dot{\phi}$ is vanishing. If this condition is not met, then the resulting solution is pathological and unbounded. Additionally, due to the driving term, at long times the particle does not settle down to the minimum of the inverted barrier. It will instead reach a final position $\phi(\xi_{\max}) \ll \phi_{\mathrm{tv}}$ or $\phi(\xi_{\max}) \gg \phi_{\mathrm{fv}}$, which are both pathological end points.

To simplify parameter dependence of this problem, we shall again, remove the dimensions from the action above, by making the following, transformations

$$\phi \to ax, \qquad \varepsilon \to 2\lambda a^4 E, \qquad \xi \to \frac{t}{a\sqrt{\lambda}}, \qquad \alpha \to \frac{\widetilde{\alpha}}{a\sqrt{\lambda}}. \tag{6.1.4}$$

The ratio $\xi/\alpha = t/\widetilde{\alpha}$, thus this simplifies the argument of the integration measure, $\sin^3(\xi/\alpha)$. With these considerations, we have,

$$S_E[\phi] = \frac{2\pi^2\widetilde{\alpha}^3}{\lambda}\int_0^{\widetilde{\alpha}\pi}\mathrm{d}t\sin^3(t/\widetilde{\alpha})\left[\frac{1}{2}\left(\frac{\mathrm{d}x}{\mathrm{d}t}\right)^2 + \frac{1}{8}(x^2-1)^2 + E(x-1)\right] = \frac{\widetilde{S}}{\lambda}. \tag{6.1.5}$$

Effectively, we have reduced the problem to more familiar terms as in (4.1.3), however, this integral is taken over a compact manifold. Our first differential equation to consider is then,

$$\frac{\mathrm{d}\widetilde{S}}{\mathrm{d}t} = 2\pi^2\widetilde{\alpha}^3\sin^3(t/\widetilde{\alpha})\left[\frac{1}{2}\left(\frac{\mathrm{d}x}{\mathrm{d}t}\right)^2 + \frac{1}{8}(x^2-1)^2 + E(x-1)\right] \tag{6.1.6}$$

In order to solve this, we need the bounce $\bar{x}$, which is obtained by the Euler-Lagrange equation,

$$\frac{\mathrm{d}^2\bar{x}}{\mathrm{d}t^2} + \frac{3}{\widetilde{\alpha}}\cot\left(\frac{t}{\widetilde{\alpha}}\right)\frac{\mathrm{d}\bar{x}}{\mathrm{d}t} = \frac{\mathrm{d}\widetilde{U}}{\mathrm{d}\bar{x}}. \tag{6.1.7}$$

Again, we would like to turn this into a system of two first order ODEs by defining,

$$v = \frac{\mathrm{d}x}{\mathrm{d}t}. \tag{6.1.8}$$

Thus, the other differential equation becomes,

$$\frac{\mathrm{d}v}{\mathrm{d}t} = -\frac{3}{\widetilde{\alpha}} \cot\left(\frac{t}{\widetilde{\alpha}}\right) v + \frac{\mathrm{d}\widetilde{U}}{\mathrm{d}x}, \tag{6.1.9}$$

with boundary conditions,

$$v(0) = v(\widetilde{\alpha}\pi) = 0. \tag{6.1.10}$$

From here on, the analysis and discussion of the undershoot and overshoot method is effectively identical.

Of course, we would like to begin our integration from $t = 0$. However, we have a singularity at $t = 0$, thus we will start at $t_0 \simeq 10^{-15}$. Similarly, $t = \widetilde{\alpha}\pi$ is another singularity of our drag term, thus we terminate the integration at $t_{\mathrm{end}} = \widetilde{\alpha}(\pi - t_0)$. In order to determine $\widetilde{B}$, we will have to integrate (6.1.6). However, we also need to determine $\widetilde{S}$ for a constant false vacuum solution. The actual value of the corrected action is given by,

$$\widetilde{B} = \widetilde{S}[\bar{x}] - \widetilde{S}[x_{\mathrm{fv}}]. \tag{6.1.11}$$

This is a more correct way to calculate $\widetilde{B}$. In the flat case, we defined a corrected potential, however, we were always free to do this, so it was best to exploit this.

6.2 Types of Solutions

6.2.1 Trivial Solutions

$\phi = \phi_{\mathrm{tv}}$ and $\phi = \phi_{\mathrm{fv}}$

The most obvious class of solutions which obey the boundary conditions are the ones that occur on the minima of the potential ϕ_{tv} and ϕ_{fv}. However, these are not very interesting solutions.

Hawking-Moss Instanton

In 1982, Hawking and Moss proposed a transition from the false vacuum to the top of the barrier [17] called the Hawking-Moss instanton shown in Figure 6.2.1. This is a solution for which $\phi = \phi_{\mathrm{top}} = \phi_{\mathrm{HM}}$, where ϕ_{top} is a local maximum of $U(\phi)$. To verify

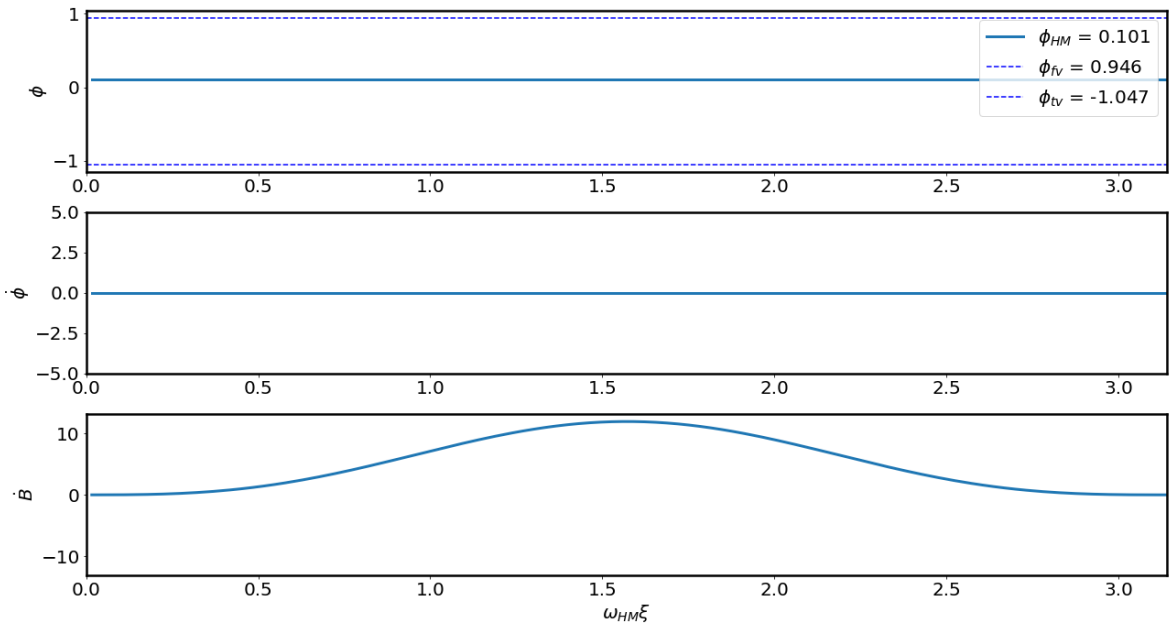

Figure 6.2.1: The Hawking-Moss Instanton, $\phi_{\rm HM}$, plotted with the gradient, $\dot{\phi}_{\rm HM} = 0$, and $\dot{B}$.

that this is a solution, we see that,

$$\left.\frac{\mathrm{d}U}{\mathrm{d}\phi}\right|_{\phi=\phi_{\rm HM}} = 0$$
$$\frac{\mathrm{d}^2\phi_{\rm HM}}{\mathrm{d}\xi^2} + \frac{3}{\alpha}\cot\left(\frac{\xi}{\alpha}\right)\frac{\mathrm{d}\phi_{\rm HM}}{\mathrm{d}\xi} = 0. \tag{6.2.1}$$

We can also calculate the action of this configuration,

$$\begin{aligned} B_{\rm HM} &= 2\pi^2\alpha^3\int_0^{\alpha\pi}\mathrm{d}\xi\,\sin^3(\xi/\alpha)\left[U(\phi_{\rm HM}) - U(\phi_{\rm fv})\right] \\ &= \frac{8\pi^2}{3}\alpha^3\Delta U\int_0^{\alpha\pi}\mathrm{d}\xi\,\sin^3(\xi/\alpha) \\ &= \frac{16}{3}\left(\frac{\pi^2}{2}\alpha^4\right)\Delta U \\ &= \frac{16}{3}V_4(\alpha)\Delta U. \end{aligned} \tag{6.2.2}$$

where $\Delta U = U(\phi_{\rm HM}) - U(\phi_{\rm fv})$ and $V_4(\alpha)$ is the 4−measure (4−volume) of $\mathbb{S}^4$. Note that we did not consider this type of solution in the flat case precisely because its

contribution to B is proportional to the volume of space-time (the volume of flat space is infinite) and so the contribution is vanishing. However, since Euclidean de Sitter space is a compact, we might believe that there is a finite contribution to Γ/V from the Hawking-Moss instanton.

Eigenvalue Decomposition of Trivial Solutions

The ϕ_{tv}, ϕ_{fv} and ϕ_{HM} solutions all describe constant configurations of the scalar field. So why are ϕ_{tv} and ϕ_{fv} solutions uninteresting as opposed to the ϕ_{HM} instanton? The secret lies in the calculation of the spectrum of eigenvalues of the second-order variation of our Euclidean action. Recall, that the condition for barrier penetration, is that our eigenvalue spectrum contains only one negative mode. This means that the functional determinant of our operator, will be imaginary, leading to an imaginary energy eigenvalue and thus, Γ/V. We can continue this analysis for a constant solution by investigating the spectrum of eigenvalues of the perturbations $\delta\phi$ about these constant solutions,

$$-\nabla_\mu \nabla_\mu \delta\phi + U''(\phi)\delta\phi = 0, \tag{6.2.3}$$

where $U''(\phi)$ is defined for the constant solutions mentioned as,

$$U''(\phi) = \begin{cases} U''(\phi_{\text{tv}}) & \text{for } \phi = \phi_{\text{tv}}, \\ U''(\phi_{\text{fv}}) & \text{for } \phi = \phi_{\text{fv}}, \\ U''(\phi_{\text{HM}}) & \text{for } \phi = \phi_{\text{HM}}. \end{cases}$$

In principle, we should consider the variations in the metric as well, however, it is possible choose a gauge in which it is only relevant to consider $\delta\phi$ in computing the eigenvalue spectrum, [12]. The radial part of (6.2.3) can be teased out by applying the standard separation techniques (as in solving the Hydrogen atom), $\delta\phi(\xi, \psi, \varphi, \theta) = R(\xi)\Psi(\psi)\Phi(\varphi)\Theta(\theta)$. The radial part of the equation is given by,

$$\frac{\mathrm{d}^2 R_{nl}}{\mathrm{d}\xi^2} + 3\omega \cot(\omega\xi)\frac{\mathrm{d}R_{nl}}{\mathrm{d}\xi} - \frac{\omega^2}{\sin^2(\omega\xi)} l(l+2)R_{nl} - \left[U''(\phi) - \lambda\right] R_{nl} = 0, \tag{6.2.4}$$

where ω^2 is given by,

$$\omega^2 = \begin{cases} \omega^2_{\rm tv} = U(\phi_{\rm tv})/3M_p^2 & \text{for } \phi = \phi_{\rm tv} \\ \omega^2_{\rm fv} = U(\phi_{\rm fv})/3M_p^2 & \text{for } \phi = \phi_{\rm fv} \\ \omega^2_{\rm HM} = U(\phi_{\rm HM})/3M_p^2 & \text{for } \phi = \phi_{\rm HM} \end{cases}$$

Provided that $n + l = M$ [29], the full spectrum of the eigenvalues for $\phi_{\rm tv}$ and $\phi_{\rm fv}$, are given by,

$$\lambda_M = \begin{cases} U''(\phi_{\rm tv}) + M(M+3)\omega^2_{\rm tv} & \text{for } \phi = \phi_{\rm tv} \\ U''(\phi_{\rm fv}) + M(M+3)\omega^2_{\rm fv} & \text{for } \phi = \phi_{\rm fv} \end{cases}$$

However, $U'' > 0$ for local minima. So for all values of M for $\phi_{\rm tv}$ and $\phi_{\rm fv}$, the eigenvalue spectrum is always positive, thus these configurations do not describe legitimate tunnelling phenomena.

On the other hand, the spectrum of the eigenvalues for Hawking Moss is given by,

$$\lambda_M = -|U''(\phi_{\rm HM})| + M(M+3)\omega^2_{\rm HM}. \tag{6.2.5}$$

The absolute value is here because $U''(\phi_{\rm HM}) < 0$. The $M = 0$ mode of Hawking-Moss is negative, $\lambda_0 < 0$. This of course gives the imaginary energy contribution leading to vacuum instability so it describes tunnelling

Of further interest is the $M = 1$ eigenvalue of Hawking-Moss,

$$\lambda_1 = -|U''(\phi_{\rm HM})| + 4\omega^2_{\rm HM}. \tag{6.2.6}$$

This is negative when,

$$\frac{|U''(\phi_{\rm HM})|}{4} < \frac{U(\phi_{\rm HM})}{3M_p^2}. \tag{6.2.7}$$

Thus under the condition (6.2.7), it is possible for the Hawking-Moss instanton to possess more than one negative eigenvalue [29] and the tunnelling contribution is obsolete.

After analytically continuing back to a Lorentzian signature in the metric, the Hawking-Moss transition represents a de Sitter space, with a constant varnish of $\phi_{\rm HM}$ over it. This is problematic as it does not respect the causal structure of the Lorentzian

space-time. It is possible to conclude that the Hawking-Moss instanton surely does not contribute to Γ/V if (6.2.7) condition is met. However, its true relevance and interpretation is not fully understood.

6.2.2 Coleman de Luccia Solution

The key class of solutions we are interested in are the Coleman de Luccia (CdL) bounces. The CdL solution is the analogue of the $O(4)$-symmetric solutions in flat spacetime but in curved space-time. They are monotonically increasing functions which cross the barrier once between $\phi(0)$ and $\phi(\xi_{\max})$. They are found by the undershoot/overshoot method as in section 4.1 Setting up the Numerical Problem. In Figure 6.2.2 we see the resulting CdL bounces at $\widetilde{\alpha} = 3$ which is an interesting case, because the initial state and final state are considerably further away from the true and false vacuum than in the flat case. Figure 6.2.3 shows another set of CdL bounces but at $\widetilde{\alpha} = 10$. We can see that for larger $\widetilde{\alpha}$, that the initial condition for the CdL bounce is much closer to the true vacuum and the overall shape of these instantons are more similar to the Minkowski instantons shown in Figure 4.2.1.

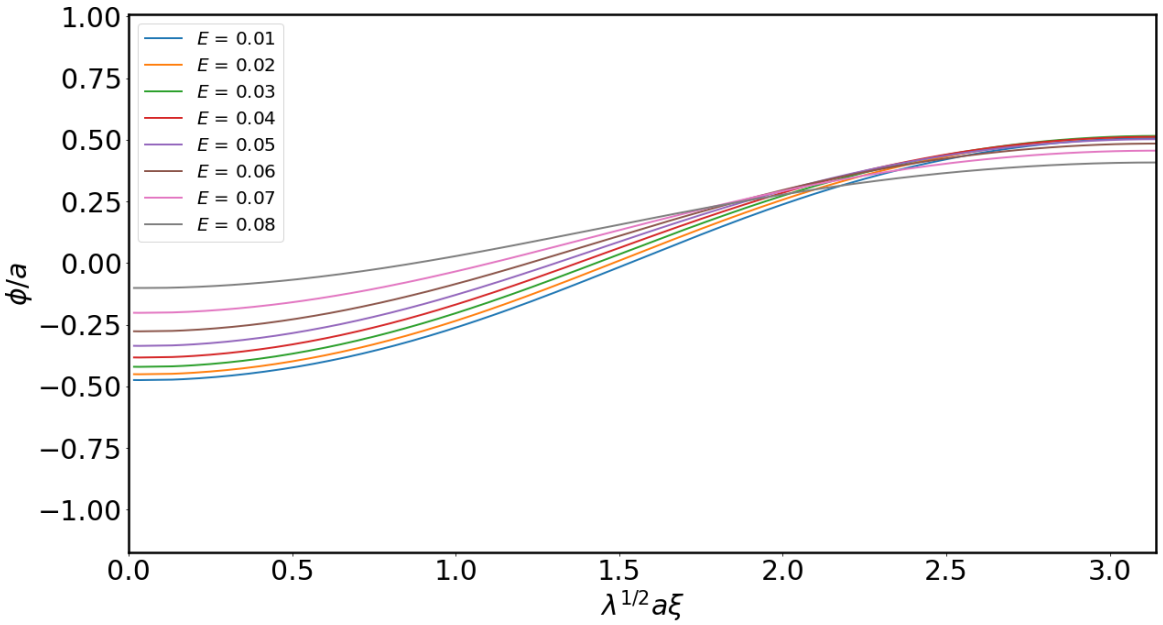

Figure 6.2.2: The Coleman de Luccia bounce for $\widetilde{\alpha} = 10$ for $E = [0.01 - 0.08]$ in steps of 0.01.

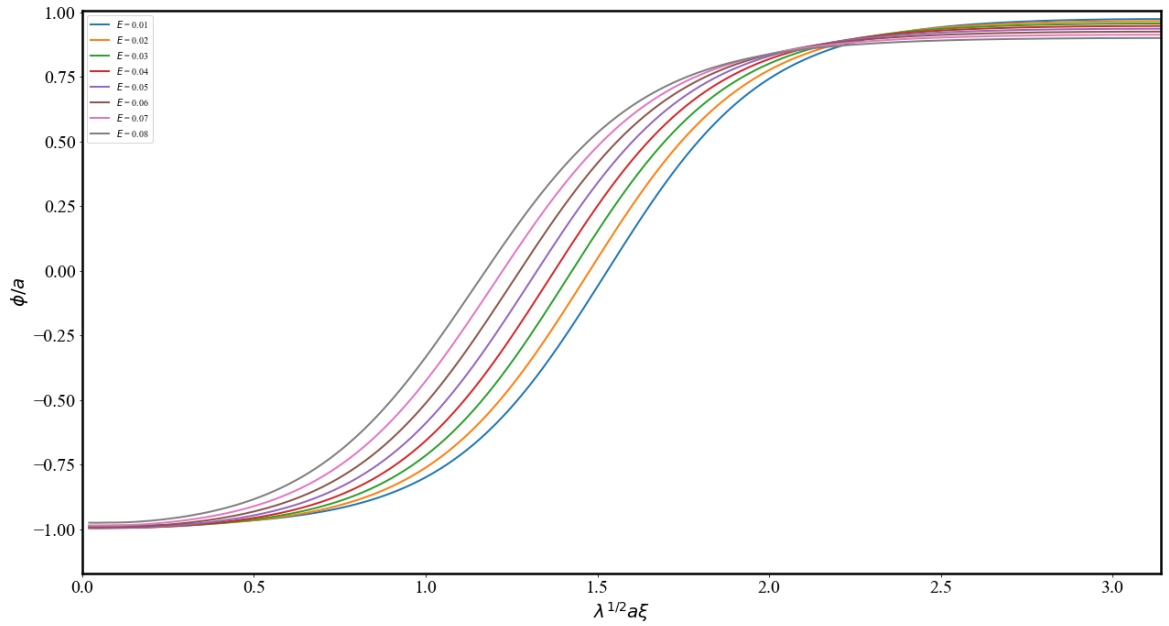

Figure 6.2.3: The Coleman de Luccia bounce for $\widetilde{\alpha} = 10$ for $E = [0.01 - 0.08]$ in steps of 0.01.

Numerical Determination of the CdL Bounce

Having discussed the CdL bounce in the theoretical framework, we can see in Figure 6.2.3 that the qualitative nature of the solution is very similar to the flat case analogue, as in Figure 4.2.1. Indeed we see that the plots shown for several values of E in Figure 6.2.3. However, we also see that the CdL bounces are qualitatively different to those shown for the flat case in Figure 4.2.1. In the flat case, the initial condition for all cases are very close to the true vacuum. However, in the case of the fixed de Sitter solution, for small E, the initial condition is initially quite far from the true vacuum. However, the same effect is seen in terms of the initial conditions $x(0)$ coming closer to x_{tv} as E increases.

6.2.3 Oscillating Solutions

The final class of solutions obeying the boundary conditions,

$$\dot{\phi}(0) = \dot{\phi}(\alpha\pi) = 0, \tag{6.2.8}$$

that are present in de Sitter spacetime are the oscillating solutions. There is no flat case analogue of these solutions. Their existence here is due to the compactness of de Sitter

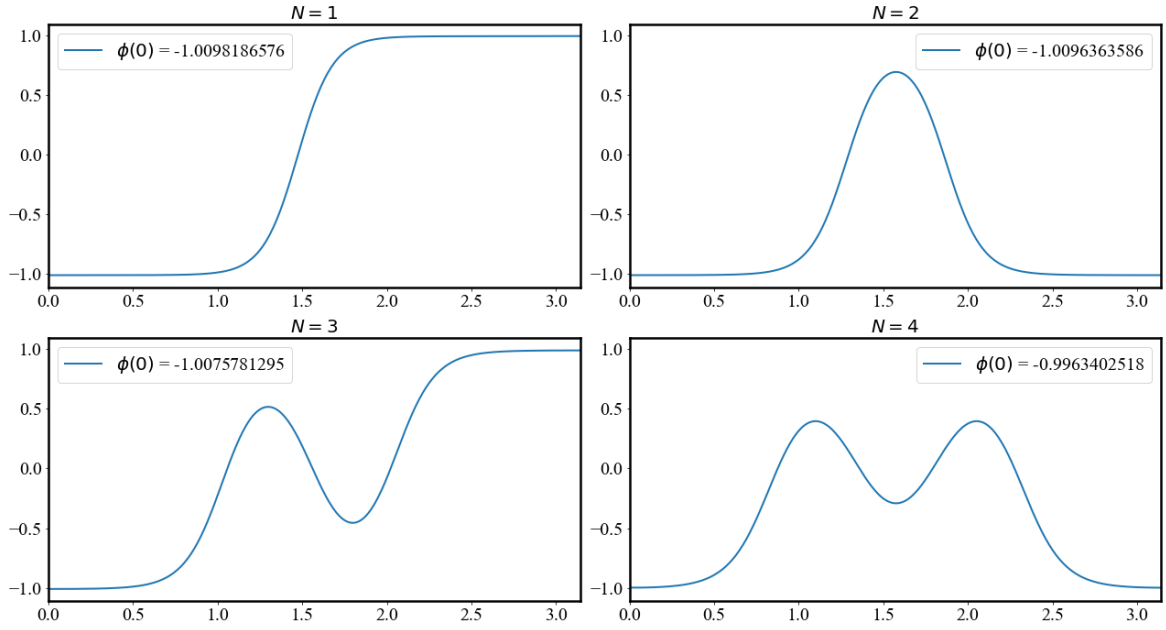

Figure 6.2.4: Plots showing the bounce solutions for potential with non-degenerate vacua for $\alpha/a^{-1}\lambda^{-1/2} = 10$ and $\varepsilon/2\lambda a^4 = 0.01$. In general for even N, we should have true-true transitions whereas for odd N, we have true-false transitions. Furthermore, we see that the $N = 1$ bounce is just Coleman-de Luccia.

space after Wick rotation which results in the fact that we can smoothly deform an instanton with N oscillations (N is called the order of the instanton) into ones with a fewer number of oscillations. Moreover, the effect of spacetime on the space of solutions produces an alternating pattern of overshoots and undershoots. Between each of these sets, we expect to find instantons of different N, but also possibly more Coleman de Luccia bounces. These solutions may in principle contribute to the vacuum decay rate as indicated by Vincentini [34].

Furthermore, recent developments show evidence indicating that a solution of order N has N negative eigenvalues in its spectrum of fluctuations [22]. The condition for Γ/V to be defined is such that the product of eigenvalues is overall negative, so that $\prod_n \lambda_n^{-1/2}$ is overall imaginary. We can see in Figure 6.2.4 that the transitions with even N are transitions which take the particle from true-vacuum to true-vacuum. It was argued by Coleman [5], that bounces with multiple negative eigenvalues push the action of such solutions away from the minimum of the stationary action - effectively, the actions of these solutions correspond to saddle points and maxima. It was later corroborated by Brown and Weinberg [2] that this is also the case in de Sitter space,

however, the interpretation of the bounce is of thermally-assisted tunnelling. Thus, it is possible for us to ignore these solutions in the calculations of the decay rate.

6.3 Filtering Hawking-Moss and Oscillating Solutions

If we were to naïvely solve the problem, for different values of $\widetilde{\alpha}$ and E, we find that the oscillating solutions will not be filtered out by this method. This is because all of these solutions obey the boundary conditions in (6.1.10). However, we have shown that oscillating bounces have several negative eigenvalues and so they must be filtered out. Moreover, under the condition provided in (6.2.7), Hawking-Moss is also a questionable contribution. This is where the order, N, of the instanton is important. The way to determine the order of the solution is to check for sign changes, m, in the array of $v(t)$. A Coleman-de Luccia bounce monotonically increases, thus we have no sign change sign changes in $v(t)$. This alludes to an order of $m+1$ for a particular solution. We can also use this to filter through solutions of a particular order. For instance, if we wanted to analyse the action B for higher N contributions.

6.4 Action and Radius of the CdL Bounce

We can see in Figure 6.4.1 increasing values of $\widetilde{\alpha}$, the curves converge on the numerical and thin-wall curves for the flat case. This is as expected from the approximation performed and leading to (5.2.5). However, due to the effect of the initial conditions collapsing on the true vacuum for large $\widetilde{\alpha}$, there is another computational constraint placed on the limit of $\widetilde{\alpha}$ we can determine these results for. The root cause of this issue is from the use of double-precision floating point numbers. This can in principle be solved by increasing to quadruple-precision floats as mentioned in 4.3 Limitations of the Solution. Even better, would be to perform these calculations on a supercomputer. The issue is that however precise we make the storage of our initial conditions whether in *double-, quadruple-* or *octuple*-precision floating point numbers, we would never reach close enough to obtain results that sufficiently converge on the flat results. So we pause in satisfaction having obtained a solution.

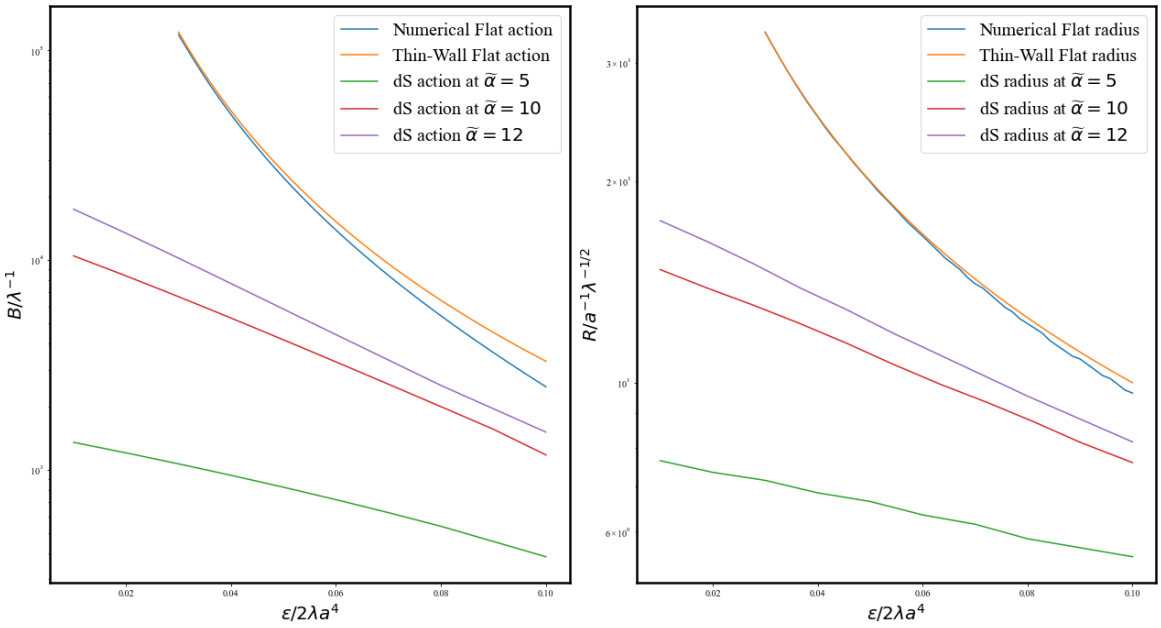

Figure 6.4.1: Plots showing the variations of B and R for several values of ε and $\alpha = 5/a\sqrt{\lambda}, 10/a\sqrt{\lambda}, 12/a\sqrt{\lambda}$.

However, by from the $\widetilde{R} - E$ graph it is quite clear that the resulting bubble on the de Sitter space is of the same order as $\widetilde{\alpha}$. In the graphs $\widetilde{\alpha}$ and $\widetilde{R}$ are expressed in the same units. So we are describing true vacuum bubbles which are of the same order of magnitude as the radius of $\mathbb{S}^4$. Ideally, these calculations should be performed at higher precision.

Chapter 7

Gravitational Instantons

Having described the case of tunnelling in a curved spacetime, we now focus our attention on the case of adding a minimal-coupling of the scalar field to the Einstein-Hilbert action.

7.1 Friedmann-Robertson-Walker Ansatz

In order to incorporate dynamical gravity, we make a further abstraction by generalising the metric. We assume the following Euclidean metric ansatz,

$$\mathrm{d}s^2 = \mathrm{d}\xi^2 + \rho^2(\xi)\,\mathrm{d}\Omega_3^2, \tag{7.1.1}$$

which is in the form of a Friedmann-Robertson-Walker (FRW) metric [3]. We now treat the metric as a dynamical variable and its dynamics as encapsulated within the scale factor, ρ. The form of the action now includes the Einstein-Hilbert Action in the *non-minimal coupling regime* is [27],

$$S_E[\phi] = \int \mathrm{d}^4x\sqrt{|g|}\left[\frac{1}{2}g^{\mu\nu}\nabla_\mu\nabla_\nu\phi + U(\phi) + \frac{1}{2}\varsigma\phi^2 R_E - \frac{1}{2}M_p^2 R_E\right]. \tag{7.1.2}$$

Non-minimal coupling implies that there is a direct coupling, ς, between Ricci scalar, R_E, and ϕ which is non-zero [24]. Minimal coupling switches off the interaction of ϕ with R_E,

$$\varsigma = 0, \tag{7.1.3}$$

whereas conformal coupling has a standard form in D-dimensions,

$$\varsigma = \frac{(D-2)}{4(D-1)}, \tag{7.1.4}$$

so in $D = 4$ we have $\varsigma = 1/6$. We work in the minimal coupling regime in this report, although instanton calculations with the non-minimal coupling term is still an active area of research in physics beyond the Standard Model [30]. The Ricci scalar in the Euclidean signature, R_E, is given by,

$$R_E = \frac{6(1-\dot{\rho}^2)}{\rho^2} - \frac{6\ddot{\rho}}{\rho}, \tag{7.1.5}$$

[3; 29]. From the Einstein tensor, we can obtain the Friedmann equation, by computing the $\mu\nu = \xi\xi$ component of $G_{\mu\nu}$,

$$\begin{aligned} G_{\xi\xi} = R_{\xi\xi} - \frac{1}{2}R_E &= -3\frac{\ddot{\rho}}{\rho} - 3\left[\frac{1}{\rho^2} - \frac{\ddot{\rho}}{\rho} - \left(\frac{\dot{\rho}}{\rho}\right)^2\right], \\ &= 3\left(\frac{\dot{\rho}}{\rho}\right)^2 - \frac{3}{\rho^2}. \end{aligned} \tag{7.1.6}$$

Of course by the Einstein field equations, we have to equate this to the corresponding component of $T_{\mu\nu}$,

$$\left(\frac{\dot{\rho}}{\rho}\right)^2 - \frac{1}{\rho^2} = \frac{1}{3M_p^2}T_{\xi\xi}. \tag{7.1.7}$$

From quantum field theory, we know that this component of the energy momentum tensor is the Hamiltonian density, ϱ, of the constituent matter fields in our particular theory. Effectively, we can write $T_{\xi\xi} = \varrho = \frac{1}{2}\dot{\phi}^2 - U(\phi)$. Moreover, we now define the Hubble parameter $H = \dot{\rho}/\rho$. Thus we have the Friedmann Equation,

$$H^2 = \left(\frac{\dot{\rho}}{\rho}\right)^2 = \frac{1}{3M_p^2}\varrho + \frac{1}{\rho^2}. \tag{7.1.8}$$

7.2 Instanton Equations and The Corrected Action

For a scalar field ϕ, the covariant derivative, $\nabla_\mu\phi = \partial_\mu\phi$ is the usual gradient operator. Noting again that scalar field is invariant under $O(4)-$transformations of (ψ, φ, θ) coordinates, thus we assume ϕ only has ξ-dependence. The Euclidean action simplifies

to,

$$S_E = 2\pi^2 \int \mathrm{d}\xi \left[\rho^3(\xi)\left(\frac{1}{2}\dot{\phi}^2 + U(\phi)\right) + 3M_p^2\left(\rho^2\ddot{\rho} + \rho\dot{\rho}^2 - \rho\right)\right]. \tag{7.2.1}$$

Here the gravitational contribution also receives a Euclidean treatment. From here on $\dot{f} = \frac{\mathrm{d}f}{\mathrm{d}\xi}$. The first step is to integrate the $\rho^2\ddot{\rho}$ term by parts,

$$S_E = 2\pi^2 \int \mathrm{d}\xi \left[\rho^3(\xi)\left(\frac{1}{2}\dot{\phi}^2 + U(\phi)\right) - 3M_p^2\rho(\dot{\rho}^2 + 1)\right]. \tag{7.2.2}$$

Since we are only interested in action difference between solutions which agree at spatial infinity, thus the corrected action for a particular solution is given by,

$$B = S_E[\phi] - S_E[\phi_{\mathrm{fv}}]. \tag{7.2.3}$$

(Note: this was performed implicitly in the case of flat space by including a correction such that for different values of ε, that $U(\phi_{\mathrm{fv}}) \equiv 0$ (4.1.8)). We expect this surface term in (7.2.2) to vanish as a result of this convention.

We also have the instanton equation of the scalar field ϕ as before,

$$\frac{\mathrm{d}^2\phi}{\mathrm{d}\xi^2} + 3\frac{\dot{\rho}}{\rho}\frac{\mathrm{d}\phi}{\mathrm{d}\xi} = \frac{\mathrm{d}U}{\mathrm{d}\phi}, \tag{7.2.4}$$

with the boundary conditions $\dot{\phi}(0) = \dot{\phi}(\xi_{\max}) = 0$. This equation is equivalent to (3.2.2), however, it is different in two ways. First, the independent variable is ξ as opposed to $\rho = \rho(\xi)$. Second, the drag term is proportional to $\dot{\rho}$. These changes are essentially cosmetic. There is a neat shortcut to obtain the Friedmann equation by applying the conserved quantity of *energy*-type from particle mechanics,

$$E = \frac{\partial\mathcal{L}}{\partial\dot{\phi}}\dot{\phi} + \frac{\partial\mathcal{L}}{\partial\dot{\rho}}\dot{\rho} - \mathcal{L} = 0, \tag{7.2.5}$$

where $\mathcal{L} = \rho^3(\frac{1}{2}\dot{\phi}^2 + U(\phi)) - 3M_p^2\rho(\dot{\rho}^2 + 1)$. From this we obtain,

$$\left(\frac{\dot{\rho}}{\rho}\right)^2 = H^2 = \frac{1}{\rho^2} + \frac{1}{3M_p^2}\left(\frac{1}{2}\dot{\phi}^2 - U\right), \tag{7.2.6}$$

$$\dot{\rho}^2 = 1 + \frac{\rho^2}{3M_p^2}\left(\frac{1}{2}\dot{\phi}^2 - U\right). \tag{7.2.7}$$

For numerical calculations, this is a problem, since the second term becomes sufficiently negative, then $\dot{\rho}$ becomes imaginary. This is easily fixed if we take the derivative with respect to ξ of (7.2.7), for which we obtain the second instanton equation for ρ,

$$\ddot{\rho} = -\frac{\rho}{3M_p^2}\left(\dot{\phi}^2 + U\right), \tag{7.2.8}$$

as pointed out in [29]. This corresponds to Friedmann's Second Equation.

The boundary condition for this differential equation is chosen to be $\dot{\rho}(0) = 1$ and $\rho(0) = 0$. These boundary conditions help us to avoid the singularity at $\xi_{\max}$, where $\xi_{\max}$ is to be determined. In the limit of large ξ, we have $\dot{\phi} = 0$, and $U \simeq U(\phi_{\rm fv})$. In this limit, (7.2.8) has approximate form,

$$\ddot{\rho} \simeq -\frac{\rho}{3M_p^2}U(\phi_{\rm fv}). \tag{7.2.9}$$

This is the equation of a simple harmonic oscillator with constant frequency, thus in the limit of large ξ, we expect $\ddot{\rho}$ and thus ρ to approach another zero, $\xi_{\max}$. $\xi_{\max}$ is determined by the position of this second zero of ρ. This can be used to determine the length over the manifold between $\xi = 0$ and $\xi = \alpha\pi$, where $\alpha = \xi_{\max}/\pi$. α is analogous to the radius of the de Sitter spacetime as we defined in (5.1.2).

Another point of interest in this problem has to do with the addition of a constant to the potential. In Minkowski space and in de Sitter space, we were always free to add a constant to the potential $U(\phi)$. However, due to the equations of motion, this constant was differentiated off, and so in our problem, we had only cared about the potential *differences*, as opposed to the absolute potential values. In the case of gravitation however, the differentiation of the constant still occurs in (7.2.4). Although, there is a contribution from this constant to the drag term through the calculation of (7.2.8). Subtracting off the contributions due to $\phi_{\rm fv}$ via (7.2.3) (which indeed has a gravitational contribution) takes care of gravitational back-reactions from the action of the uniform false vacuum solution and results in a vanishing B outside the bubble of the true vacuum over the space.

Chapter 8

Numerical Results with Gravity

8.1 Numerical Problem in Dynamical Gravity

As before, we start with the action of the scalar field minimally-coupled to the Einstein-Hilbert action,

$$S_E = 2\pi^2 \int \mathrm{d}\xi \left[\rho^3 \left(\frac{1}{2}\dot{\phi}^2 + U \right) - 3M_p^2 \rho(\dot{\rho}^2 + 1) \right]. \tag{8.1.1}$$

As before we shall simplify the parameter dependence of the action,

$$\phi \to ax, \qquad \xi \to \frac{t}{a\sqrt{\lambda}}, \qquad \varepsilon \to 2\lambda a^4 E. \tag{8.1.2}$$

But we also have the parameters,

$$M_p \to a\widetilde{M}_p, \qquad \rho \to \frac{\rho}{a\sqrt{\lambda}}. \tag{8.1.3}$$

In this manner, we see that,

$$\dot{\rho} = \frac{\mathrm{d}\rho}{\mathrm{d}\xi} = \frac{\mathrm{d}\widetilde{\rho}}{\mathrm{d}t} = \dot{\widetilde{\rho}}, \tag{8.1.4}$$

is dimensionless. Putting this all together, we have the following form of the re-defined action,

$$\begin{aligned} S_E &= 2\pi^2 \int \frac{\mathrm{d}t}{a\sqrt{\lambda}} \left[\frac{\lambda a^4 \widetilde{\rho}^3}{a^3 \lambda^{\frac{3}{2}}} \left(\frac{1}{2}\dot{x}^2 + \widetilde{U} \right) - 3\frac{a^2 \widetilde{M}_p^2}{a\sqrt{\lambda}} \widetilde{\rho} \left(\dot{\widetilde{\rho}}^2 + 1 \right) \right] \\ &= 2\pi^2 \int \frac{\mathrm{d}t}{a\sqrt{\lambda}} \left(\frac{a}{\sqrt{\lambda}} \right) \left[\widetilde{\rho}^3 \frac{1}{2} \left(\dot{x}^2 + \widetilde{U} \right) - 3\widetilde{M}_p^2 \widetilde{\rho} \left(\dot{\widetilde{\rho}}^2 + 1 \right) \right] \\ &= \frac{1}{\lambda} \left\{ 2\pi^2 \int \mathrm{d}t \left[\widetilde{\rho}^3 \frac{1}{2} \left(\dot{x}^2 + \widetilde{U} \right) - 3\widetilde{M}_p^2 \widetilde{\rho} \left(\dot{\widetilde{\rho}}^2 + 1 \right) \right] \right\} = \frac{\widetilde{S}}{\lambda} \end{aligned} \tag{8.1.5}$$

which has the same form as before (4.1.3). Furthermore, we have the following re-definitions of the instanton equations,

$$\begin{aligned} \frac{\mathrm{d}^2 x}{\mathrm{d}t^2} &= -3\frac{\dot{\widetilde{\rho}}}{\widetilde{\rho}} \frac{\mathrm{d}x}{\mathrm{d}t} + \frac{\mathrm{d}\widetilde{U}}{\mathrm{d}x}, \\ \frac{\mathrm{d}^2 \widetilde{\rho}}{\mathrm{d}t^2} &= -\frac{\widetilde{\rho}}{3\widetilde{M}_p^2} \left(\dot{x}^2 - \widetilde{U} \right). \end{aligned} \tag{8.1.6}$$

Now, our problem is to solve these equations but using the Runge-Kutta method as before. But first we transform the equations by defining, $v = \dot{x}$ and $w = \dot{\widetilde{\rho}}$. We have a system of four coupled differential equations,

$$\frac{\mathrm{d}v}{\mathrm{d}t} = -3\frac{\dot{\widetilde{\rho}}}{\widetilde{\rho}} v + \frac{\mathrm{d}\widetilde{U}}{\mathrm{d}x}, \qquad v = \frac{\mathrm{d}x}{\mathrm{d}t}, \tag{8.1.7}$$

$$\frac{\mathrm{d}w}{\mathrm{d}t} = -\frac{\widetilde{\rho}}{3\widetilde{M}_p^2} \left(\dot{x}^2 - \widetilde{U} \right), \qquad w = \frac{\mathrm{d}\widetilde{\rho}}{\mathrm{d}t}. \tag{8.1.8}$$

With these equations solved, we can then integrate,

$$\frac{\mathrm{d}\widetilde{S}}{\mathrm{d}t} = 2\pi^2 \left[\widetilde{\rho}^3 \frac{1}{2} \left(\dot{x}^2 + \widetilde{U} \right) - 3\widetilde{M}_p^2 \widetilde{\rho} \left(\dot{\widetilde{\rho}}^2 + 1 \right) \right]. \tag{8.1.9}$$

If $\bar{x}$ is a particular bounce (without discrimination of the order of the instanton), and x_{fv} is the constant false vacuum configuration, then the action of a particular bounce is given by,

$$B = \widetilde{S}[\bar{x}] - \widetilde{S}[x_{\mathrm{fv}}], \tag{8.1.10}$$

as required by (7.2.3).

Furthermore, we can determine the Ricci scalar for the spacetime over the course of the transition. In units of $\widetilde{M}_p^2 = 1$ (which we adopt from here on), the Ricci scalar (7.1.5) transforms as $R_E \to \lambda a^2 \widetilde{R}_E$, thus we have,

$$\widetilde{R}_E = 6\left[\frac{1-w^2}{\widetilde{\rho}^2} - \frac{1}{3}\left(v^2 - \widetilde{U}\right)\right]. \tag{8.1.11}$$

8.2 Scale Factor for Hawking-Moss

The Hawking-Moss instanton again provides a good example of when we can solve the instanton equations analytically. The equation of the Hawking-Moss scale factor, ρ, (7.2.8) becomes,

$$\ddot{\rho} = -\frac{U(\phi_{\mathrm{HM}})}{3M_p^2}\rho, \tag{8.2.1}$$

provided $U(\phi_{\mathrm{HM}}) > 0$, we have the equation of a simple harmonic oscillator. Under the boundary conditions for a compact manifold with $\xi_{\max}$ as the *period* of ξ, $\rho(0) = \rho(\xi_{\max}) = 0$. For $\omega_{\mathrm{HM}}^2 = U(\phi_{\mathrm{HM}})/3M_p^2$, the scale factor is,

$$\rho_{\mathrm{HM}}(\xi) = \omega_{\mathrm{HM}}^{-1}\sin(\omega_{\mathrm{HM}}\xi). \tag{8.2.2}$$

For this particular case, the radius of the resulting 4-sphere can be determined. The value of $\xi_{\max} = \omega_{\mathrm{HM}}^{-1}\pi$, thus the radius of the 4-sphere is nothing but,

$$\alpha_{\mathrm{HM}} = \omega_{\mathrm{HM}}^{-1}, \tag{8.2.3}$$

thus,

$$\rho_{\mathrm{HM}}(\xi) = \alpha_{\mathrm{HM}}\sin^2\left(\xi/\alpha_{\mathrm{HM}}\right). \tag{8.2.4}$$

Thus the metric of the resulting spacetime from the ansatz (7.1.1) is nothing but,

$$\mathrm{d}s^2 = \mathrm{d}\xi^2 + \alpha_{\mathrm{HM}}^2\sin^2\left(\xi/\alpha_{\mathrm{HM}}\right)\mathrm{d}\Omega_3^2. \tag{8.2.5}$$

Which is identical to (5.1.5).

The Hawking-Moss transition leads to a de Sitter space (5.1.5). Next, we consider the

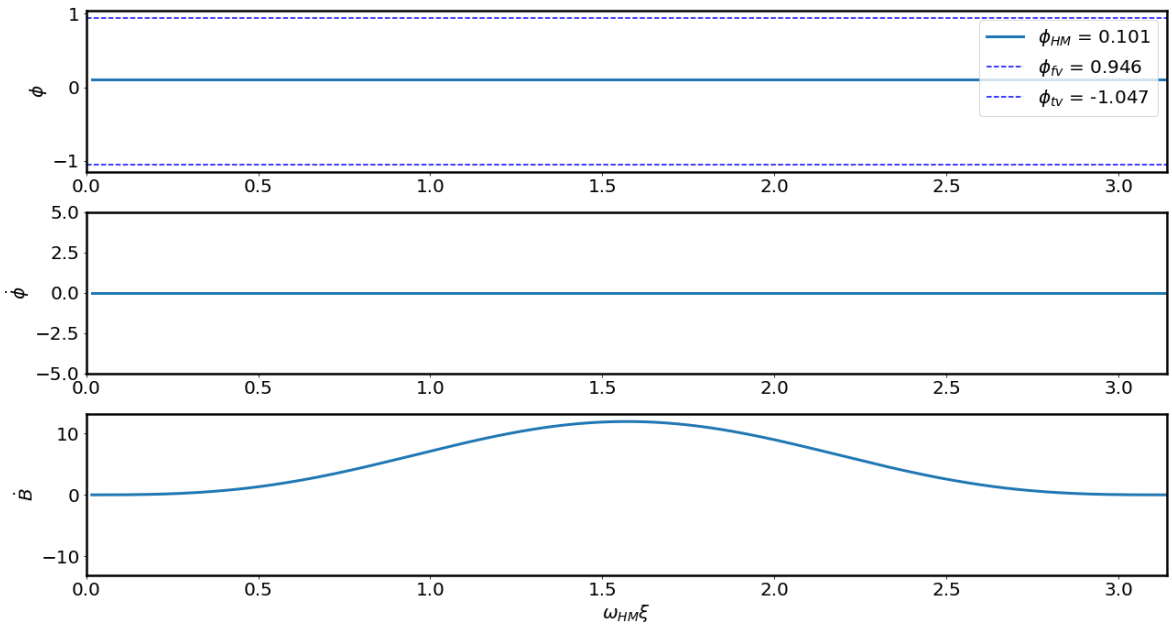

Figure 8.2.1: The Hawking-Moss Instanton, $\phi_{\rm HM}$, plotted with the gradient, $\dot{\phi}_{\rm HM} = 0$, and $\dot{B}$.

action for the Hawking-Moss instanton, $B_{\rm HM}$. $\dot{B}$ for the Hawking-Moss instanton is shown in Figure 8.2.1. An approximate solution of the decay coefficient, B is,

$$B_{\rm HM} \;=\; 24\pi^2 M_p^4 \left[\frac{1}{U(\phi_{\rm fv})} - \frac{1}{U(\phi_{\rm HM})}\right]. \tag{8.2.6}$$

We have taken care to subtract off the action $S[\phi_{\rm fv}]$ which is where the term containing $U(\phi_{\rm fv})$ comes from. This solution describes a universe dominated by a constant potential $U(\phi_{\rm HM})$. Let $V_0 = U(\phi_{\rm fv})$, in the limit $V_0 - U(\phi_{\rm HM}) \ll V_0$, then we can approximate $U(\phi_{\rm HM}) \simeq U(\phi_{\rm fv})$ and approximate $B_{\rm HM}$ to be,

$$B_{\rm HM} \simeq \frac{4\pi}{3}\alpha_{\rm HM}^3 \frac{\Delta U}{T_{\rm GH}}, \tag{8.2.7}$$

where the *Gibbons-Hawking temperature*, $T_{\rm GH}$, associated with the horizon of this space-time,

$$T_{\rm GH} = \frac{\omega_{\rm HM}}{2\pi}. \tag{8.2.8}$$

The action is given as a ratio of energy density, ΔU, integrated over a 2-sphere of radius $\alpha_{\rm HM}$, divided by $T_{\rm GH}$. Thus the energy of this solution is $E_{\rm HM} = \frac{4\pi}{3}\alpha_{\rm HM}^3 \Delta U$. We see this by calculating Γ/V,

$$\frac{\Gamma}{V} = \exp\left(-\frac{E_{\rm GH}}{T_{\rm GH}}\right), \tag{8.2.9}$$

which is a Boltzmann factor. So we conclude that the Hawking-Moss instanton is a thermal transition. With the scale factor ρ as in (8.2.2), the Hubble rate, $H = \dot{\rho}/\rho$ is given by,

$$H = \frac{\dot{\rho}_{\rm HM}}{\rho_{\rm HM}} = \omega_{\rm HM}\cot(\omega_{\rm HM}\xi). \tag{8.2.10}$$

Both the scale factor and the Hubble rate obtain from numerical calculations are shown in Figure 8.2.2, the profiles of which clearly agree with the predictions from the calculations of (8.2.2) and (8.2.10). This is seen through the normalisation of the axes in Figure 8.2.2. For instance, we see that from (8.2.2) that if we represent the Hawking-Moss instanton in units of $\omega_{\rm HM}$, then we are left with $\rho_{\rm HM}(\xi) = \sin(\omega_{\rm HM}\xi)$. Thus we expect that when $\omega_{\rm HM}\xi = \pi/2$, then the scale factor $\rho_{\rm HM}$, should peak at 1 as seen in Figure 8.2.2. Moreover, the Hubble rate H is clearly a cotangent function, as predicted in (8.2.10) which is vanishing at $\omega_{\rm HM}\xi = \pi/2$.

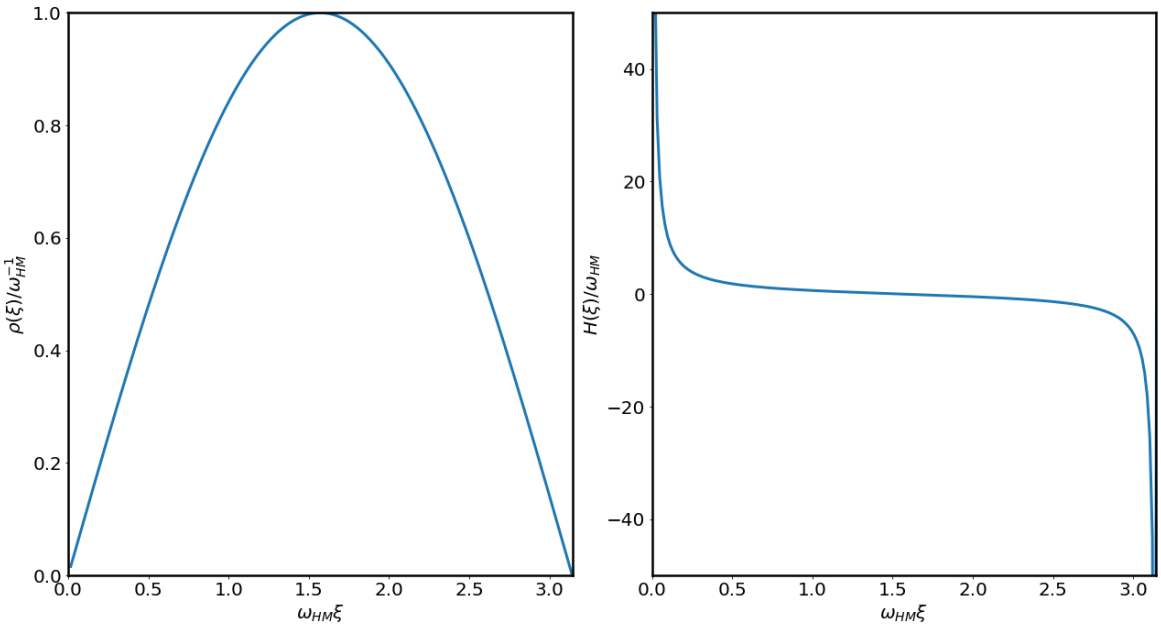

Figure 8.2.2: The evolution of the Euclidean scale factor, $\rho(\xi)$, and the Euclidean Hubble parameter, $H = \dot{\rho}/\rho$.

8.3 Coleman-de Luccia Analytical Solution

In order to calculate the B for the CdL bounce, we ought to calculate the correction $S_E[\phi_{\rm fv}]$. The correction to the bounce is due to a constant $\phi = \phi_{\rm fv}$ solution, so that,

$$S_E[\phi_{\rm fv}] = 2\pi^2 \int \mathrm{d}\xi \left[\rho^3 U(\phi_{\rm fv}) - 3M_p^2 \rho(\dot{\rho}^2 + 1)\right]. \tag{8.3.1}$$

Now we want to solve for ρ in this case, the simplest way to do this is to solve (7.2.8), so that,

$$\ddot{\rho} = -\frac{U(\phi_{\rm fv})}{3M_p^2}\rho, \tag{8.3.2}$$

which has a solution,

$$\rho(\xi) = \omega_{\rm fv}^{-1} \sin(\omega_{\rm fv}\xi), \tag{8.3.3}$$

where $\omega_{\rm fv}^2 = U(\phi_{\rm fv})/3M_p^2$. Then, by substituting into $S_E[\phi_{\rm fv}]$, we find,

$$S_E[\phi_{\rm fv}] = -\frac{24\pi^2 M_p^4}{U(\phi_{\rm fv})}. \tag{8.3.4}$$

The Euclidean action is obtained by substituting (7.2.7) into (7.2.2) and so we have,

$$\begin{aligned} S_E &= 2\pi^2 \int \mathrm{d}\xi \left[\rho^3 \left(\frac{1}{2}\dot{\phi}^2 + U\right) - 6M_p^2\rho - \rho^3\left(\frac{1}{2}\dot{\phi}^2 - U\right)\right], \\ &= 4\pi^2 \int \mathrm{d}\xi \left[\rho^3 U(\phi) - 3M_p^2\rho\right]. \end{aligned} \tag{8.3.5}$$

Using this simplified action, we can again split the action into parts as we did in (3.3.4)

- Outside the bubble, $\phi = \phi_{\rm fv}$, the action reduces to,

$$B_{\rm outside} \simeq 0. \tag{8.3.6}$$

- Within the wall we can approximate ρ to be constant, $\bar{\rho}$ and so,

$$B_{\rm wall} = 2\pi^2 \bar{\rho}^3 S_1, \tag{8.3.7}$$

  where $S_1 = \int \mathrm{d}\phi \, [U(\phi) - U(\phi_{\rm fv})]$.

- Inside the wall, $\dot{\phi} = 0$ and $U = U(\phi_{\rm tv})$ we need to perform a change of variables

$$\mathrm{d}\xi = \mathrm{d}\rho \left[1 - \rho^2 \left(U(\phi_{\rm tv})/3M_p^2\right)\right]^{-1/2},$$

$$B_{\rm inside} = -12\pi^2 M_p^4 \int_0^{\bar{\rho}} \mathrm{d}\rho\rho^3 \left[1 - \rho^2 U(\phi_{\rm tv})/3M_p^2\right]^{\frac{1}{2}} - (\phi_{\rm tv} \to \phi_{\rm fv}), \tag{8.3.8}$$

where $(\phi_{\rm tv} \to \phi_{\rm fv})$ refers to the first term but all instances of $\phi_{\rm tv}$ are replaced by $\phi_{\rm fv}$. Solving this integral leads to the following,

$$B_{\rm inside} = 12\pi^2 M_p^4 U(\phi_{\rm tv})^{-1} \left\{ \left[1 - \bar{\rho}^2 U(\phi_{\rm tv})/3M_p^2\right]^{\frac{3}{2}} - 1 \right\} - (\phi_{\rm tv} \to \phi_{\rm fv}). \tag{8.3.9}$$

- Overall the decay coefficient is given by,

$$\begin{aligned} B &= B_{\rm inside} + B_{\rm wall} + B_{\rm outside}, \qquad (8.3.10)\\ &= 2\pi^2\bar{\rho}^3 S_1 + 12\pi^2 M_p^4 U(\phi_{\rm tv})^{-1} \left\{ \left[1 - \bar{\rho}^2 U(\phi_{\rm tv})/3M_p^2\right]^{\frac{3}{2}} - 1 \right\} - (\phi_{\rm tv} \to \phi_{\rm fv}). \end{aligned}$$

It was argued in [6] that there are essentially two cases that are of critical importance plotted on Figure 8.3.1. The idea being that the energy density difference between us and that of the state we are living in is always zero, as we cannot directly measure the vacuum energy density of space-time.

The case of interest to us displayed in Figure 8.3.1 (b), where $U(\phi_{\rm tv}) = 0$ and $U(\phi_{\rm fv}) = \varepsilon$. This describes the case for which the transition of spacetime is from de Sitter space (with a positive cosmological constant) to another de Sitter space with a (different positive cosmological constant). In order to determine B and R for this case, we need to use the result obtained from l'Hôpital's rule,

$$\lim_{U(\phi_{\rm tv})\to 0} \frac{12\pi^2 M_p^4}{U(\phi_{\rm tv})} \left[(1 - \bar{\rho}^2 U(\phi_{\rm tv}/3M_p^2)^{\frac{3}{2}}) - 1\right] = -\frac{\bar{\rho}^2}{2M_p^2}. \tag{8.3.11}$$

Then we can substitute this into (8.3.10), and take the derivative with respect to $\bar{\rho}$ so we have,

$$\begin{aligned} B &= 2\pi^2\bar{\rho}^3 S_1 - 6\pi^2 M_p^2 \bar{\rho}^2 - \frac{12\pi^2 M_p^4}{\varepsilon} \left[(1 - \bar{\rho^2}\varepsilon/3M_p^2)^{\frac{3}{2}}) - 1\right]\\ \frac{\mathrm{d}B}{\mathrm{d}\bar{\rho}} &= 6\pi^2\bar{\rho}^2 S_1 - 12\pi^2 M_p^2\bar{\rho} + 12\pi^2 M_p^2\bar{\rho} \left[(1 - \bar{\rho^2}\varepsilon/3M_p^2)^{\frac{1}{2}} - 1\right] = 0\\ \left[\bar{\rho}S_1 - 2M_p^2\right]^2 &= 4M_p^2 \left[1 - \varepsilon\bar{\rho}^2/3M_p^2\right]. \end{aligned}$$

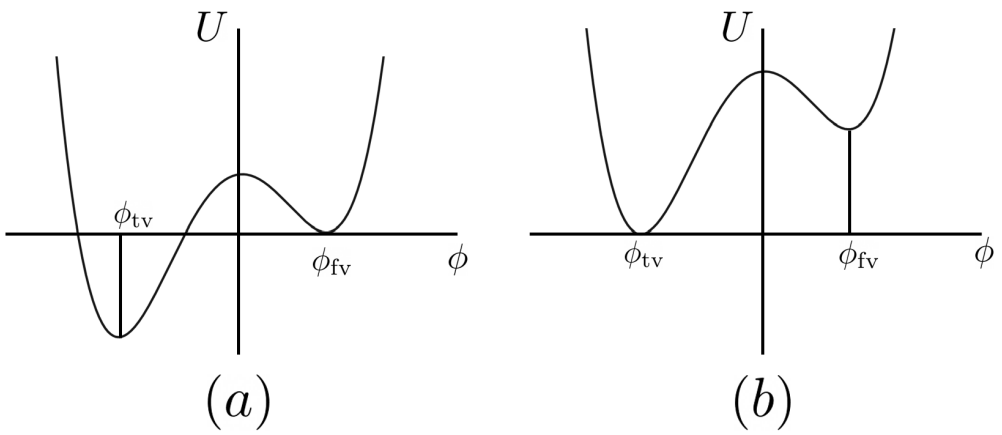

Figure 8.3.1: (a) This case is appropriate if we are living in a universe in the false vacuum state ($U(\phi_{\rm fv}) = 0$ and $U(\phi_{\rm tv}) = -\varepsilon$). This configuration describes a transition from dS to Anti-de Sitter spacetime (AdS). (b) This case is appropriate if the false vacuum decay has already occurred in the past ($U(\phi_{\rm fv}) = +\varepsilon$ and $U(\phi_{\rm tv}) = 0$). This is the same potential as the flat, curved and gravitational cases. This configuration describes a transition from dS to dS of different energy density.

On re-arrangement of this for $\bar{\rho}$, the value of the bubble radius is given in terms of that of the flat case R_0,

$$\bar{\rho} = \frac{R_0}{1 + (R_0/2\Lambda)^2}, \tag{8.3.12}$$

where $\Lambda = (\varepsilon/3M_p^2)^{-1/2} = \omega_{\rm fv}^{-1}$ is the cosmological horizon of de Sitter space. This is equally the Schwarzschild radius of a sphere of energy density ε and $R_0 = 3S_1/\varepsilon$ is equivalent to (3.3.9). Substituting $\bar{\rho}$ into the action again and performing some algebra, we have an expression for the action B,

$$B = \frac{B_0}{[1 + (R_0/2\Lambda)^2]^2} \tag{8.3.13}$$

where B_0 is the action in the flat case as in (3.3.10). Thus we expect that the radius and the action in the gravitational case is much smaller that that in the flat case.

8.4 Numerical Results for Coleman-de Luccia Bounce

After filtering out the bounces with order, $m \neq 1$, we are left with the CdL bounce, as shown in Figure 8.4.1.

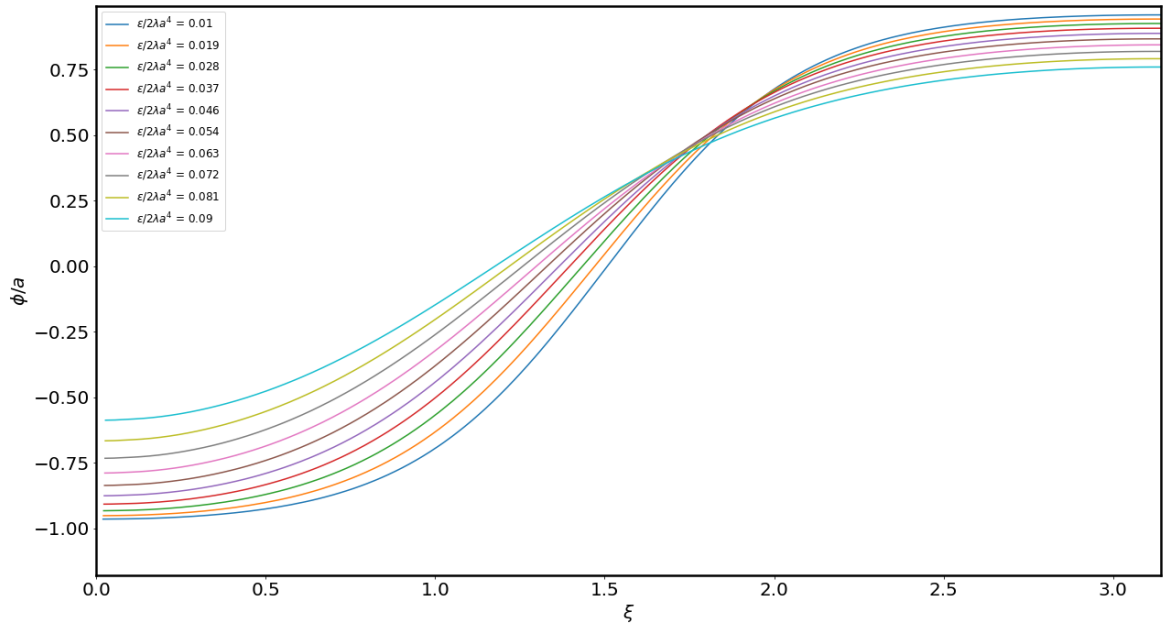

Figure 8.4.1: A plot showing the CdL bounces obtained for $E = [0.01, 0.09]$.

Furthermore, in Figure 8.4.2, we see plots showing the corresponding scale factor as a result of solving (7.2.8). The form of ρ and H in Figure 8.4.3 are in considerable agreement with those obtained for the Hawking-Moss instanton in Figure 8.2.2.

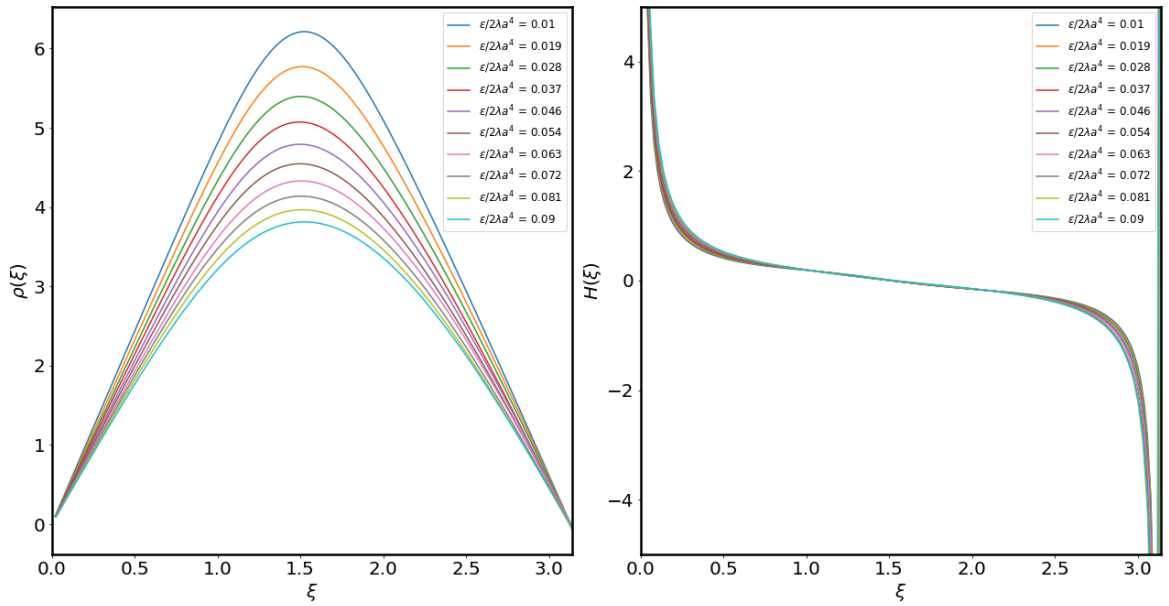

Figure 8.4.2: A plot showing the scale factors and Hubble parameter for the corresponding CdL bounces for $E = [0.01 - 0.09]$.

In Figure 8.4.3, we show one CdL scale factor and Hubble rate for $E = 0.05$ along with the corresponding scale factor and Hubble rate for the Hawking-Moss instanton. We see that when the ξ-axis is scaled so that the corresponding solution is defined between $\xi = 0$ and $\xi = \pi$. Then the only difference between the curves of the scale factors is the peak of the curves. The Hubble rates for the different configurations also significantly agree with one another.

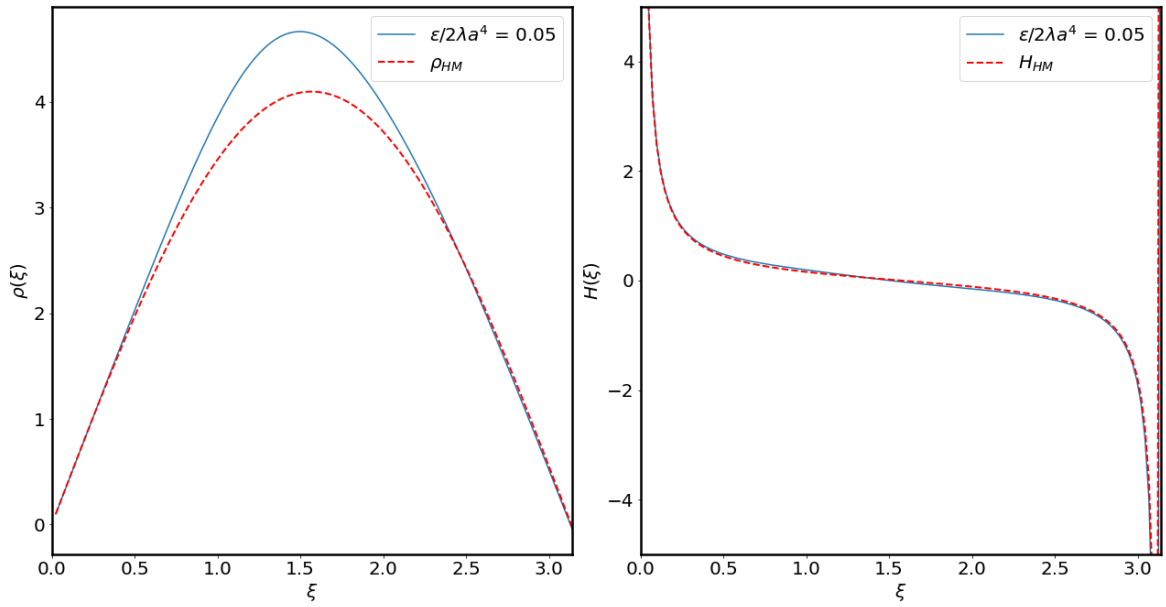

Figure 8.4.3: A plot showing the scale factors and Hubble parameter for the corresponding CdL bounces for $E = [0.01 - 0.09]$.

Having confirmed the solutions of the instanton equations, we now turn our attention to the action of the CdL solutions.

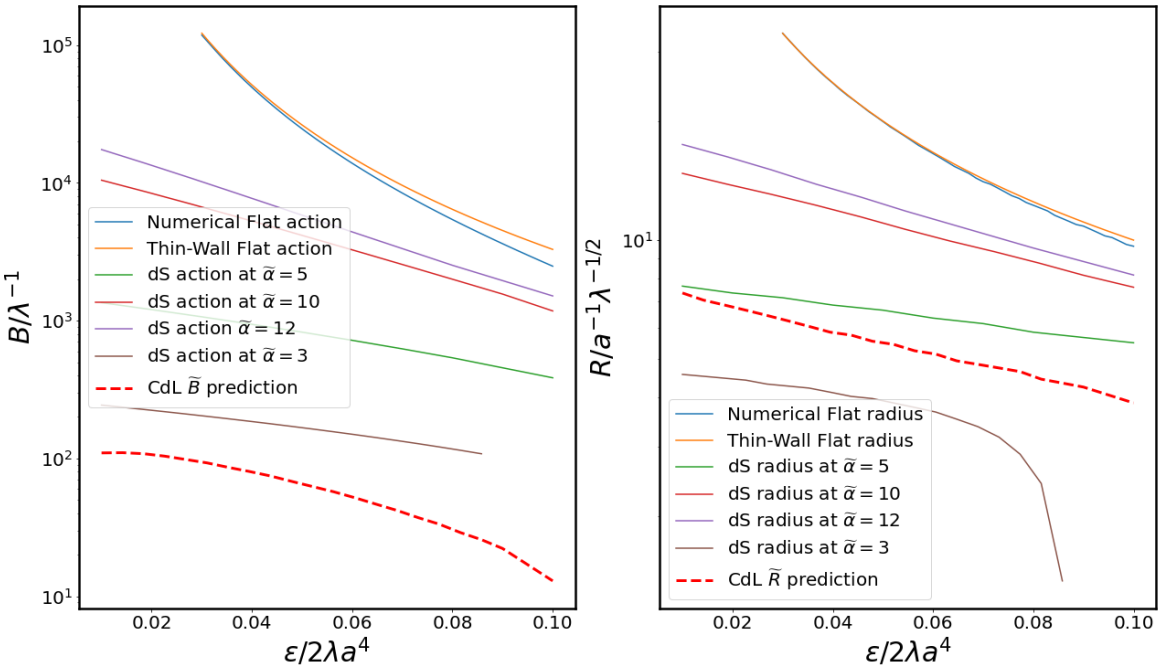

Figure 8.4.4: A plot showing the action and radius of the CdL bounces in the gravitational case (shown in red and dashed), compared to the previous results of de Sitter space and flat case.

The results shown are pretty interesting, as we see that the action for the CdL bounce with gravity is much smaller than say the action for a CdL bounce in a de Sitter space with $\widetilde{\alpha} = 3$. Thus we see that in our particular case, that gravitation makes the bubble materialization more likely, but the resulting bubbles are quite large compared to the bubble produced at $\widetilde{\alpha} = 3$. This is just as expected for the case of tunnelling from a positive false vacuum to a zero false vacuum as described in [6]. Although the size of the resulting bubbles are smaller than all cases expected for $\widetilde{\alpha} = 5, 10, 12$

8.5 The Fixed Background Approximation

Consider our usual potential with non-degenerate vacuum states. Previously, we had altered the energy density difference between ϕ_{tv} and ϕ_{fv} by shifting the value of ε. However, if we now add a constant parameter U_0 to the potential, so that we have

$$U(\phi) = U_0 + U_F(\phi) = U_0 + \frac{\lambda}{8}\left(\phi^2 - a^2\right)^2 + \frac{\varepsilon}{2a}(\phi - a) \tag{8.5.1}$$

this will change the geometry of the spacetime for different values of U_0. Previously, in the Minkowski spacetime this would not have made any difference, as only the derivative of the potential appears in the equations of motion. However, in the gravitational case, this extra degree of freedom contributes a back-reaction on the dynamics of the scalar. However let us consider the instanton equations in the limit $\varepsilon \ll U_0$,

$$\ddot{\phi} + \frac{3\dot{\rho}}{\rho}\dot{\phi} = \frac{\mathrm{d}U}{\mathrm{d}\phi}, \tag{8.5.2}$$

$$\ddot{\rho} = -\frac{\rho}{3M_p^2}\left(\frac{1}{2}\dot{\phi}^2 - U(\phi)\right). \tag{8.5.3}$$

In the limit of large U_0, the term in linear ε is vanishing. Furthermore, the term linear in λ, is small with respect to U_0 between the true and false vacuum. This is relevant as this is the region over which the all transitions occur. Thus in this limit the potential is approximately constant.

The equation of $\ddot{\rho}$ is approximately,

$$\ddot{\rho} \simeq \frac{\rho}{3M_p^2}\left(\frac{1}{2}\dot{\phi}^2 + U_0\right) \simeq -\frac{U_0}{3M_p^2}\rho, \tag{8.5.4}$$

in the limit of $\dot{\phi} \ll 1$. Thus the equation of the scale factor is solved easily to be,

$$\rho(\xi) = \alpha \sin\left(\xi/\alpha\right), \tag{8.5.5}$$

with $\alpha = (U_0/3M_p^2)^{\frac{1}{2}}$. Our metric ansatz (7.1.1) becomes,

$$\mathrm{d}s^2 = \mathrm{d}\xi^2 + \alpha^2 \sin^2\left(\xi/\alpha\right)\mathrm{d}\Omega_3^2, \tag{8.5.6}$$

which we have seen before as the de Sitter metric (5.1.5). Furthermore, the Ricci scalar of de Sitter space is given by,

$$R = \frac{12}{\alpha^2}, \tag{8.5.7}$$

which is standard in $D = 4$ dimensions [3] and a constant.
The equation of motion in the fixed background approximation is given by,

$$\frac{\mathrm{d}^2\phi}{\mathrm{d}\xi^2} + \frac{3}{\alpha}\cot\left(\frac{\xi}{\alpha}\right)\frac{\mathrm{d}\phi}{\mathrm{d}\xi} = \frac{\mathrm{d}U_F}{\mathrm{d}\phi}, \tag{8.5.8}$$

and since, the leading order contribution, U_0, to $U(\phi)$ is differentiated off on the right side of the above, $\mathrm{d}U_F/\,\mathrm{d}\phi$ is the leading order contribution to the right-hand side of (8.5.8). This was considered by Rajantie and Stopyra in [29] though for a different potential with an additional ϕ^6 term. In their particular set up, it was found that as U_0 is increased, the shape of the CdL bounce is smoothly deformed into the Hawking-Moss solution beyond a critical shift $U_{0\mathrm{crit}}$. This will also be a point of investigation in the next part of this report.

8.6 Confirming the Fixed Background Approximation

Consider the potential,

$$\widetilde{U}(x) = \frac{1}{8}(x^2-1)^2 + E(x-1) + \widetilde{U}_0. \tag{8.6.1}$$

We previously discussed in the limit that $\varepsilon \ll U_0$ that the calculations should fall to those of a fixed de Sitter background). Translating this relation into our dimensions, we have, $E \ll \widetilde{U}_0/2$. Given this condition, we should expect to approach the limit of a fixed background. We consider solving the equations (8.1.7) and (8.1.8) in this limit. We see in Figure 8.6.1 that for $E = 0.05$ as $\widetilde{U}_0$ is increased, the Coleman-de Luccia bounce flattens. The solution never reaches the false vacuum and it becomes more difficult for a transition to the true vacuum to occur. For $\widetilde{U}_0 > 0.184$ the transition achieves a perfect relaxation on the Hawking-Moss instanton. Beyond this point, the CdL bounce does not exist. This is interpreted as thermal effects becoming more important compared to the effects of quantum tunnelling [2; 29].

We can determine the effects on the Ricci scalar under the limit of increasing U_0 Figure 8.6.2. It is apparent that $\widetilde{R}_E$ becomes constant over a greater range of ξ as U_0 is increased. The interpretation here is that the Coleman-de Luccia type instantons deform the spacetime around the region of transition as a wave travelling up the 4-sphere. As this wave travels, it induces a change in curvature over the manifold. In the example of $U_0 = 0.1$, we have an approximate CdL configuration. For this configuration, at approximately the centre of the instanton, we see the greatest change in curvature on the manifold due to the transition from true to false vacuum. As the

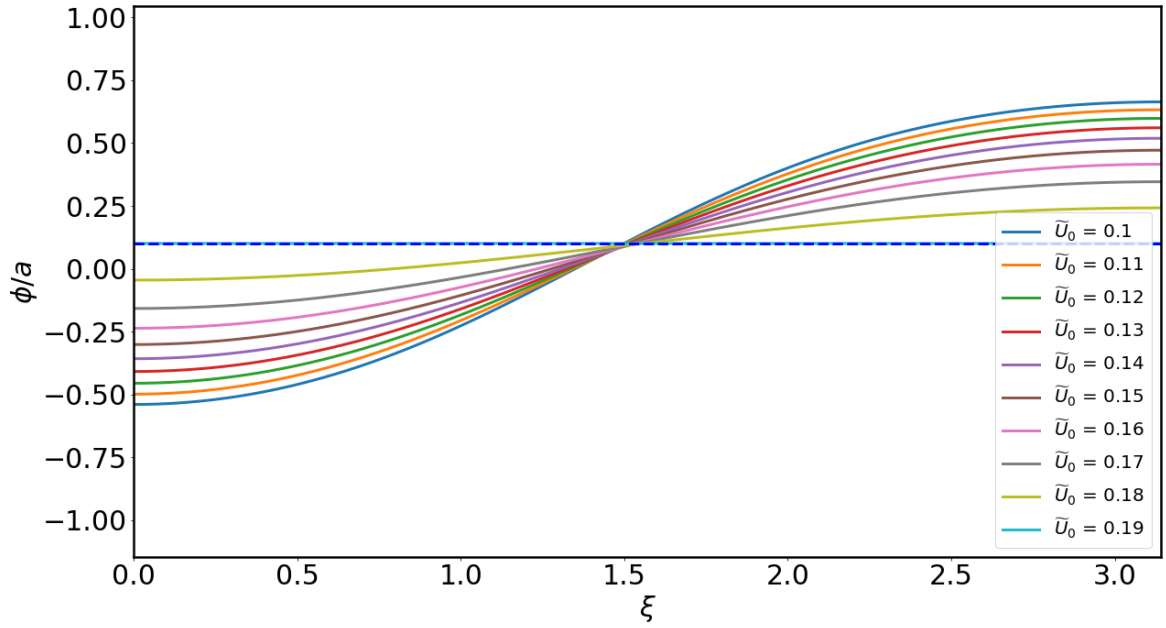

Figure 8.6.1: The bounces for $\widetilde{U}_0 = [0.01 - 0.19]$ for $E = 0.05$. We see that what are initially Coleman-de Luccia bounces deform into the Hawking-Moss instanton for this potential. The ξ-axis is normalised to the corresponding value of radius of the 4−sphere, $\alpha = \xi_{\max}/\pi$ of each bounce.

value of $\widetilde{U}_0$ is increased, the Ricci scalar $\widetilde{R}_E$ tends to homogeneity over the entire 4-sphere. Thus we have a manifold with constant positive curvature leading to a fixed de Sitter background.

However, at the poles of the 4−sphere ($\xi = 0$ and $\xi = \pi$ normalised for the radius of the particular sphere), we see that the scalar is rather singular. It is possible to show that this is an artefact of the size of the integration step chosen in the Runge-Kutta calculation. In particular, in the Figure 8.6.2, the size of the integration step is $\mathrm{d}\widetilde{\xi} = 0.001$. It was found that if the size of the step is decreased to $\mathrm{d}\widetilde{\xi} \ll 0.01$, the Ricci scalar becomes flatter over a larger domain of $\widetilde{\xi}$. In Figure 8.6.3, we see that the smaller integration step results in a spatially-homogeneous Ricci scalar curvature. Furthermore, we can see that as the integration step is decreased, the $\widetilde{R}_E$ converges on the predicted value of the Ricci scalar as in (8.5.7) for a universe dominated by a spatially-homogeneous scalar field configuration of the Hawking-Moss instanton.

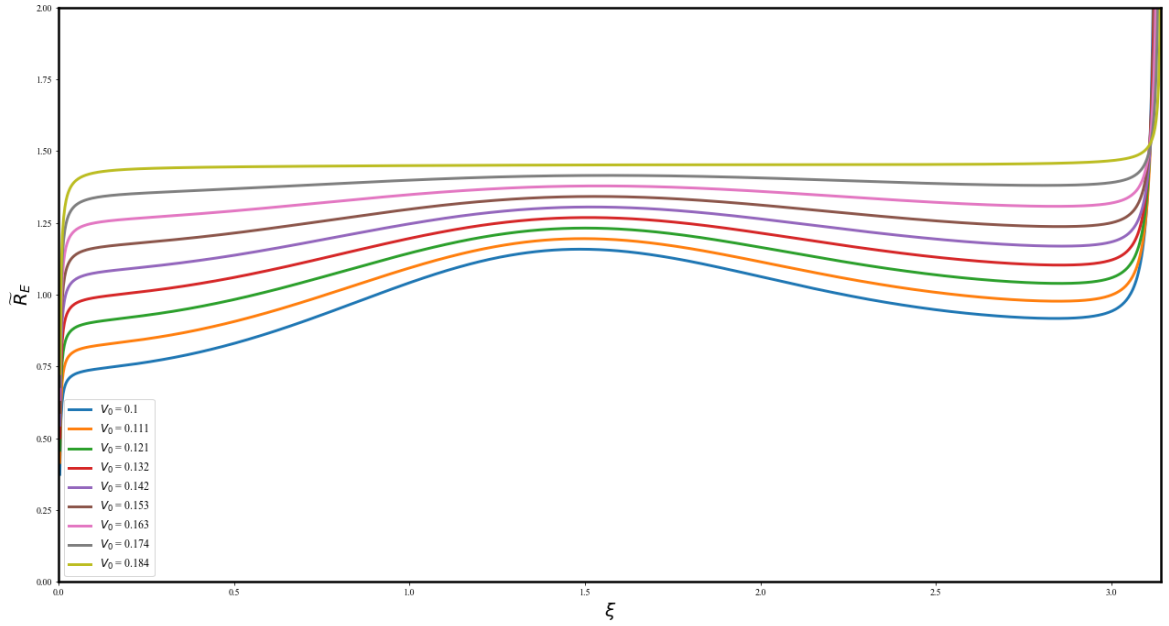

Figure 8.6.2: Plots showing the Ricci scalar, $\widetilde{R}_E$ as a function of ξ. With increasing values of U_0, we see that the Ricci scalar becomes flatter and flatter. The integration time-step for the bold lines is $\mathrm{d}\widetilde{\xi} = 0.01$

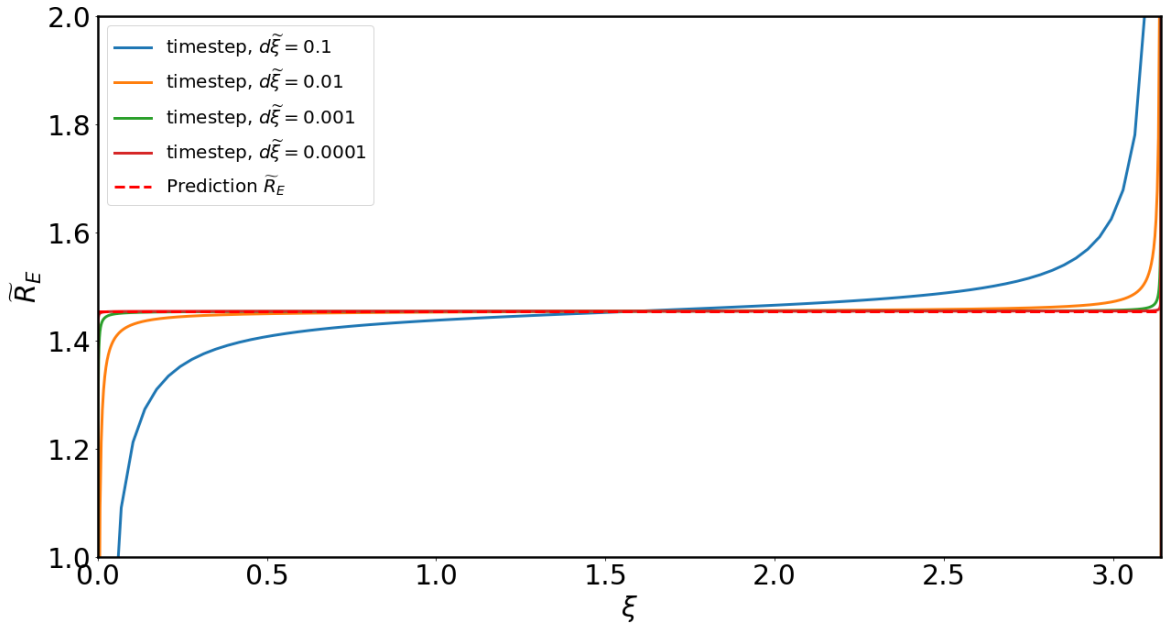

Figure 8.6.3: Plot showing the calculation of the bounce at the critical potential shift $\widetilde{U}_{0\mathrm{crit}} = 0.184$

An improved calculation of Figure 8.6.2 with a better time-step of $\mathrm{d}\xi = 0.001$, is shown in Figure 8.6.4, showing that indeed the issue with the calculations is the size of $\mathrm{d}\xi$.

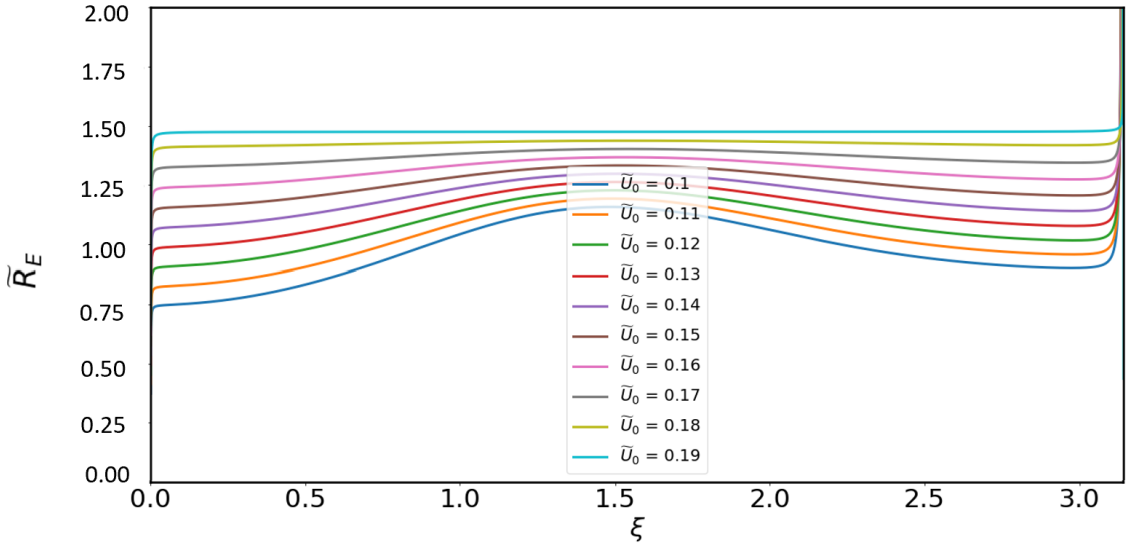

Figure 8.6.4: Plots showing the improved calculation of $\widetilde{R}_E$ using smaller step size of $\mathrm{d}\widetilde{\xi} = 0.001$.

This confirms that in the limit of increasing U_0, the Ricci scalar becomes homogeneous over the domain of ξ. Thus the FRW ansatz (7.1.1) is a true de Sitter space with a constant scalar curvature and is thus fixed.

Chapter 9

Concluding Remarks

In our journey through the aspects of false vacuum decay, we first developed the formalism of the bounce and demonstrated that it agreed with the standard WKB formalism for tunnelling in quantum mechanics. We then defined the metastable state and showed the spectrum of eigenvalues of the second variation of the action contained a negative eigenvalue which was the root cause of the metastability. This paved the way for us to perform similar calculations in the case of a scalar field with self-interaction potential with two non-degenerate minima in Minkowski space. It was found the we were to calculate the decay rate per unit time per unit volume and showed the fully renormalised expression for this amplitude. What followed was a numerical demonstration of the solutions as well as the determination of the action of the bounce, B, and the centre of the instanton, R.

We then introduced de Sitter space, an example of a maximally-symmetric spacetime which is a vacuum solution to the Einstein Field Equations and showed that the space of solutions is more flavourful than the flat case. We showed that the case of Euclidean de Sitter space, that the monotonic bounce is not a unique solution with the specified boundary conditions and we have a more complicated space of solutions with constant configurations (Hawking-Moss instanton) and the oscillating bounces of order N. We confirmed via the calculation of eigenvalues that the only relevant contribution to the tunnelling amplitude was the Coleman-de Luccia instanton. In terms of numerical results, we showed that the curves for the radius and action converge on the Minkowski space results for large de Sitter radius. The reason for this was that the curvature of spacetime decreases with larger de Sitter radius.

Dissatisfied with the exclusion of General Relativity, we introduced the corresponding calculation in the presence of gravitation by coupling the scalar field to the Einstein-Hilbert action in the minimal-coupling regime. We found that the action of the bubbles formed through tunnelling were easier to form if the transition was from dS-dS as opposed to dS-AdS. It was also found that for a small energy density difference between the true and false vacuum, shifting the false vacuum zero to positive values eventually leads to the transition deforms the Coleman-de Luccia instantons into Hawking-Moss instantons which results in a spacetime with constant positive curvature - a true de Sitter spacetime.

There are many aspects of the theory of vacuum decay that we have ignored in this report. Such as the inclusion of a finite temperature or in the case of gravity, inclusion of the non-minimal coupling term for the Ricci Scalar. Though these are fascinating aspects of the theory that the author would have included given more time, they were nonetheless, beyond the scope of the goals of this project. Though they are interesting additions which would surely improve our understanding of the language and origins of the Universe we live in.

Appendices

Appendix A

Gaussian Integrals

A.1 Contour Integration

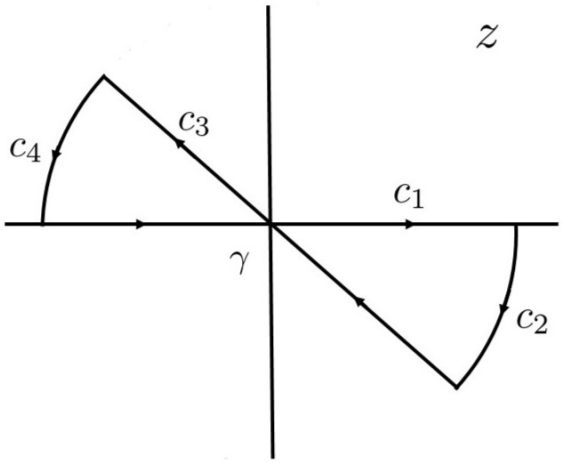

Figure A.1.1: Contour of Integration.

When we discussed the path integral, it was mentioned that the Gaussian integrals were simply a mathematical nuance that we would take to be identities. Here, we will discuss the precise solution of Gaussian integrals with purely imaginary arguments in their exponent. The integration procedure is described in [25].

Consider the following integral with positive and real a with real variable p,

$$I = \int_{-\infty}^{\infty} \mathrm{d}p \exp\left(-iap^2\right). \tag{A.1.1}$$

If we replace p with a complex variable z and consider the integral over the closed contour γ, we can write also,

$$J = \oint_\gamma \mathrm{d}z \exp\left(-iaz^2\right), \tag{A.1.2}$$

where the contour γ is shown in Figure A.1.1 and integration along the real axis corresponds to the integral in (A.1.1). We note that the integral can be split up as $\oint_\gamma = \sum_{i=1}^{4} \int_{c_i}$. By Cauchy's Theorem, (A.1.4) vanishes as no poles are enclosed by the contour. So algebraically, we can write $\int_{c_1} = -\int_{c_2} - \int_{c_3} - \int_{c_4}$. Dealing with integration over c_2 (and c_4 as they are essentially the same),

$$\begin{aligned}
\int_{c_2} \mathrm{d}z e^{-iaz^2} &= iR \int_0^{-\frac{\pi}{4}} \mathrm{d}\theta e^{i\theta} e^{-iaR^2(\cos(\theta)+i\sin(\theta))^2}, \\
&= iR \int_0^{-\frac{\pi}{4}} \mathrm{d}\theta e^{i\theta} e^{-iaR^2(\cos(2\theta)+i\sin(2\theta))}, \\
&= iR \int_0^{-\frac{\pi}{4}} \mathrm{d}\theta e^{i\theta} e^{-iaR^2\cos(2\theta)} e^{aR^2\sin(2\theta)},
\end{aligned}$$

Now if we transform the integral $\theta \to -\theta$ in which we exploit the parity properties of $\sin\theta$ and $\cos\theta$,

$$\int_{c_2} \mathrm{d}z e^{-iaz^2} = -iR \int_0^{\frac{\pi}{4}} \mathrm{d}\theta e^{-i\theta} e^{-iaR^2\cos(2\theta)} e^{-aR^2\sin(2\theta)}.$$

We now employ the triangle inequality,

$$\left| \int_a^b f(z)\,\mathrm{d}z \right| \leq \int_a^b |f(z)|\,\mathrm{d}z,$$

$$\left| \int_{c_2} \mathrm{d}z e^{-iaz^2} \right| \leq R \int_0^{\frac{\pi}{4}} \mathrm{d}\theta e^{-aR^2\sin(2\theta)}.$$

If we define $\beta = 2\theta$, we can write,

$$\left| \int_{c_2} \mathrm{d}z e^{-iaz^2} \right| \leq \frac{R}{2} \int_0^{\frac{\pi}{2}} \mathrm{d}\beta e^{-aR^2\sin(\beta)}.$$

Using Jordan's Inequality for $0 \leq \beta \leq \frac{\pi}{2}$,

$$\frac{2\beta}{\pi} \leq \sin\beta \leq \beta,$$

we have,

$$\begin{aligned}\left|\int_{c_2} \mathrm{d}z e^{-iaz^2}\right| &\leq \frac{R}{2}\int_0^{\frac{\pi}{2}} \mathrm{d}\beta e^{-aR^2\sin(\beta)}, \\ &\leq \frac{R}{2}\int_0^{\frac{\pi}{2}} \mathrm{d}\beta e^{-2aR^2\beta/\pi}, \\ &\leq \frac{\pi}{4aR}\left(1-e^{-aR^2}\right).\end{aligned} \tag{A.1.3}$$

Since the LHS of (A.1.3) is real and positive it must vanish in the limit $R \to \infty$. The integral over c_4 vanishes using similar arguments. Now we are left with the integration along c_3 which is a rotated contour of the real variable x. We can write this as $z = (1-i)x$, so we are left with,

$$\begin{aligned}\int_{-\infty}^{\infty} \mathrm{d}p \exp\left(-iap^2\right) &= (1-i)\int_{-\infty}^{\infty} \mathrm{d}x \exp\left(-2ax^2\right), \\ &= e^{-i\frac{\pi}{4}}\sqrt{\frac{\pi}{2a}} = \sqrt{\frac{\pi}{ia}}.\end{aligned}$$

Indeed the naïve integration agrees with a more sophisticated analysis in complex analysis.

Appendix B

Functional Determinants

B.1 Evaluating Functional Determinants

How do we evaluate functional determinants? We can borrow from linear algebra that for some matrix $\mathbf{M}$ with eigenvalues λ_n, then $\det \mathbf{M} = \prod_n \lambda_n$. Suppose ψ is eigenfunction of the differential operator such that

$$(-\partial_\tau^2 + W)\psi = \lambda\psi \tag{B.1.1}$$

where W is some function of τ. We can label the eigenfunctions by the eigenvalues such as $\psi_\lambda(\tau)$ which obey the boundary conditions $\psi_\lambda(T/2) = 0$ and $\partial_\tau\psi_\lambda(T/2) = 1$ which obeys the eigenvalue equation (B.1.1). Now we define two such potentials $W^{(1)}$ and $W^{(2)}$, each of whom have corresponding solutions $\psi_\lambda^{(1,2)}(\tau)$. Now we construct some function

$$\det\left[\frac{-\partial_\tau^2 + W^{(1)} - \lambda^{(1)}}{-\partial_\tau^2 + W^{(2)} - \lambda^{(2)}}\right] \tag{B.1.2}$$

This is a meromorphic function which has a zero at $\lambda^{(1)}$ and a simple pole at $\lambda^{(2)}$. A meromorphic function is holomorphic (complex differentiable) in some open subset $U \subset \mathbb{C}$ except at some points which are simple poles. As a result of Liouville's Theorem from complex analysis, two meromorphic functions with the same poles and zeros are proportional to one another. So we can construct a function

$$\frac{\psi_\lambda^{(1)}(T/2)}{\psi_\lambda^{(2)}(T/2)} \tag{B.1.3}$$

where this function also has the same zero and pole. We can separate out the parts that correspond to the same λ and choose to deal with the $\lambda = 0$ solution

$$\frac{\det\left[-\partial_\tau^2 + W\right]}{\psi_0(T/2)} = \pi\hbar N^2 \tag{B.1.4}$$

where the right hand side is a convenient choice of normalisation. We can rearrange the (B.1.4) into

$$N(\det[-\partial_\tau^2 + \omega^2])^{-\frac{1}{2}} = (\pi\hbar\psi_0(T/2))^{-\frac{1}{2}}\,. \tag{B.1.5}$$

Effectively, we are solving the differential equation

$$-\frac{\mathrm{d}^2\psi_0}{\mathrm{d}\tau^2} + \omega^2\psi_0 = 0 \tag{B.1.6}$$

together with the boundary conditions the solution is

$$\psi_0(\tau) = \omega^{-1}\sinh\left[\omega\left(\tau + T/2\right)\right] \tag{B.1.7}$$

so $\psi_0(T/2) = \omega^{-1}\sinh(\omega T)$ so $N\det[\partial_\tau^2 + \omega^2]^{-\frac{1}{2}} = [\pi\hbar\omega^{-1}\sinh(\omega T)]^{-\frac{1}{2}}$

Appendix C

Variations in the Einstein Hilbert Action

C.1 Variation of $\sqrt{-g}$

There are only two real barriers to solve obtaining Einstein's Equations, $\delta\sqrt{-g}$ and $\delta R_{\mu\nu}$. Let's deal with $\delta\sqrt{-g}$, we can simply write,

$$\delta\sqrt{-g} = \frac{1}{2\sqrt{-g}}\delta g. \tag{C.1.1}$$

In order to make progress, let's look at,

$$\begin{aligned} g_{\mu\sigma}g^{\mu\rho} &= \delta^{\rho}_{\sigma} \\ \delta g_{\mu\sigma}g^{\mu\rho} + g_{\mu\sigma}\delta g^{\mu\rho} &= 0 \\ \delta g_{\mu\sigma}g^{\mu\rho} &= -g_{\mu\sigma}\delta g^{\mu\rho} \\ \delta g_{\nu\sigma} &= -g_{\rho\nu}g_{\mu\sigma}\delta g^{\mu\rho} \end{aligned} \tag{C.1.2}$$

This relation will turn variations of the metric into variations of the inverse metric. For a non-singular matrix M we have, $\ln(\det(M)) = \mathrm{Tr}(\ln(M))$, now we take the variation to obtain the identity,

$$\frac{1}{\det M}\delta(\det M) = \mathrm{Tr}(M^{-1}\delta M). \tag{C.1.3}$$

we have used the cyclic property of the trace to ignore the the fact that M and δM do not commute in general. Using $\det M = g$, we can write (C.1.3) as,

$$\frac{\delta g}{g} = g^{\mu\nu}\delta g_{\mu\nu}.$$

However, we would like this in terms of $\delta g^{\mu\nu}$, so we can use our formula derived in (C.1.2), to write

$$\delta g = -g(g_{\mu\nu}\delta g^{\mu\nu}). \tag{C.1.4}$$

This is just what we need to write the correct form of (C.1.1),

$$\delta\sqrt{-g} = -\frac{1}{2}\sqrt{-g}g_{\mu\nu}\delta g^{\mu\nu}, \tag{C.1.5}$$

which completes the proof.

Acknowledgements

This dissertation is firstly dedicated to my parents, *Ammi* and *Dad*, who have always inspired me to work hard and to think critically and for their constant love, support and advice. Secondly, to my grandparents: *Syed Mohammad Zakria* (1938-2021) and *Syeda Musarat Zakria* (1945-2021). They were my first teachers and role models.

I would like to thank *Prof. Arttu Rajantie* for his invaluable insights and wisdom in answering my questions with patience and finesse. I have had the unique pleasure to discuss physics with some of the finest minds in the World. Moreover, I would like to thank all of my teachers during my time on as a student of the Theory Group. Their fantastic methods of teaching have bestowed on to me an understanding of the inner workings of the Universe (which is no small feat). They are truly the giants whose shoulders I stand on to see further than I previously could.

Finally to my lovely girlfriend *Nour Bensiali* for her patience and support in my meandering conversations and for providing love and support in the most difficult of times.

Bibliography

[1] Banks T.; Bender C.M.; Wu T.T., *Coupled Anharmonic Oscillators. I. Equal-Mass Case*, (1973), Phys.Rev.D, Vol 8.

[2] Brown, A.R.; Weinberg, E.J., *Thermal derivation of the Coleman de Luccia tunnelling prescription*, (2007), Phys. Rev. D, Vol. 76.

[3] Carol S.M., *Spacetime and Geometry: An Introduction to General Relativity*, (2019), Cambridge University Press.

[4] Coleman S., *Fate of the false vacuum: A semi-classical theory*, (1977), Phys.Rev.D, Vol. 15.

[5] Coleman, S., *Quantum Tunnelling and Negative Eigenvalues*, (1988), Nuclear Physics B, Vol 298, Issue 1, [pg:178-186].

[6] Coleman S, *Gravitational Effects on and of vacuum decay*, (1980), Phys.Rev.D, Vol. 21.

[7] Coleman S., *Uses of Instantons* from *Aspects of Symmetry - Selected Erice Lectures*, (1985), Cambridge University Press, ISBN: 9780511565045.

[8] Coleman S.; Callan Jr. C.G, *Fate of the False Vaccum II: First Quantum Corrections*, (1977), Phys.Rev.D, Vol. 16.

[9] Coleman S.; Glaser V. Martin, *A. Action minima among solutions to a class of Euclidean scalar field equations*, Commun.Math.Phys. Vol. 58, 211–221 (1978), https://doi.org/10.1007/BF01609421

[10] Degrassi, G.; Di Vita, S.; Elias-Miró, J., *'Higgs mass and vacuum stability in the Standard Model'*, (2012), J.High Energ.Phys. 2012, 98.

[11] Garriga, J., *Instantons for vacuum decay at finite temperature in the thin-wall limit*, (1994), Phys.Rev.D, Vol 49.

[12] Gratton S.; Turok N.; *Homogeneous Modes of Cosmological Instantons*, (2001), Phys.Rev.D, Vol. 63.

[13] Griffiths D.J., *An Introduction to Quantum Mechanics*, (1995), Pearson Education.

[14] Guralnik G. S.; Hagen C. R.; Kibble T.W.B., *Global Conservation Laws and Massless Particles*, (1964), Phys. Rev. Lett., Vol. 13.

[15] Hackworth J. C., Weinberg E. J., *Oscillating Bounce Solutions and Vacuum Tunnelling in de Sitter Spacetime*, (2004), arXiv: hep-th/0410142v1.

[16] Hartman T., *Lecture Notes on Classical de Sitter Space*, Cornell University.

[17] Hawking S.W.; Moss I.L., *Supercooled phase transitions in the very early universe*, (1982), Phys.Lett.B, Vol. 110.

[18] Hida Y; Li X.S.; Bailey D.H., *Quad-Double Arithmetic: Algorithms, Interpretation, and Application*, (2000), Lawrence Berkeley National Laboratory Technical Report LBNL-46996.

[19] Higgs, P. W. , *Broken Symmetries and the Mass of the Gauge Bosons*, (1964), Phys. Rev. Lett., Vol. 13.

[20] Kahan W., *Lectures notes on the Status of IEEE Standard 754 for Binary Floating-Point Arithmetic*, (1997), UC Berkeley, Department of Elect. Eng. Computer Science.

[21] Kobsarev I.Y.; Okun L.B.; Voloshin M.V., *Bubbles in Metastable Vacuum*, (1974), ITEP—81, USSR.

[22] Lavrelashvili G., *Number of negative modes of the oscillating bounces*, (2006), Phys.Rev.D, Vol. 73.

[23] Linde A. D., '*Decay of the False Vacuum at Finite Temperature*, Nucl. Phys. B, 216, (1983), 421 [erratum: Nucl. Phys. B **223** (1983), 544] doi:10.1016/0550-3213(83)90072-X

[24] Markkanen T.; Rajantie A.; Stopyra S., *Cosmological Aspects of Higgs Vacuum Metastability*, (2018), Frontiers in Astronomy and Space Sciences, https://doi.org/10.3389/fspas.2018.00040 .

[25] Nakahara M., *Geometry, Topology and Physics*, (2003), Taylor Francis Group, Second Edition.

[26] Osborn H., *Lectures on Advanced Quantum Field Theory*, (2007), Department of Applied Mathematics and Theoretical Physics, University of Cambridge.

[27] Parker L.; Toms D., *Quantum Field Theory in Curved Spacetime*, (2009), Cambridge Monographs on Mathematical Physics, Cambridge University Press

[28] Peskin M.E.; Schoeder D.V., *An Introduction to Quantum Field Theory*, (1995), First Edition, Westview Press.

[29] Rajantie A.; Stopyra S., *Standard Model Vacuum decay in a de Sitter Background*, (2017), arXiv: 1707.09175v1 [hep-th]

[30] Rajantie A.; Stopyra S., *Standard Model Vacuum Decay with Gravity*, (2016), arXiv:10606.00849v1 [hep-th].

[31] Riley K.F.; Hobson M.P.; Bence S.J., '*Mathematical Methods for Physics and Engineering*', Third Edition; (2006), Cambridge University Press.

[32] Shifman M.A., ITEP lectures on particle physics and field theory. Vol. 1, 2. World Sci.Lect.Notes Phys., 62:1–875, 1999.

[33] Tanabashi M.; et al (Particle Data Group), *Review of particle physics*, (2018), Phys.Rev.D, Vol. 98, doi:10.1103/PhysRevD.98.030001 .

[34] Vicentini S., *New bounds on vacuum decay in de Sitter space*, (2022), arXiv: 2205.11036v1 [gr-qc].

[35] Weinberg E., *Hawking Moss bounces and vacuum decay rates*, (2007), arXiv: hep-th/0612146v2.

[36] Zee A., *Quantum Field Theory in a Nutshell*, (2010), Second Edition, Princeton University Press.